THE CONDUCTANCE OF MOLTEN SALTS AT CONSTANT VOLUME

A Thesis
presented for the degree of
Doctor of Philosophy
in the
University of London
by

Derek John Fray

London, May 1965

ABSTRACT

This work describes the design and construction of an apparatus for measuring conductance and volume changes up to 1000°C and 1000 atm. Using this apparatus, the volumes and conductances of potassium nitrate and sodium nitrate were measured up to 1000 atm. and 500°C.

To obtain correct compressibilities for these salts, the solubility of argon has to be taken into account and a reliable method of doing this has been developed. From the results the values of the activation volume and the energies at constant pressure and volume are derived. The values of E_V range from 1 to 1.5 Kcal for potassium nitrate and from 1.8 to 2.2 Kcals for sodium nitrate. The values of $\Delta V^{\ddagger}$ are 4 - 10ml for KNO_3 and 3 - 5 ml for $NaNO_3$. These are described in relation to theories of transport in fused salts and the structure of the liquids.

It is concluded that the critical void free volume theory due to Cohen and Turnbull is the most applicable of the contemporary theories to conductance in molten nitrates. It is found that the ratio E_V/E_p and the quantity $\Delta V^{\ddagger}$ for molten nitrates are similar to those for other liquids, and that hence,

the mechanism of transport is dependent only on the short range attractive and repulsive forces and not on the long range coulombic forces.

TABLE OF CONTENTS

			Page
CHAPTER	1.	INTRODUCTION	1
	1.	General	2
	2.	Structure of Fused Salts	3
	3.	Structure of Nitrates	6
	4.	Theories of Transport in Fused Salts	9
	5.	Solubility of Gases	22
	6.	Previous Work at High Pressures	25
	7.	Origins of Present Work	30
CHAPTER	2.	EXPERIMENTAL	34
	1.	General	35
	2.	Circuit Diagram	36
	3.	Design of High Pressure Equipment	36
	4.	Ancillary Equipment	48
	5.	Safety Precautions	52
	6.	Furnace Design	56
	7.	Cell Design	60
	8.	Dilatometer and Probe	61
	9.	Methods of Operation	64

TABLE OF CONTENTS (cont'd)

		Page
CHAPTER 3.	RESULTS	73
1.	General	74
2.	Conductance	74
3.	Volume	81
4.	Analysis	84
5.	Calibration of Pressure Gauge	90
6.	Experimental Errors	91
CHAPTER 4.	DISCUSSION OF RESULTS	93
1.	Conductivities	94
2.	Volumes	105
3.	Compressibilities	107
4.	Gas Solubility	118
5.	Measurements at Constant Volume	124
6.	Discussion of the Activation Energy at Constant Volume in conjunction with the Volume of Activation	132
7.	Analysis	137
8.	Errors in Derived Quantities	139

TABLE OF CONTENTS (cont'd)

		Page
CHAPTER 5.	GENERAL DISCUSSION	141
1.	General	142
2.	Transport Theories	142
3.	Comparison with other data	149
4.	Conclusions and suggestions for further work.	153
	APPENDIX	155
	ACKNOWLEDGEMENTS	169
	REFERENCES	170

C H A P T E R 1

INTRODUCTION

1. GENERAL

Most measurements of the transport properties of molten salts have been made at atmospheric pressure. The interpretation of the effect o f temperature on the properties is, therefore, complicated by the fact that both the transport rate and the density change simultaneously with temperature at constant pressure. Fused salts have more free volume than most other liquids, but little is known of how this space is distributed, nor how it affects transport properties. As the transport properties of the liquid are undoubtedly sensitive functions of the amount and the nature of the unoccupied volume present, the results of transport experiments at constant volume are likely to be of great value in indicating the direction which theoretical treatments could most profitably be developed.

To evaluate precise energies of activation at constant volume, it is necessary to measure the pressure dependence of a transport property and the change in volume of the melt with pressure at a series of temperatures. Although diffusion may be considered the more fundamental property,

in that transport of an individual species is studied, conductance has the practical advantage in that measurements can be made more accurately and also continuously. From conductance measurements, the activation energy at constant pressure is found to vary with temperature, but so far none of the diffusion measurements made have been of sufficient accuracy to detect a similar dependence.

It is, therefore, proposed to study the effect of pressure and temperature on the conductance and volume of fused salts. In this initial work, nitrates will be studied as they are non-corrosive and have low melting points but, eventually, it is intended to extend the measurements to the alkali halides.

2. STRUCTURE OF FUSED SALTS

Compared to solids and gases, our understanding of the structure of the liquid state is very unadvanced. A solid may be regarded as an ordered regular arrangement of atoms and a gas is usually considered as a random distribution of atoms or molecules. Liquids, however, have proved to be more difficult to describe, especially fused salts where long range coulombic forces as well as short range forces are acting.

For molten salts, the change in volume on fusion is approximately 20% and Bockris and Richards[1] showed by velocity of sound measurements that only 2% of this volume change comes from the positional fluctuation of the ions, the rest is distributed randomly throughout the melt.

X-ray diffraction techniques have proved to be one of the most useful experimental methods in elucidating the structure of liquids. Zarzycki[2] and Levy et al[3] have shown from radial distribution functions that a high degree of short range order exists in fused salts but no long range order. Comparison with the solid salt showed that the internuclear distance and the co-ordination number decreased on fusion by 5% and 20% respectively. In the second co-ordination shell, the average number of ions was apparently about half that found in solid NaCl.

The simplest theory of the molten state consistent with these observations is the vacancy model, originated by Frenkel[4] and developed by Bresler[5]. The liquid is regarded as a disordered form of the solid and it is assumed that the major part of the large volume change on fusion is due to the formation of Schottky defects. These occur in every sixth position

in the interpenetrating lattices causing the breakdown of long range order. It was thought that this model should apply especially to fused salts where there is a strong coulombic force to maintain close neighbour contact. This theory has now been superseded by the hole model in which the structure of the liquid is regarded as a disordered form of the corresponding solid incorporating holes of varying size.[6] Lumsden however, has suggested that it is not necessary to regard the liquid structure as being derived from that of the same solid. For example, liquid NaCl can be considered as a disordered form of the zinc blende structure which already exhibits fourfold co-ordination. The hole theory is discussed in more detail in the following section in connection with theories of transport.

The liquid state can be considered from an alternative point of view.[7] Zernicke and Prins suggested that a liquid resembles a compressed gas in which the free volume is small compared with the space occupied by the atoms and on melting, a uniform expansion of the lattice occurs.[8] Swalin's and Cohen and Turnbull's[9] theories were derived from this model assuming that the free volume, instead

of being uniformly associated with each cell, is randomly distributed throughout the liquid. These models will be discussed more fully later.

It is not the purpose of this work to review the statistical mechanical approach to the liquid state but these theories will be briefly discussed in the section concerned with transport in molten salts.

3. THE STRUCTURE OF NITRATES

Theories of fused salt structure are usually applied to alkali halides which are considered typical ionic liquids. With nitrates some additional aspects must be examined. For instance, compared to typical ionic salts, the nitrates show low melting points, small volume changes on fusion, high entropies of fusion and a low ratio of the heats of activation for viscous flow and conductance. It has been supposed that the low melting points of the alkali nitrates can be accounted for by anion-cation association. This association was thought to be due to the fact that in the crystal the three-fold axis of each nitrate ion is constrained in the crystal but on melting, the restriction is removed and closer packing of the ions becomes possible. Although the

change in volume of the nitrates is much less than the alkali halides, the unoccupied volume in the liquids is very similar. Cleaver[10] found that just below the melting point of potassium chloride and potassium nitrate, the concentration of defects is approximately the same and that the low melting point of the nitrate is related to the ease with which defects can be formed in the solid salt and not to the presence of complexes.

Ubbelhode[11] and Førland[12] consider that the high entropy of fusion is one of the major reasons why nitrates have low melting points. The entropy can be broken down into three parts due to position, orientation and association. Førland suggests that the orientation entropy predominates whilst Ubbelhode regards the association entropy as the largest part of the fusion entropy.

Although the activation energies for nitrates and chlorides are very similar, the transport parameters of the nitrates are smaller than those of the chlorides. Janz and James[13] using the data in their paper, conclude that this is due to the small value of the exponential term in the Arrhenius equation and suggest that as the temperature is raised, the exponential term for the nitrate approaches that of

the chloride. Moreover, the thermodynamic properties of the halide and nitrate melts are very similar [14] and it is, therefore, concluded that except for the melting point phenomena the nitrates resemble the chlorides.

b) MODEL OF THE NITRATE ION

There are two conflicting opinions of the shape of the nitrate ion. Janz and James [13] considered that the nitrate ion consists of a sigma bond framework formed by the overlap of sp^2 hybrid orbitals on the nitrogen with p orbitals on the oxygen, and π bonds in which there is a large measure of delocalisation. X-ray data shows that the N-O distance is 1.218 Å and the O-N-O bond angle 120°, and empirical calculations give the radius of the nitrate ion between 1.78 Å to 2.3 Å. Due to the presence π bonds, a disk of 2.31 Å radius and 2.2 Å thickness was suggested. A spherical ion would involve rotation and for this to occur an entropy of fusion of 25 e.u. would be required. This has not been observed experimentally and it was thought that a spherical ion is only likely to exist at extremely high temperatures. Furukawa [15] calculated that completely free rotation of the nitrate ion requires a volume of at least 37%

larger than the actual value.

Conversely, Rhodes[16] treated nitrate ions as hexagonal close-packed spheres of radius 2.32 Å. In the case of potassium nitrate, the nitrate ions occupy 42.6 ml per gram ion, leaving 12 ml for the cations. However at 350°C, from the molar volumes of mixed nitrate melts of potassium and calcium and assuming that the calcium ions fit into the interstices between the nitrate ions, the actual volume was less than the calculated value. It was then suggested that the nitrate ions must have contracted together.

Angell[17] assumed that the nitrate ion rotates freely and behaved as a spherical ion of radius 2.19 Å. This radius was calculated by Kleppa and Hersh[18] from the high temperature Cs Cl structure of $RbNO_3$ and $TlNO_3$.

It is concluded that although a disk model may be favoured at low temperatures, treating the nitrate ion as an equivalent sphere will not be greatly in error. However, this question is further examined in the discussion section.

4. THEORIES OF TRANSPORT IN FUSED SALTS

e) CONDUCTANCE

The majority of fused salt transport measurements have been interpreted in terms of the rate theory or

the theory of transition states. This principle was applied by Bockris, Kitchener, Ignatowicz and Tomlinson [19] assuming that in the absence of an electric field the three dimensional jumps average out, but in the presence of a potential gradient, the activation energy is lowered in the direction of the field. The conductance equation is given by

$$\Lambda_i = \frac{1}{6} z e_o F_L^2 \exp\frac{-\Delta G_o^*}{RT} \qquad (1.1)$$

where z is the valence of the ions, e_o the electronic charge, F the Faraday, h Planck's constant, L is the jump distance and ΔG_o^* the energy of activation.

Bockris, Crook, Bloom and Richards [20] derived a similar equation but were in error, as they combined the one dimensional and three dimensional jump schemes. [67] Their model consisted of spherical ions amongst which are randomly mixed a number of holes, equal to the volume change upon fusion. Conductance involved the migration of ions by a series of jumps from one equilibrium position to another and that each jump requires an energy of activation. In liquids, the activation energy for the mechanism of jumping of an ion into a hole may be regarded as consisting of two parts. Firstly, the energy required for the formation

of the holes and secondly, the energy necessary for the molecule to move into a hole. Results have shown that plots of activation energies against temperature where the volumes are allowed to change, are of variable slope showing that the factors contributing to the activation energy are complex.

The rate theory has produced little advance in explaining the energies in terms of measurable properties of the salts and no clear account has been given of the variation of activation energy with temperature. As no other theory has been derived specifically for conductance, the relation between conductance and diffusion will be examined.

The Nernst-Einstein equation which relates diffusion, D_i, and conductance, Λ, was originally derived for dilute electrolyte solutions and is given by

$$D_i = \frac{RT}{z F^2} \Lambda \qquad (1.2)$$

where z is the ionic charge and F is the Faraday. This equation is only known to apply in very dilute solutions [21], where the concentration of ions is very low and in ionic solids where the concentration of defects controls both conductance and diffusion [22].

For fused salts, conductivities have been calculated from diffusion coefficients using the Nernst-Einstein equation but it was found that the experimental conductivity values were much smaller than the calculated values. According to Sundheim (23), the values for NaCl are 40% low, for $NaNO_3$ 40% low and for CsCl 21% low; the deviation increases with increasing temperature.

The deviations from the Nernst-Einstein equation have been accounted for in several ways. Bockris and Hooper (24) suggested that movements are possible which do not contribute to conductance but by simultaneous movement of a cation and anion contribute to diffusion. This was originally suggested for solids but should be more applicable to molten salts where the large free space would increase the probability of paired vacancy formation. The concentration of such holes would also, increase with temperature.

Klemm (25, 26) and Laity (22, 27) have proposed that interference between ions, moving in opposite directions, under the influence of an applied field is responsible for the deviation.

The use of the Nernst-Einstein equation does not seem to be a fruitful approach, although Angell (28) used the equation to obtain values of E_D from E_Λ.

However, although there may be no direct relation between diffusion and conductance it is useful to examine theories of diffusion since the fundamental physical models involved may be applicable to conductance.

b) DIFFUSION

1. The Hole Theory

Furth's hole theory[77] has been applied by Bockris and Richards[1] to the calculation of thermodynamic properties of fused salts and, in conjunction with the activated state theory, by Bockris and Hooper[24] to diffusion in alkali halides.

The hole model differs from the vacancy model in that the holes are not Schottky defects but are randomly distributed and arise by means of density fluctuations. These holes, which need not be spherical, are assumed to vary in size from those which are too small to accomodate an ion, to others into which ions or ion pairs can migrate. Combining the hole theory with X-ray measurements, Bockris[29] suggests that the liquid may have a tighter interionic packing and if it were not for the holes, there would be a volume decrease on melting. Furth considered

that the holes in the liquid were analogous to the molecules and molecular clusters in dense gases rather than to vacancies in the solid state, but his calculations showed that the size of the average hole was smaller than that of a single gas molecule. From the size distribution proposed by Furth, Bockris and Richards[1] showed that the most probable hole size is given by

$$V_h = 0.68\left(\frac{kT}{\gamma}\right)^{3/2} \qquad (1.3)$$

where γ is the liquid-vapour interfacial tension. To calculate the size of a hole in the melt, the measured surface tension of the liquid was used. The use of the macroscopic surface tension in calculating the size of an ionic hole has been discussed by Riess et al[30] who concluded that the effect of curvature of the hole on the surface tension is not large. At the same time, Stillinger[31] considers the use of macroscopic surface tension to be very inaccurate. Blander et al[32] used a similar assumption in calculating gas solubilities in melts and found the result was only correct within an order of magnitude.

From this theory, Bockris and Hooper[24] derived

the following formula for the heat of activation at the melting point:-

$$(\triangle H_h)_m = 3.55\ RT_m \qquad (1.4)$$

where $\triangle H_h$ is the work of hole formation per mole of holes. They found that this could be applied to molten salts within ±50%. This work was extended to other liquids by Nanis and Bockris (33) who used a slightly different equation,

$$\triangle E = 3.74\ RT_m \qquad (1.5)$$

where $\triangle E$ is the energy of activation of self-diffusion. However from the graph in their paper, it is seen that the energies for Na in $NaNO_3$, Na in NaI and Sr in $SrCl_2$ are identical whereas the melting points are 307, 659, and 873°C respectively.

According to the hole theory the activation energy is identified with the surface energy of formation of the hole. This view, as recognised by Frenkel (34) and Nachtrieb (35) also leads to the expectation that the energy of diffusion be proportional to the heat of vaporisation but experiment shows no such correlation between the two quantities (8).

2. The Density Fluctuation Theory

Swalin[8] devised this theory from the quasi-random model and assumed that transport in liquid metals results from local density changes by means of which the atoms can move small and variable distances. The self-diffusion coefficient was found to be represented by

$$D = 1.29 \times 10^{-8} \, T^2 / \Delta H_v \beta^2 \ cm^2 \ sec^{-1} \quad (1.5)$$

where ΔH in the heat of vaporisation, β is related to the slope of the morse curve and may be evaluated from the force constant data of Waser and Pauling[36]. A direct result of the theory is that there is no activation energy and the slope of $\log_{10} D$ versus $1/T$ should have a value of 2 RT and be independent of the properties of the diffusing species. This theory has been applied mainly to liquid metals where it is found that the activation energy is proportional to the temperature and the diffusion coefficient is approximately proportional to T^2.

For molten salts, E/RT has an average value of 3.6 which is considerably higher than that predicted by Swalins's theory. Even if this theory was recalculated using a more realistic distribution

function and a coulombic energy equation, it is doubtful whether it would apply to fused salts, due to the large amount of free volume. A theory is, therefore, needed which considers the free volume and ion movements of approximately atomic dimensions instead of microjumps.

3. Critical Void Free Volume Theory

In this theory, the movement of the particles does not depend on an activation energy but on the distribution of free volume in the liquid. It has an advantage over the rate theory that the temperature dependence of transport is stated in terms of other measurable properties.

Cohen and Turnbull's free volume theory [9] is based on the concept that an ion can only move when a void above a critical size appears adjacent to it. The critical void size is that which just allows a neighbouring ion to jump into the original position following the displacement. The voids are considered to arise by the distribution of the free volume existing in the liquid and not as a result of an activation in the ordinary sense. These ideas are similar to Rice's [107] theory of diffusion in crystals.

A relation was derived between the diffusion coefficient, D, and the free volume, v_f.

$$D = gau \exp(- \gamma v^{*}/v_f) \quad (1.6)$$

where g is a geometric factor, taken as 1/6, a is the jump distance or approximately the ion diameter, u is the gas kinetic velocity, $(3kt/m)^{\frac{1}{2}}$, γ is a constant to correct for the overlap of free volume which should lie between $\frac{1}{2}$ and 1, and v^{*} is the critical void volume. The free volume is assumed to be equal to the thermal expansion above a temperature T_o, where the free volume starts to appear. This is given by

$$v_f = \alpha \bar{v}_m (T - T_o) - \bar{v}_p \beta p \quad (1.7)$$

where α is the mean value of the coefficient of expansion in the range T to T_o and $\bar{v}_m$ is the mean molar volume. The second term gives the pressure dependence where β is the mean compressibility, and $\bar{v}_p$ the mean molecular volume for the pressure increment P. The complete expression for diffusion is then

$$D = ga(3kT/m)^{\frac{1}{2}} \exp -\gamma v^{*}/\left[\alpha \bar{v}_m (T - T_o) - \bar{v}_p \beta P\right]. \quad (1.8)$$

T_o is assumed to be equal to the glass transition temperature but when T_o is zero the equation is similar in form to that obtained from the rate theory.

Cohen and Turnbull applied their theory to organic liquids and liquid metals and found that v^* was near to the van der Waals volume for organic liquids and the ion core size corresponding to the highest valence state of the metal. Values of $\gamma v^*/\bar{v}_m$ for fused salts have been calculated by Lunden[38] and Angell[39] taking $\bar{v}_m$ as the volume of the ion. The void size was approximately that of the ion and, considering the similarity of E_D for cation and anion, Angell concluded that the free volume in molten salts was distributed between cations and anions in proportion to their sizes.

A critical test of the theory is the temperature dependence of transport. The diffusion coefficient can be written:-

$$D = AT^{\frac{1}{2}} \exp(-K/T - T_o) \qquad (1.9)$$

$$\text{and } \frac{d \ln D}{d(1/T)} = \frac{-E_D}{R} = -\tfrac{1}{2}T - K \left(\frac{T}{T - T_o}\right)^2 \qquad (1.10)$$

Plots of $\log_e D$ against $1/T$ should be curved but as measurements on molten salts have only been carried out over small temperature ranges the curvature is scarcely noticeable.

This theory has been applied by Angell [28] who used glass forming melts in the system $Ca(NO_3)_2$ and KNO_3 and found an exponential dependence of conductance on $1/(T - T_o)$, where T_o is the glass transition point. He applied various values of T_o to his data and selected the one which gave the best fit. This corresponded very well with the experimentally observed transition point [40]. A graph was constructed relating T_o and the mean cationic strength of various molten salts and mixtures. However, the ratio of the void volume to the ion volume was found to be in the range 0.5 to 0.25, which is about half that found by Cohen and Turnbull for molecular liquids. Moreover, the values of the pre-exponential constant calculated from the Cohen and Turnbull formula were an order of magnitude greater than the measured values.

4. STATISTICAL MECHANICAL THEORIES

Rice and Allnatt [41] have examined the equilibrium properties of an idealised ionic melt consisting of anions and cations of the same size and electronic configuration, except for the change of sign. Transport was defined in terms of rigid

core collisions between two particles followed by a Brownian type movement in the fluctuating force field of the neighbouring ions. Rice[42] examined the relaxation behaviour of this simplified melt and together with Allnatt[41] concluded that only short range forces affect the motion of ions and, therefore, transport coefficients, excluding conductance, should be similar to those in liquid inert gases.

With regard to conductance, Rice[42] considers that there will be frictional forces arising from the asymmetry of the local ionic structure. This asymetry will be greater for conductance than diffusion due to the movement of the surrounding ions under a potential gradient.

Calculations showed that the viscosity of liquid potassium chloride, where $r_{K^+} \approx r_{Cl^-} \approx r_A$ may be compared with those of liquid argon with reasonable agreement. If, however, coulombic forces were considered the values were too large by a factor of 4.

Further evidence was given by Angell and Tomlinson[43]. If transport properties were determined by the coulomb potential, the values of D_+ and D_- for TlCl should lie above those for RbCl.

In fact, it was found that they fell below those for CsCl which is to be expected for a salt with a high van der Waals energy, a cation with a Xe core and a higher polarisability than Cs. The low values of the transport properties of lead chloride compared to those of cadmium chloride were related to the high polarisibility of the lead ion. The importance of short range forces was stressed by Stillinger [44] and Reiss and Mayer [45] in calculating compressibilities and surface tensions of molten salts.

4. SOLUBILITY OF GASES

As the pressure is transmitted by a gas it is essential to have some knowledge of the gas solubility. Measurements of inert gas solubilities in molten fluorides have been made by Grimes et al [32, 46, 47] by equilibrating the salt with gas, removing the salt, flushing out the gas and determining the inert gas content with a mass spectroscope. Copeland [48] used an alternative method where the solid nitrate was subjected to argon pressure, the salt melted, and from the pressure change, the solubility of the gas was calculated. Depression of the freezing point was used by Frame, Rhodes and Ubbelohde [49] to

calculate the solubilities of various gases in nitrate melts. For oxygen and nitrogen the depression was less than 0.01°C which indicated that the solubilities were less than 10^{-5} mole/ cc of salt.

Bockris, Pilla and Barton [50] attempted to determine the change in volume on fusion by measuring the pressure change of an inert gas over the system. To obtain values of the volume changes which agreed with previous measurements, they had to allow for a gas solubility of 10^{-8} mole/ cc of salt.

The solubility of a gas depends upon its partial pressure and is given by Henry's law:-

$$P_g = k X_1 \qquad (1.11)$$

where P_g is the pressure of the gas, k is a proportionality constant, known as Henry's law constant, and X_1 is the amount of gas in the liquid. Henry's law is only strictly applicable at low pressures because at high pressures the law becomes less exact and it is found that the proportionality constants exhibit considerable variation [51].

For fluoride melts [32, 46, 47] the law is obeyed within the experimental precision of ±5%, but the pressures used did not exceed 2.07 atm.

Copeland [48] made no mention of the applicability of the law to his results. It is suggested by Frohlich, Tauch, Hogan and Peer [52] that solubilities may be considered as linear functions of pressure provided that corrections for the deviations from the ideal gas law are applied.

The solubility of most gases in liquids decreases with increasing temperature. However, Grimes et al [32, 46, 47] found that the gas solubilities increased with increasing temperature to give position heats of solution. This occurs for relatively insoluble gases.

Blander, Grimes, Smith and Watson interpreted their results using a similar model to Uhlig [53]. This model assumes that provided the dissolved gas does not interact with the liquid, the free energy change on solution is related to the surface energy of the hole created by the gas. The following reaction was considered

$$X_{(g,\ C_g)} = X_{(d,\ C_d)} \qquad (1.12)$$

where C_g is the concentration of the gas and C_d is the concentration of the gas in the liquid. The free energy change on solution was equated to the surface energy of the hole by the following equation:-

$$-RT \ln \frac{C_d}{C_g} = kA \gamma_{mic} \qquad (1.13)$$

where for a spherical atom kA is $18.08r^2$ (r is the radius of the gas atom in Å), and γ_{mic} is the microscopic surface tension. By assuming that the microscopic surface tension is the same as the macroscopic surface tension, it was found that the calculated values of the solubility were within an order of magnitude of those found experimentally.

5. PREVIOUS TRANSPORT MEASUREMENTS AT HIGH PRESSURES

Much work has been done on the effect of pressure on the properties of liquids and solids but it is only recently that the results have been applied to transport theories. It was not until 1951 that transport properties were studied at constant volume when Jobling and Lawrence [54] examined the viscosities of benzene and carbon tetrachloride.

a) DIFFUSION

Values of the pressure dependence of self-diffusion of carbon tetrachloride [55], diffusion

of iodine in carbon tetrachloride [56] and the self-diffusion of 2,2 dimethylhexane [57] were used by Cohen and Turnbull to test their theory. The experimental values were slightly less than those given by the theory. However, when a similar calculation was applied to liquid metals, the theoretical values were greater by a factor of ten than those found experimentally by Petit and Nachtrieb [35, 58]. Consequently, Cohen and Turnbull modified the pressure dependent term in their expression to $\bar{v} \Delta\beta \Delta P$, where $\Delta\beta$ is the compressibility difference between β_T and β_{T_0}. This is described more fully in the discussion.

Nachtrieb and Petit [35, 58] measured the activation volume in liquid gallium and mercury and found that the values were approximately 1/20 of those for the solid. This is consistent with the view that in the solid a vacancy has to be formed before diffusion can occur while in the liquid, the activation volume merely represents a dilation accompanying jumping.

Tricklebank, Nanis and Bockris [59] determined the self diffusion coefficients of sodium 22 in molten sodium nitrate at 350°C and up to 800 bar and found the activation volume was 10.7 ± 1.4 cm^3.

The extension of this work by Nagarajan, Nanis and Bockris [60] showed that the activation energy at constant pressure did not change with pressure and the activation energy at constant volume was 0.72 ± 0.17 kcal mole^{-1}. These workers [61] have also examined diffusion in $CsNO_3$ and the viscosities of these melts. However, not too much reliability should be attached to these results as will be shown in the discussion.

b) CONDUCTANCE

A number of workers have examined the effect of pressure on the electrical conductivity of ionic crystals. Jost and Nehlep [62] have measured the conduction of AgCl and AgBr to 300 atm and 300°C. Similar measurements have been made by Shapiro and Kolthoff [63, 64] on AgBr and this work was extended by Kurnick [65] to AgBr doped with $CdBr_2$. Activation energies for both Frenkel and Schottky defects, mobility energy for silver vacancies and interstitials, and the activation and mobility volumes were calculated.

Cleaver [10] measured the pressure dependence of the conductivity of pure potassium nitrate and potassium nitrate doped with 0.015 mole% $Ba(NO_3)_2$

and found that the volume of activation for the migration of cation vacancies was 9 ml/mole at the melting point.

The first attempts to measure the effect of pressure on the conductances of ionic solutions were made by Colladon and Sturn in 1827 [66], since then there have been a large number of measurements but very little application to transport theories. In 1961, Brummer and Hills [67] measured the temperature and pressure dependence of conductance of dilute electrolyte solutions in water, methanol and nitrobenzene. It was found that energies of activation at constant pressure and constant volume are substantially different and that E_p was a function of temperature, whereas, E_v was not. However, both were sensitive functions of the volume of the system. Their work will be discussed in detail in conjunction with the present results.

Conductivity measurements have been carried out on molten sodium nitrate by Copeland et al [48] at 369°C at atmospheric pressure and at 362 atm. where it was found that the specific conductance had decreased by 5.7%.

c) DENSITY

Bridgeman[68] has investigated a wide range of organic liquids and some rare gases at several temperatures and at pressure up to 80,000 atm. It was found that most liquids contract by 20 - 30 % of their initial volume when the pressure is raised from 1 atm to 1200 atm. The compressibilities decreased by about a half in the same pressure range.

The compressibilities of molten salts at 1 atmosphere pressure have been determined by Bockris et al[1] by the indirect method of measuring ultrasonic velocities and applying the equations:-

$$\beta_T = \frac{\gamma V}{u_1^2 M} \qquad (1.14)$$

and

$$\gamma - 1 = \frac{u_1^2 \alpha^2 TM}{C_p} \qquad (1.15)$$

where β_T is the isothermal compressibility, γ is the ratio of the specific heats, V is the volume, u_1 is the ultrasonic velocity, M is the molecular weight, T is the temperature and C_p is the specific heat at constant pressure. The ultrasomic velocities were redetermined by Higgs and Litovitz[69] who found slightly lower values than Bockris, but

the experimental error obscures any effect these results would have on β_T. This method suffers from the disadvantage that the compressibility is obtained at atmospheric pressure and no indication is given of its pressure dependence. More recently, Owens[70], has determined the density of molten nitrates up to 10,000 atm using a direct piston method but the results are not available.

7. ORIGINS OF PRESENT WORK

Activation energies for conduction in fused salts at constant pressure are not independent of temperature[71, 73, 74]. Klemm[72] differentiated the Arrhenius equation,

$$\Lambda = \Lambda_\infty \exp\left(-\frac{H}{RT}\right) \qquad (1.16)$$

and obtained,

$$\frac{d \ln \Lambda}{d\,(1/RT)} = H_{app} = H - \frac{T\,dH}{dT} - \frac{d \ln \Lambda_\infty}{d\,(1/RT)} \qquad (1.17)$$

Assuming that Λ_∞ is independent of temperature, it is seen from the differential that the temperature dependences of H and H_{app} differ radically whenever $\frac{d H}{dT}_{app} \neq 0$. For potassium nitrate E_P decreased by 20 % in the temperature range 340°C to 440°C[73] and in the case of sodium nitrate a decrease of 10 %

occurred for an increase in temperature of $50^{o}C$ [74].

Using the absolute rate theory equation for conductance,

$$\lambda_{\infty} = \frac{1}{6}\frac{ZeF}{h} L^2 \exp\left(-\frac{\Delta G_o}{RT}\right) \qquad (1.18)$$

and the following expressions for the energies at constant pressure and volume:-

$$E_p = RT^2 \left(\frac{\partial \ln K}{\partial T}\right)_P, \qquad (1.19)$$

$$E_v = RT^2 \left(\frac{\partial \ln K}{\partial T}\right)_V. \qquad (1.20)$$

Brummer and Hills [67] obtained

$$E_p - E_v = (\Pi + P)\Delta V^{\ddagger} + \frac{2}{3} RT^2\alpha \qquad (1.21)$$

where Π is the internal pressure, $\Delta V^{\ddagger}$, the activation volume and $2/3\ RT^2\alpha$ is derived from the temperature dependence of the jump distance. It is obvious from this equation that it is unlikely that both E_v and E_p are independent of temperature since Π, $\Delta V^{\ddagger}$, and $\frac{2}{3} RT^2\alpha$ are functions of temperature.

The slope of $\ln \Lambda$ versus $1/T$ is $\Delta U^{\ddagger}$, at constant volume, and $\Delta U^{\ddagger} + (\Pi + P)\Delta V^{\ddagger} + 2/3\ RT^2\alpha$, at constant pressure. Not only is the second expression more complex but as $\Delta V^{\ddagger}$ depends on the volume, a change in volume must alter E_p.

If the 2/3 $RT^2\alpha$ term can be neglected, the internal pressure taken as $\frac{T\alpha}{\beta}$, and the activation volume as $- RT \left(\frac{\partial \ln K}{\partial P} \right)_T$, the equation approximates to

$$E_p - E_v \simeq RT^2 \frac{\alpha}{\beta} \left(\frac{d \ln K}{dP} \right)_T \qquad (1.22)$$

when P is small. This is the same as the expression used by Hiraoka, Osugi and Jono [75, 76] in the interpretation of their diffusion work.

The purpose of this work is to determine the values of E_v, E_p and ΔV^* for molten salts and to examine them in relation to contempory theories of transport in molten electrolytes.

Measurement of the activation energy at constant volume affords a critical test of the hole theory. The total activation energy for the mechanism of ions jumping into a hole or vacant site may be regarded as the sum of the jump energy and the energy of hole formation. In the absence of any structural changes over a limited temperature range and if the volume of the liquid is kept constant, the number of holes may be regarded as unchanged. The activation energy obtained from measurements at constant volume is E_v, the energy of jumping. From hole theory Bockris and Hooper [24] suggest this should be very small

compared to the activation energy at constant pressure.

If it is assumed that conductivity can be applied to the Cohen and Turnbull equation, 1.8, the equation can be tested in two ways. At constant volume the conductance should vary as $T^{\frac{1}{2}}$ and from the equation, the pressure dependence of conductance can be estimated using values of T_o given by Angell [28], and by assuming that v^* approximates to v_m.

Measurements at high pressures on molten salts should give some indication of which theory is most applicable as each theory suggests a completely different pressure dependence of transport. As measurements have been obtained on other systems at constant volume, comparisons of the data should exemplify the differences and similarities between molten electrolytes and ordinary liquids.

C H A P T E R 2.

EXPERIMENTAL SECTION

1. GENERAL

The design of high pressure equipment depends on the pressure and temperature at which the measurements are to be made. It was intended that the apparatus should work up to 1000°C and 1000 atmospheres although in the present work the maximum temperature was only 500°C. As the eventual working temperature of 1000°C exceeds the point where metals start to lose their strength, the bomb must be heated internally.

The cost and ease of manufacture are related to the size of the bomb, and this in turn, is controlled by the dimensions of the furnace. To obtain accurate conductance and volume measurements, vessels are required which are approximately half an inch in diameter, open at one end, and maintained within $\pm 2^{\circ}$C over a length of one and half inches. Although there are considerable advantages in thermal behaviour at high pressures in a horizontal furnace, only a vertical furnace will accomodate the vessels with economy of space.

Argon is most suitable as the compressive medium as it does not react with metals, has a smaller compressibility than either helium or nitrogen and is readily available in a high degree of purity.

Moreover, furnace windings appear to suffer less embrittlement in argon.

2. PRESSURE CIRCUIT

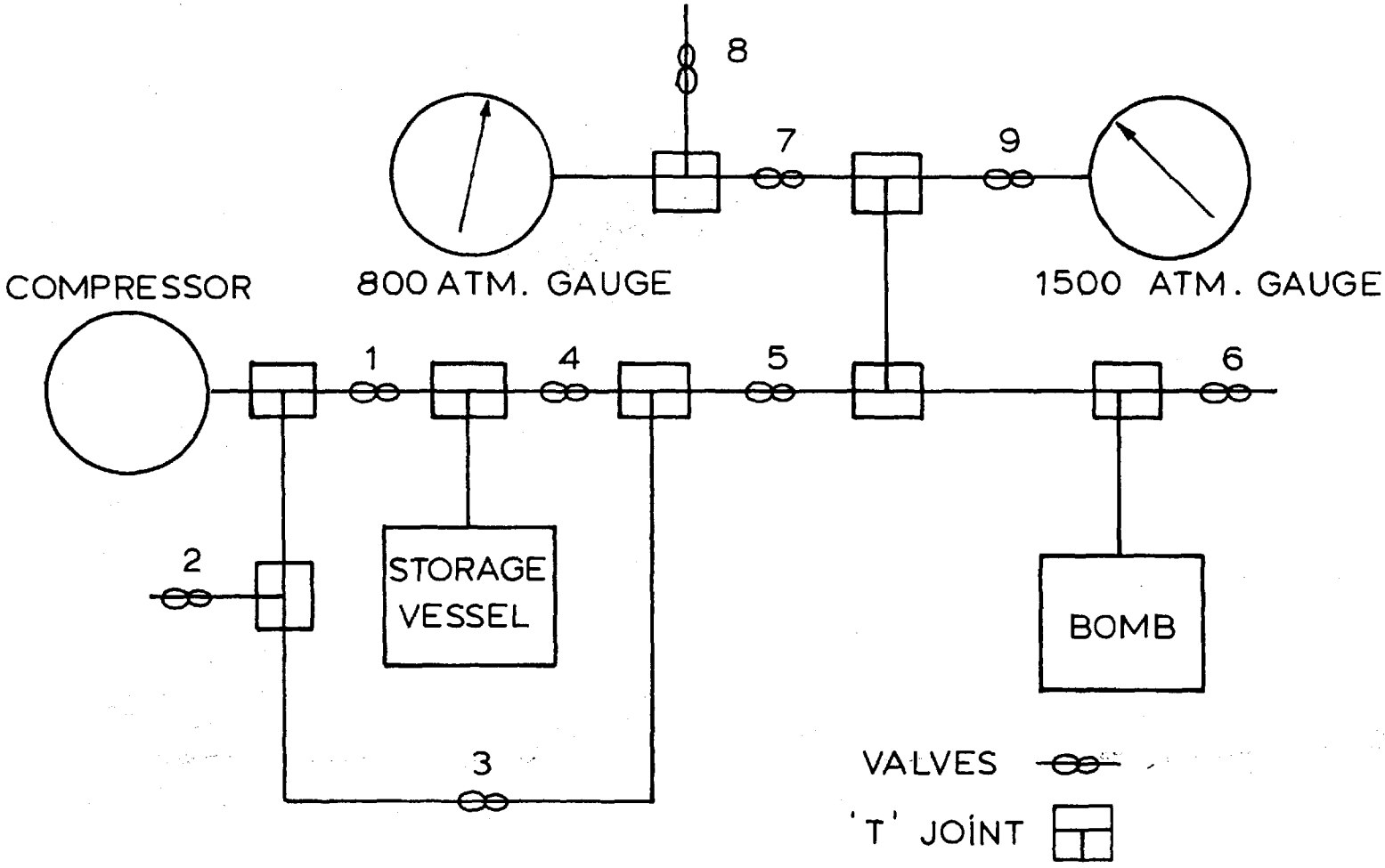
The circuit diagram is shown on page 37. The gas enters the pump through a filter from the cylinder and, after compression, is given a further filtration to remove oil droplets before passing into the bomb.

There are two pressure gauges, calibrated to 800 atm. and 1500 atm. respectively. Up to 500 atm. the low pressure gauge is used but at greater pressures, valve 7 is closed and the pressure read on the 1500 atm. gauge. If valve 7 should leak, valve 8 can be opened to relieve the pressure. The pressure inside the bomb is reduced by opening valve 4 to allow the gas to flow into the storage vessel where it can be used for the initial compression in the next run.

3. DESIGN OF HIGH PRESSURE EQUIPMENT

a) FACTORS AFFECTING DESIGN

All pressure vessels have to be designed in such a way that no permanent deformation occurs during use. The pressure is not the only factor controlling the



PRESSURE CIRCUIT DIAGRAM

onset of failure; temperature, thermal stress, fatigue and corrosion are just as important.

1. Internal Pressure

For safe design it is essential to have some criterion of elastic failure which gives the pressures necessary to cause the material at the bore to yield and for the vessel to burst.

Most experimental evidence shows that for ductile materials the Octahedral Shear Stress criterion is valid (78). This states that

$$\sigma_p = \frac{\sigma_y}{\sqrt{3}} \left(\frac{k^2 - 1}{k^2} \right) \qquad (2.1)$$

where σ_p is the yield pressure, σ_y is the 0.1% proof stress and k is the ratio of the external diameter to the internal diameter. However, the true margin of safety between the working and bursting pressures is given by the formula:- (78)

$$\frac{P_b}{P} = \frac{2\sigma_u}{P} \left(\frac{k - 1}{k + 1} \right) \qquad (2.2)$$

where P_b is the bursting pressure, P is the working pressure, σ_u is the ultimate tensile strength of the material, and k is the ratio of the diameters.

According to Dodge (79) a thread will not shear if the threaded length is equal to the thread diameter. In calculating stresses in threads it was necessary to make an allowance for the tightening up stress which may be as high as 50% of the pressure stress. Where the thread diameter was greater than its length, the total load was divided by the area taking the strain to give the shearing force on the thread.

The accepted safety factor when working at 1000 atm. is 2.5 on the yield point or the 0.1% proof stress of the material. When the apparatus was at 1000 atm. all the stresses were less than a third of the 0.1% proof stress of the materials and gave a safety factor of at least seven on the bursting pressure.

2. Temperature

Temperature has two distinct effects on the mechanical behaviour of pressure vessels. Firstly, there is creep which occurs in all ductile materials under continuous load, but only becomes a serious factor above a critical temperature which for medium alloy steels is 350°C higher than the anticipated internal wall temperature. The second effect is due

to the thermal stresses, which are set up in the wall by a temperature gradient causing each part of the vessel to expand an amount which is dependent on the temperature. The combined thermal and pressure stresses in an internally heated bomb are always lower than the largest stress acting independently. The maximum temperature gradient a vessel can support without yielding at the bore is given by (78).

$$T_y = \frac{(1 - v)}{\alpha E} \sigma_y \left[\frac{k^2}{k^2 - 1} - \frac{2}{\ln k} \right]^{-1} \qquad (2.3)$$

where T_y is the temperature gradient, v is Poissons ratio, α is the coefficient of linear expansion, E is Young's modulus, and k is the ratio of the diameters. For a medium sized pressure vessel the maximum permissible temperature gradient is about 150°C. An approximate calculation shows for a bomb 4" in diameter with a wall thickness of 1" and a furnace at 1000°C surrounded by refractory the temperature gradient in the wall is 20°C. To find the stress on the internal wall the radial, tangential and axial components of the thermal stress are combined with those due to the internal pressure. With an internal pressure of 1000 atm. and a temperature gradient of 20°C in the wall, the stress acting on the inner wall of the bomb described above is 7,800 p.s.i. or 530 atm. which effectively doubles the

safety factor.

3. Fatigue

The majority of cases of fatigue failure occur in pumps and compressors where there are continual fluctuating stresses. There was no failure in either the compressor or the pressure vessels.

4. Corrosion

Argon is inert and as the gas is dried there should be no corrosion. However, it was found that, during use, a thin coating of rust appeared on the inside walls presumably due to the water absorbed in the refractories when the bomb was left open to the air. This could be cleaned off with emery paper leaving a perfectly smooth surface.

Both nitrogen (80) and helium (81) attack steel but only under more extreme conditions than those under consideration.

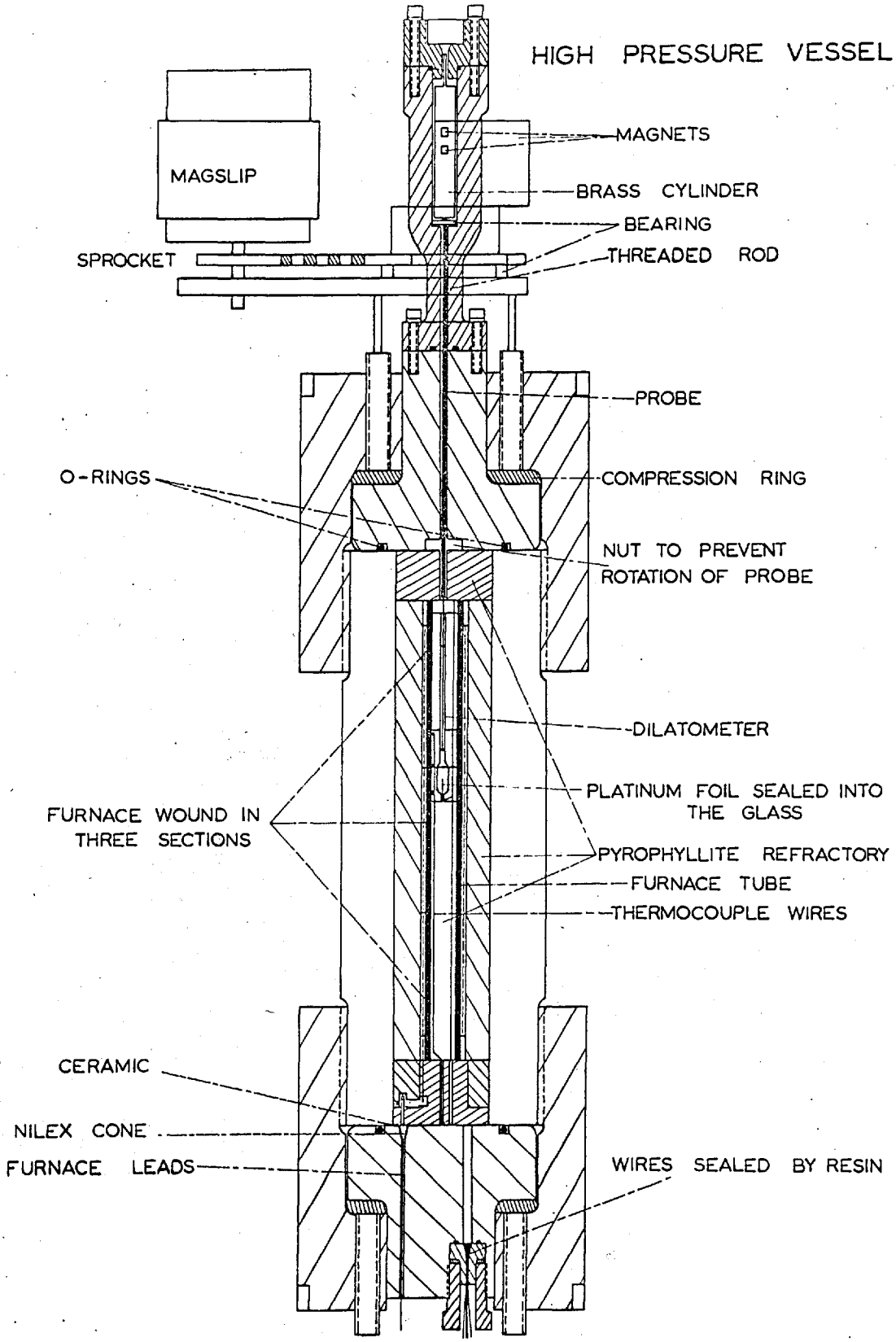
b) CONSTRUCTION OF BOMB AND STORAGE VESSEL.

The materials available for high pressure construction are restricted to steels, nimonics and beryllium copper. Plain carbon steels are occasionally

used, but alloy steels are preferred because of the better physical properties that can be developed by heat treating. The alloy steel chosen for most parts of the bomb, storage vessel and filter was En 24. The device to measure the volume changes was activated magnetically and the high strength material selected was beryllium copper. The bomb and storage vessel were essentially cylinders in the annealed condition, which were purchased from Keetons Sons and Co. Ltd., Sheffield, already drilled out to size and only required facing and threading. A 2.5% beryllium copper rod was kindly donated by Telcon Metals Ltd., Crawley, in the solution treated condition. As beryllium is toxic, the rod was machined under oil as recommended by Paul, Benedek and Warschauer (88) and then heat treated for 3 hours at 315°C to give an ultimate tensile strength of 70 - 75 t.s.i. and a yield strength of 62 - 68 t.s.i. After heat treatment it was almost impossible to machine.

There are several factors influencing the choice of closure including, size of vessel, working pressure, number of electrical leads entering the bomb and the frequency with which the closure will be removed. It was anticipated that during the

preliminary experiments the closures would be dismantled frequemtly and, therefore, it was essential that the closures be easily removed and that the sealing faces, which are pressed tight, should not turn against one another. For medium diameter vessels, such as the bomb, the most suitable closure was the compression head and for larger cylinders the cap ring closure. Both closures incorporate a ring of bolts which bear on closing plugs and provide the compression necessary to effect the gasket seal onto the face of the cylinder. These closures need not be removed entirely, but only loosened, after which the complete head can be removed. The compression head was used for both ends of the bomb and is shown on page 44. One plug was attached to the hollow beryllium copper cylinder, whilst the furnace leads and thermocouple wires were brought into the bomb through the other. As the external diameter of the storage vessel was larger than that of the bomb, a cap ring closure was used in which the ring, containing the bolts, was threaded inside the open end of the cylinder. The material for the closures was received as 7" diameter round En 24. This was machined out roughly to size, heat treated to 60/65 t.s.i.


HIGH PRESSURE VESSEL
MAGSLIP
MAGNETS
BRASS CYLINDER
BEARING
SPROCKET
THREADED ROD
PROBE
O-RINGS
COMPRESSION RING
NUT TO PREVENT ROTATION OF PROBE
DILATOMETER
PLATINUM FOIL SEALED INTO THE GLASS
FURNACE WOUND IN THREE SECTIONS
PYROPHYLLITE REFRACTORY
FURNACE TUBE
THERMOCOUPLE WIRES
CERAMIC
NILEX CONE
FURNACE LEADS
WIRES SEALED BY RESIN

tensile strength to give a greater hardness than the cylinder so as to resist the tendency for the threads to seize when the bomb was under load. All the bolts were B.S.F. "Unbrako" socket cap screws of 95 t.s.i. tensile strength which were ground flat at the compression end.

By immersing the bomb in a coolant it was hoped that the gaskets would not rise above 100°C. For this temperature and 1000 atm. there was a considerable choice of gaskets but the most convenient were P 90° shore 'O' rings. These have proved themselves perfectly satisfactory, only requiring occasional renewal. To prevent extrusion, the 'O' rings were placed in grooves in the plugs machined to the specifications recommended by the manufacturers. The sealing faces were lapped flat with diamond paste and were protected by aluminium caps when the bomb was dismantled.

c) FURNACE LEADS

Methods of bringing insulated leads into high pressure vessels have been described by many workers (81, 82, 83, 84) but the method suggested by Bett and Weale (85) was the simplest. This embodied a

small Nilex steel cone which has the same coefficient of expansion as the hollow ceramic cone into which it is inserted. This unit fitted into the high pressure face of the plug. All the surfaces were lapped with diamond paste to a perfect fit and sealed with "Durofix" to maintain a gas-tight seal until the pressure forced the components together. Nickel wires, of sufficient length to protrude outside the plug, were brazed on to the metal cone and insulated with varnish impregnated cotton. To separate the Nilex from the ceramic required a sharp tap with a hammer on the end of the nickel wire. However, the only way the ceramic could be removed was by breaking it. Electrical leaks occasionally occurred when corrosion products linked the Nilex to the bomb but these were soon rectified by cleaning the top of the ceramic.

d) THERMOCOUPLE LEADS

The easiest way of bringing a large number of thin wires into a bomb is to use some form of resin seal. Lazarre [86] cemented a bundle of eleven wires into a hole with araldite for liquid pressures up to 4000 atm., and Gugan [87] has used araldite to cement individual wires into narrow, cylindrical holes for

use at 5000 atm. Two sets of workers (88, 89) have used Stycast 2850 GT resin, which has better properties than araldite. However, it was found that the shelf life of the stycast resin was only six months.

Ten 0.0145" chromel-alumel wires were sealed into two small plugs, which were held in the larger plug by a hollow bolt which compressed an 'O' ring between the small plug and its seating.

The correct amount of low temperature catalyst was carefully weighed out and stirred thoroughly into the resin. After evacuation to remove air, the resin was painted on to the thermocouple wires and these pushed into the hole through the small plug. The hole tapered from $\frac{3}{8}$" to $\frac{1}{8}$" over a $\frac{1}{4}$" and was coated with a silicone mould release compound. The rest of the hole was filled with resin by applying a vacuum to the sealing face of the plug with the other end immersed in resin. To prevent the resin running out, small pieces of paper were slid over the wires and pushed on to the plug. Before setting the resin was warmed to increase the fluidity. As there was no adhesion to the steel, the pressure forced the resin cone into the conical socket to form a gas-tight seal.

4. ANCILLARY EQUIPMENT

a) COMPRESSOR

The gas was compressed by a single stage Hofer 1000 HK3 compressor driven by a 3 phase motor at 74 r.p.m. The suction pressure was 80-200 atm. at a suction capacity of 3 litre/hour giving a discharge pressure of 1000 atm. Compression was effected by a reciprocating piston which was sealed by stuffing boxes lubricated with oil. The valves in the compressor were simple plate-valves and, as these leaked when dust adhered to their polished surfaces, it was essential to pass the gas through a filter before it reached the compressor. For dissipating the heat generated by compression, the cylinder and pressure pipes were provided with water cooling. To ensure that the compressor could not be started without adequate cooling, a pressure operated switch which cut out if the water pressure fell below 10 p.s.i. was incorporated in the motor circuit.

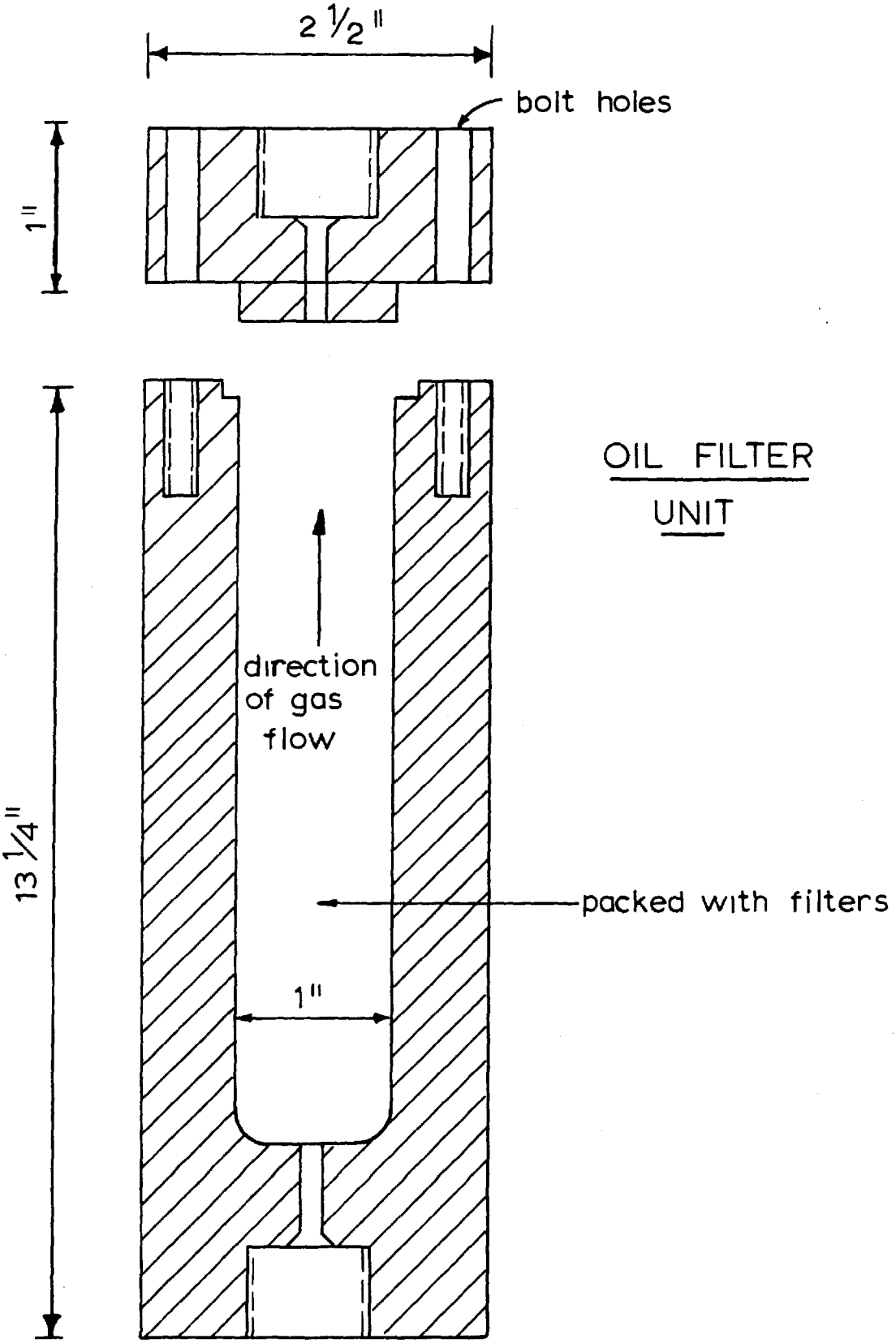
The oil separator feeding the stuffing boxes was filled with oil; this was renewed when gas could be heard escaping past the piston.

b) FILTER

As the discharged gas became contaminated with oil it was filtered after leaving the compressor. The filter unit was made from 50/60 t.s.i. tempered En 24 steel to give a safety factor exceeding three and is shown on page 50. To remove most of the oil, coarse copper gauze was placed at the bottom of the filter. The gas then flowed upwards through "Odox" filter pads dispersed with fine quartz wool and silica gel. Final filtration was given by 10 pm millipore pads. The filter proved very effective because only slight signs of carburisation, indicative of burnt oil, were found on the furnace refractories.

c) PRESSURE GAUGES

Two "Budenburg" test gauges, with 10 inch diameter scales, and reading up to 800 and 1500 atmospheres respectively were used to measure the pressure. To avoid permanently deforming the Bourdon tube it is recommended (79) that this type of gauge is used only up to two-thirds of its maximum pressure. This recommendation was followed



OIL FILTER UNIT

in the present work. The gauges were calibrated against a "Budenburg" precision balance using facilities kindly made available by Dr. K.E.Weale of the Chemical Engineering Department of Imperial College.

d) TUBING AND CONNECTORS

The austenitic stainless steel tubing had an external diameter of $\frac{3}{8}$ inches and a bore of $\frac{1}{8}$ inch and was purchased, together with the necessary connectors, from the American Instrument Company.

Most of the valves were of the "Hofer" straight through type, but a "Hofer" fine adjustment valve was fitted to regulate the flow of gas into the bomb.

The 'T' pieces and elbows were manufactured in the department's workshop of 2" round annealed En 24 steel.

e) COOLING SYSTEM

Because the removable closures prevented cooling by the normal method of a water jacket, the bomb was immersed up to the bottom of the beryllium copper top in a small tank filled with transformer oil of low viscosity and good thermal conductivity. To cool the oil, it was circulated by a small D.C. pump through

a copper coil immersed in cold water. When the furnace was at 500°C and the bomb at 1000 atm. the temperature of the bath remained below 35°C and the surface of the bomb never exceeded 50°C.

The main disadvantage of this method of cooling is the penetration of the oil inside the closures. A small positive pressure was always maintained in the bomb during removal of the closures, to prevent ingress of oil and contamination of the refractory.

f) LIFTING TACKLE

A 5 cwt. "Felco" movable hoist was employed to lift the bomb in and out of the cooling tank. The hoist straddled the safety cabinet above the bomb.

5. SAFETY

a) SAFETY PRECAUTIONS

Compressed gas contains a considerable amount of stored energy which is released in the form of a shock wave and flying fragments if the vessel should fail. The effects of shock waves were studied by Loving (90) who set off charges of TNT in a protective chamber, measured the pressure wave, and derived the following formula:

$$P = K \frac{W}{V} \qquad (2.4)$$

where P is the design pressure in p.s.i.g., W is the weight of the explosive in pounds, V is the volume of the chamber in cubic feet and K is a constant depending on the type of explosive, and equal to 20,000 for TNT. The TNT equivalent of 100 ml of gas at 1000 atm. was calculated from the stored energy in B.t.u. assuming that the energy release of 25,000 B.t.u. is produced by the explosion of 8-12 pounds of TNT (91). The value was 0.0378 lbs. of TNT giving a pressure wave of 6.4 p.s.i.g. which the cabinet could easily withstand.

No precise calculations can be done to evaluate the missile hazard and, consequently, the design was based upon other workers experience. According to Comings (92) for small pressure vessels for which an ample safety factor can be provided, barricades can be neglected. However, it is usual to have some form of protection. Porter, Lobo, and Sliepcevich (93) consider that $\frac{1}{2}$" boiler plate alone is sufficient to stop most missiles which might be produced in a laboratory scale explosion. With this in mind, the safety cabinet was made from $\frac{1}{2}$" mild

steel sheet bolted on to three inch angle iron at every ten inches with $\frac{5}{8}$" bolts. This framework was securely bolted to the floor. To reduce the chance of rupturing the steel sheet, all high-pressure vessels were mounted at least 8" from the wall (94). Over the door opening, an admiralty blast mat was hung which could arrest any flying pieces of metal.

The valves were mounted on the front panel with the valve stems protruding through the steel sheet. The ends of the valves were covered with a steel plate to prevent the valve stems blowing out in case of failure. When high pressure tubing fails, it is liable to whip about; it was therefore securely anchored at frequent intervals. The gauges were mounted on top of the safety cabinet above eye level with ample space for the blow-off back to operate.

b) TESTING

A thorough examination for flaws and cracks was given to all the materials. A specimen of beryllium copper was examined metallographically. It showed little porosity, and it was concluded that it was safe to use. To ensure that catastrophic

failure would not occur at high gas pressures, all the fittings were hydraulically tested up to 1000 atm. Measurements of the diameters of the pressure vessels were made before and after testing and at 1000 atm. There was no change and to ensure that no deformation occurred during use these measurements were checked periodically. All the joints which had leaked at high pressure were tightened, and the oil washed out of the circuit with carbon tetrachloride. Many more leaks were observed when testing with gas and these were detected with soap solution and with a rubber tube used as a stethoscope.

In case the preliminary calculations of the inner wall temperature were inaccurate, a check was made by painting a thermocolour on the inside wall. When the furnace was at 500°C and 1000 atm. the colour did not alter showing that the wall temperature had not risen above 70°C.

6. FURNACE DESIGN

a) FURNACE

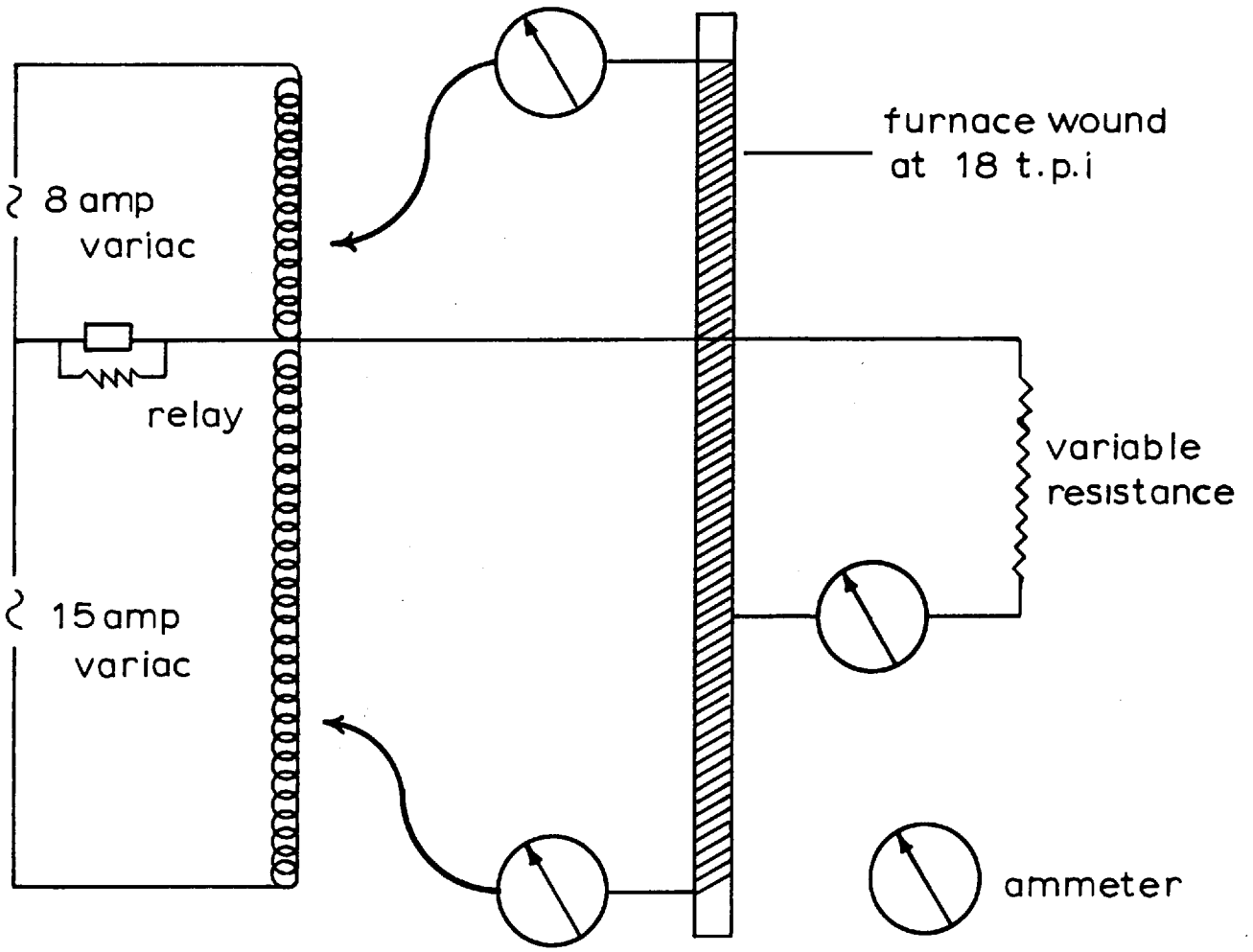
The major difficulties of attaining consistent high temperatures at pressure are the loss of heat through convection and the movement of the hot zone up the furnace tube [95]. According to Johannin and Vodar [96] increasing the pressure of nitrogen from 1 atm. to 1000 atm. increases the heat transported by laminar convection by 10^5 to 10^6. Smyth and Adams [95] found that a furnace which required 10 amps at 22 volts to attain a temperature of 1400°C at 1 atm. required 30 amps at 75 volts for the same temperature at 1200 atm. To counteract the movement of the hot zone at high pressures, the furnaces either have auxiliary windings [84] or are centre tapped [83]. The ~~former~~ latter method was adopted because keeping the inner wall temperature below 100°C requires at least $\frac{1}{2}$" of refractory; this leaves insufficient space for two sets of windings.

The furnace was wound on a lathe with 0.022" nichrome wire at 18 t.p.i. on an alumina tube 10" long, $\frac{1}{2}$" internal diameter, and 11/16" external diameter, giving a resistance of 40 ohms. The

wound furnace was coated with alumina paste and fired to insulate the leads from the windings. It was found that the best arrangement consisted of two tappings dividing the winding into three portions.

To obtain the necessary power distribution at high pressure, one variac supplied the power to the bottom and middle windings with a set of variable resistances in parallel across the middle windings. The top winding was controlled by another variac fed from the same power source as the first, as shown in the circuit diagram on page 58. To keep the temperature of the constant zone at 400°C, the power input at 1000 atm. was 8 amps at 150 volts in the bottom winding, 2 amps at 150 volts in the middle winding and none in the top compared with 3 amps at 35 volts in the top winding and 2 amps at 40 volts in each of the bottom windings at atmospheric pressure.

The temperature was controlled by a series V Kelvin Hughes proportional controller. The chromel-alumel control thermocouple was placed approximately in the centre of the furnace against the alumina insulation. Although the furnace control was within ±0.2°C at 1000 atm, the temperature gradient was



ELECTRICAL CIRCUIT FOR BOMB FURNACE

irregular as was shown by the thermocouples positioned every half inch. The maximum difference over the even temperature zone was always less than 4°C. However, the cell capillary only occupied ½ inch of the furnace tube over which the temperature gradient was less than 1°C.

The furnace performance varied with the compressive gas. Argon and nitrogen were roughly the same, while helium having better thermal conductivity required less power difference between the on-off positions of the mercury switch to maintain the same temperature control.

b) REFRACTORIES

The main problem of using standard insulators which are based on porous dead space is the penetration of gas at high pressure. This can either be overcome by placing the furnace insulation against the wall of the bomb [96] and water cooling the outside of the bomb or using a dense refractory such as soapstone or pyrophyllite [97]. Norwegian soapstone was tried, but it was found to be too inhomogenous to machine, and appeared to be a better conductor than expected. It was found that pyrophyllite purchased from Carters (Merchants) Ltd.,

was easy to machine, a poor conductor and had very little shrinkage on firing. The pyrophyllite was roughly machined and heated up to 750°C over three days. When cool, it was finally machined and refired at 1050°C. Where possible, the whole of the free space inside the bomb was filled with refractory to reduce convection currents and diminish the gas volume.

c) THERMOCOUPLES

Two negative, and four positive thermocouple wires were brought out of the bomb. One negative and positive were for the control thermocouple, while the remainder formed three thermocouples with a common negative which were arranged at ½" intervals alongside the vessel in the furnace. Chromel-Alumel thermocouples were used as they have a greater thermal e.m.f. and a lower pressure e.m.f. than platinum-rhodium [98, 99]. The e.m.f. was read on a portable Cambridge potentiometer.

7. CELL DESIGN

The salts studied were the nitrates which are low melting and can be used in Pyrex without corrosive attack [13]. The conductivities are

of the order of 1 ohm^{-1} cm^{-1} necessitating a capillary cell with a cell constant of 500 cm^{-1}. The design, consisting of a 1 mm diameter capillary, 2.5 cm long, with two 4mm diameter reservoirs, is shown on page 62. The platinum cylindrical electrodes, $\frac{1}{2}$ cm by 2 mm, were made from platinum foil welded to thick platinum wires. Before being fixed in the cells, the electrodes were platinised by passing a small current through a solution of platinic chloride and lead acetate. The current was reversed every half minute for about ten minutes. To remove the platinic solution from the surface of the electrodes, dilute sulphuric acid was electrolysed between them. When clean, the platinium cylinders were heated to red heat in a flame before the wires were sealed into the walls of the reservoirs. All glassware was annealed in a gas flame as the compressibility of glass varies with internal strain (100).

8. DILATOMETER AND PROBE.

With the exception of dilatometry, very few of the methods of measuring volume changes are applicable at high temperatures and pressures. The advantages of dilatometry are, that many results can

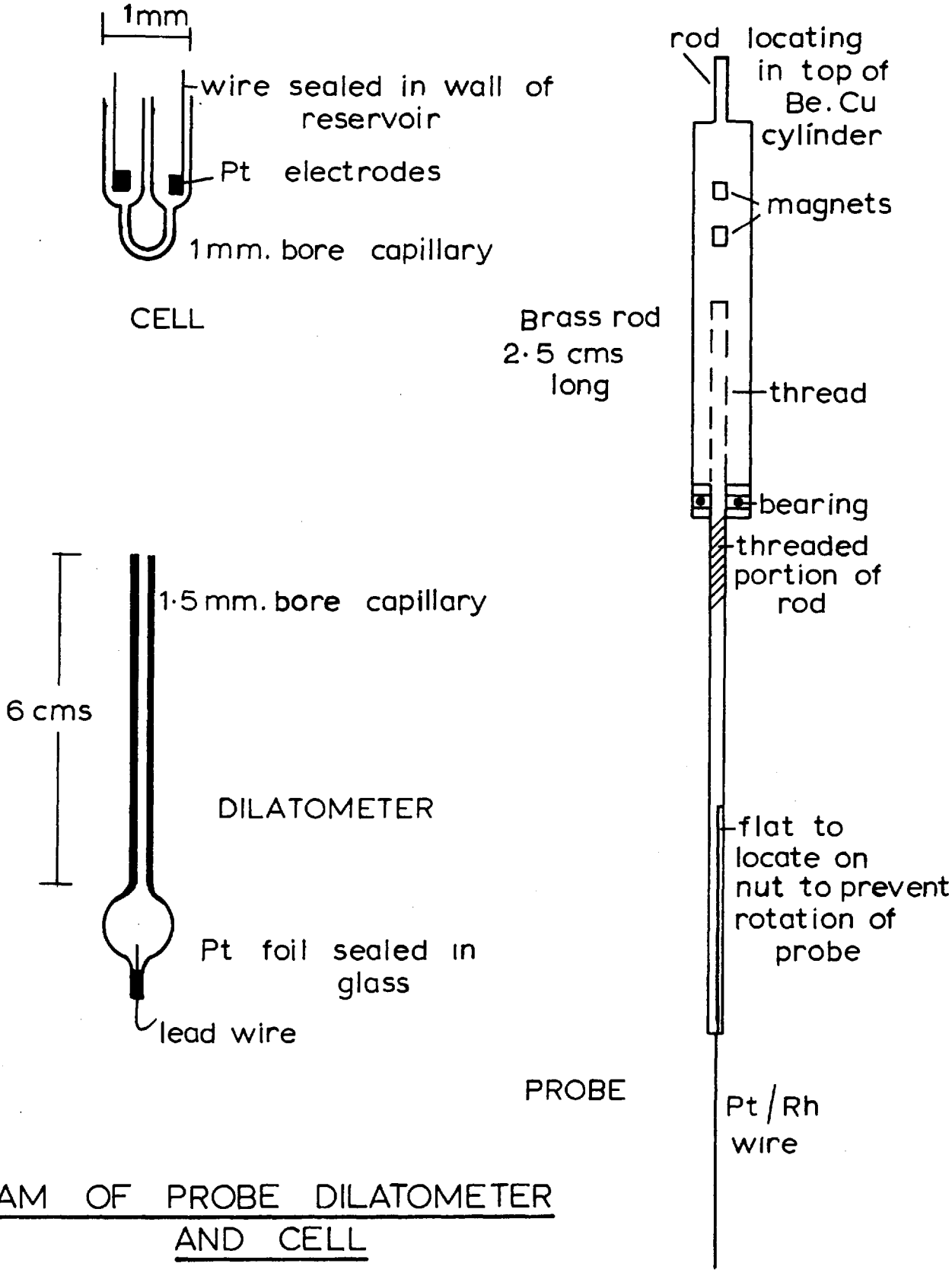


DIAGRAM OF PROBE DILATOMETER AND CELL

be obtained without renewing the cell, and that high accuracy can be attained by using a large bulb and narrow neck. This method was used and the level of liquid in the capillary was determined electrically by a probe consisting of a steel rod with one end threaded and a platinum-rhodium wire brazed on the other. The adherence of the melt to the wire and the meniscus effects depended on the size and rotation of the probe. The wire was 0.042 mm in diameter and could only move in a vertical direction. The unit, shown on page 62, was made up of a brass rod, containing two small magnets, which could rotate freely on a single thrust ring around the threaded end of the probe. There was a flat on the steel rod which rested against a small screw to prevent the probe rotating. The Pt/Rh wire was bent slightly to ensure that its point was always in the centre of the capillary. Rotation of the brass rod caused the probe either to rise or fall depending on the direction of rotation.

The magnets in the brass rod were actuated by a magnet outside the beryllium copper housing which was driven by remote control by two "Magslips".

The neck of the dilatometer was made out of precision bore tubing. At the bottom of the bulb,

a piece of platinum foil was pinch-sealed into the glass. A lead was taken from the foil via the resin seal to the conductivity bridge. The other lead from the bridge was connected to the bomb as this was in electrical contact with the probe. Contact of the probe with the liquid surface caused the conductivity reading to decrease suddenly.

9. METHODS OF OPERATION

a) ASSEMBLY OF BOMB

With reference to the diagram on page44 , the bottom plug was supported on a tripod and the lowest refractory fitted over the protruding furnace leads and thermocouple wires. These wires were sheathed in silica, welded together, and surrounded with pyrophyllite. The furnace tube was placed in position and the leads attached to the Nilex by a grub screw connector. After fitting the bottom collar of refractory, the main pyrophyllite was slid round the furnace tube. This unit was checked for electrical leaks with an insulation tester before being lowered into the bomb. The end closure was screwed down and the leads connected

to the potentiometer, furnace and controller. After inverting, the bomb was ready for the cell or dilatometer to be placed in position, the top portions of refractory added, and the top closure screwed down.

b) FILLING

Two methods are suggested in the literature for filling small vessels. Boardman et al [101] poured the molten salt into the vessel and Shartsis and Spinner [102] added powdered material and then melted. Neither of these techniques worked, due to the formation of bubbles in the capillaries. The vessels were filled by completely immersing them in the melt, which had been dried by bubbling dry argon through it for 24 hours, and evacuating. To adjust the liquid level to $\frac{1}{2}$ cm above the electrodes in the cell, and to 3 cm in the capillary of the dilatometer, the excess salt was removed piecemeal by inserting fine glass capillaries into the vessels, waiting until they were full of salt, and then removing.

c) ANALYSIS

The salts used were of Analar grade, purchased from Hopkins and Williams, but in case dissociation of the nitrate had occurred during a run, a check was made by dipping a potassium iodide-starch paper moistened with dilute acid into a solution of the salt. The liberated iodine showed that nitrite ions were present. An accurate spectrophotometric method was used to determine the exact amount of nitrite present (103). The weight of salt in the cells was found by weighing the cells after a run, dissolving out the salt and making up to 250 ml, drying the cells, and reweighing. It was essential that the cells were not damaged as it was intended to remeasure the cell constant. To 35 ml of salt solution, 1 ml of 5-N Hydrochloric acid was added, followed by 5 ml of 0.2% aqueous solution of sulphanilamide. This was allowed to stand for 2 minutes before adding 1 ml of 0.5% solution of ammonium sulphamate and after a further 2 minutes 1 ml of 0.1% solution of N-(1-Napthyl)- ethylenediamine dihydrochloride was added. The mixture was diluted to 50 ml and allowed to stand for 3 minutes before being compared with standards in a Unicam Spectrophotometer.

c) CONDUCTANCE

1. Determination Of The Cell Constant

The cell constant was determined before and after each set of runs by measuring the cell conductance with 0.1N potassium chloride solution at a temperature known within $\pm 0.1^{\circ}C$. Comparison with the standard conductance for this solution gave the cell constant. According to Brummer (104), the change of cell constant with temperature is given by

$$S_t = \frac{S_o}{1 + \alpha t} \qquad (2.6)$$

where S_t is the cell constant at the temperature and S_o is the cell constant and α is the coefficient of expansion. A change of $350^{\circ}C$ reduces the cell constant by 0.1% but as the cell constants were only determined to within $\pm 0.2\%$, this can be neglected. The cell constant also changes with pressure:-

$$S_o = S_p \left(1 - \beta \frac{P}{3} \right) \qquad (2.7)$$

where β is the compressibility of glass. A pressure change of 1000 atm. only affects the cell constant by 0.1%.

2. Conductance Bridge

The choice of bridge depends critically on the accuracy with which the other variables can be measured. The temperature is known with $\pm\frac{1}{2}^{o}C$. For alkali nitrates a change of $\frac{1}{2}^{o}C$ alters the conductance by 0.2% and, therefore, it is only necessary to have a bridge reading to within $\pm$0.2%.

A Pye conductance bridge, incorporating an oscilloscope detector was used to measure the conductivity. The bridge was of the fixed frequency type (300 and 5,000 c/sec) and the scale was stated to be accurate to 0.2%. The measurements were carried out on the 5,000 c/sec range. Ubbelohde et al [105] and other workers [106] showed that polarisation effects can be neglected and that any variation of conductances of the melt is negligible over large frequency changes. Values of conductance during cell constant determinations and nitrate runs were checked with a bridge made up of standard resistance which could be fed with a variable frequency. An earpiece was used as a detector and no change in the value of conductance was noted with change of frequency from 1000 c/s to 12,000 c/s.

3. MEASUREMENT

To prevent salt getting on to the refractories in the pressure vessel and shorting the conductance leads, the cell was transferred from the salt bath to a furnace with a temperature gradient where the salt could be solidified from the bottom. This prevented the formation of bubbles when the salt was remelted. The adhering salt was washed off and the cell dried.

The cell with its long platinum leads sheathed in alumina was placed in the furnace on the pyrophyllite plug and its leads welded to the chromel conductivity leads in the furnace. These leads were connected via the resin seal to the conductance bridge. By shorting out the cell, the leads resistance was measured.

The salt was melted from the top of the cell and the conductivity values at 1 atm. compared with those found in the literature. If there was any difference, the cell was removed and the cause found. To melt the salt from the bottom either caused the cell to leak or large bubbles to form beneath the electrodes. On completion of the measurements of conductivity versus temperature at 1 atm., the

pressure was slowly increased to 200 atm. and the power input varied continuously to keep the salt molten. When an even temperature zone had been obtained at the requisite pressure, the temperature was varied by altering the control position on the controller. Measurements with argon, nitrogen, and helium at various temperatures were completed at 200 atm. intervals up to and down from 1000 atm.

b) VOLUME MEASUREMENTS

1. Calibration

A dilatometer was filled with mercury and the variation of the volume with temperature determined with the probe. The change of level of mercury in the capillary with a known temperature change was compared with the value calculated from the density values in the literature (123) and the known weight of mercury in the dilatometer. There was very good agreement.

2. Measurement

The dilatometer was weighed before being filled with salt. After filling the dilatometer, it was quickly transferred from a portable furnace to the bomb furnace without solidifying the salt as remelting caused bubbles to accumulate at the base of the capillary. To keep the vessel upright and to prevent it moving, a hollow rod of pyrophyllite was slid over the capillary.

The probe was screwed into the plug without the top on the beryllium copper and the unit lowered. When the probe was in position, the electrical circuit and the ease of rotation were checked before putting the bomb in the oil bath.

The technique of measurement was to locate the liquid surface and assign to this position an arbitary number of turns. The change in liquid level with temperature and pressure was determined relative to this value. The pressure was altered very slowly to prevent movement of the dilatometer by the gas. Measurements in argon and nitrogen at various temperatures were carried out at 200 atm. intervals to and from 1000 atm. Corrections had to be applied to the readings as the bomb expanded

longitudinally with pressure. The effect of temperature was neglected as a change of 100°C over 3 inches of the probe only increases the length of the probe by 0.002" which is negligible compared with the accuracy of measurement.

On completion of a run the dilatometer was reweighed. The experimentally observed volume change with temperature was compared with that calculated from the weight of salt and the density equations found in the literature.

CHAPTER 3

RESULTS SECTION

1. GENERAL

The results for the change of volume and conductance with pressure at various temperatures are shown as graphs. The original results are tabulated in the appendix.

2. CONDUCTANCE

a) CELL CONSTANTS

The cell constants were determined with 0.1 N KCl before and after use and are shown in table 3.1. A different solution was used for each determination.

TABLE 3.1

Cell Constants

Cell Number	Cell Constant	
	Before	After
1	424	425
2	547	-- *
3	492	494
4	596	597
5	499	502

* Cell broke during use

The reason for the determinations not being the same was due to the use of different solutions. As the difference was within the experimental error of the determination, it was ignored and an average of the two values taken as the cell constant.

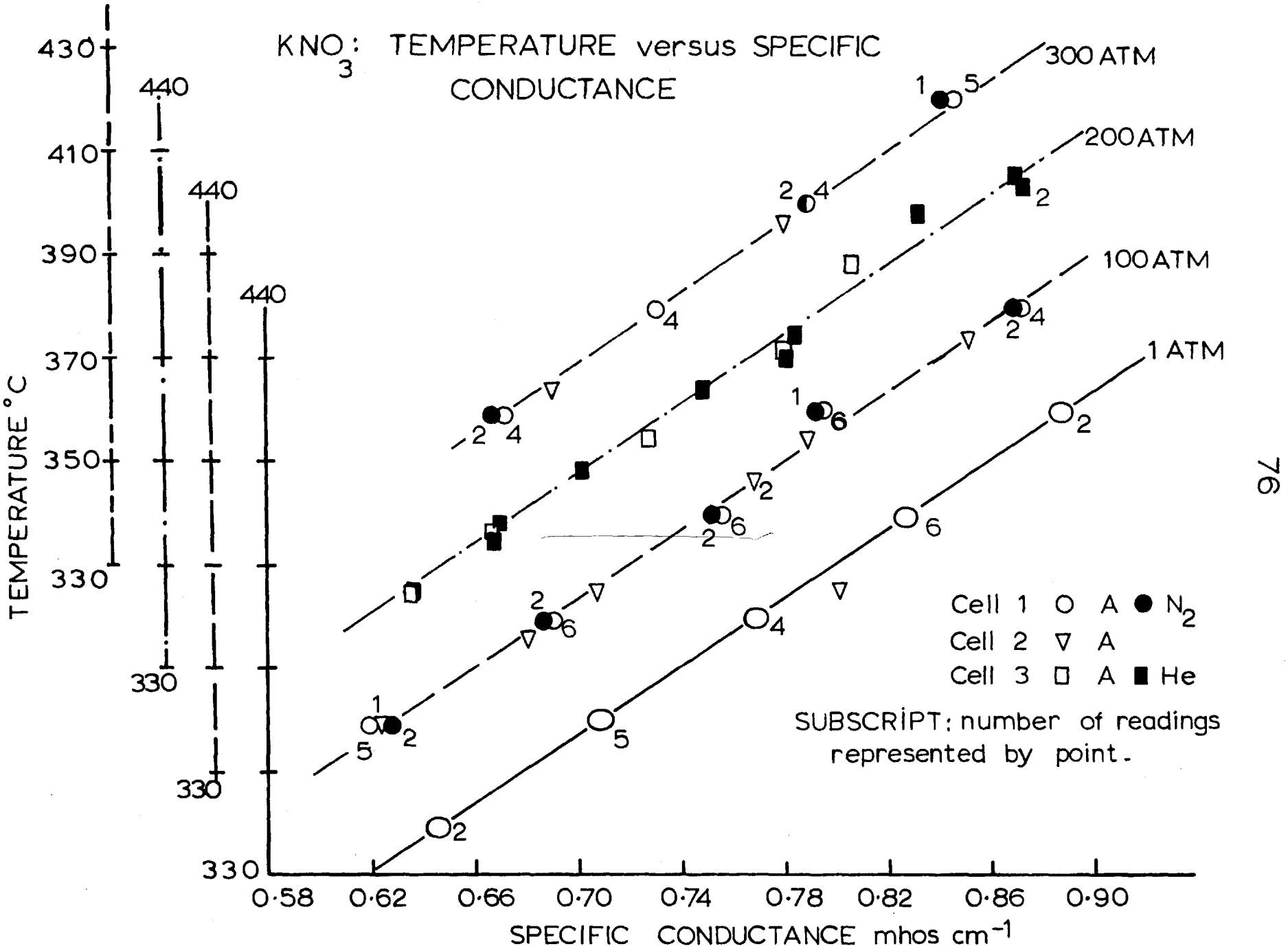
The experimentally determined values of the conductance were corrected for the resistance of the leads, which was about 5 ohms, and then multiplied by the cell constant to give the specific conductance.

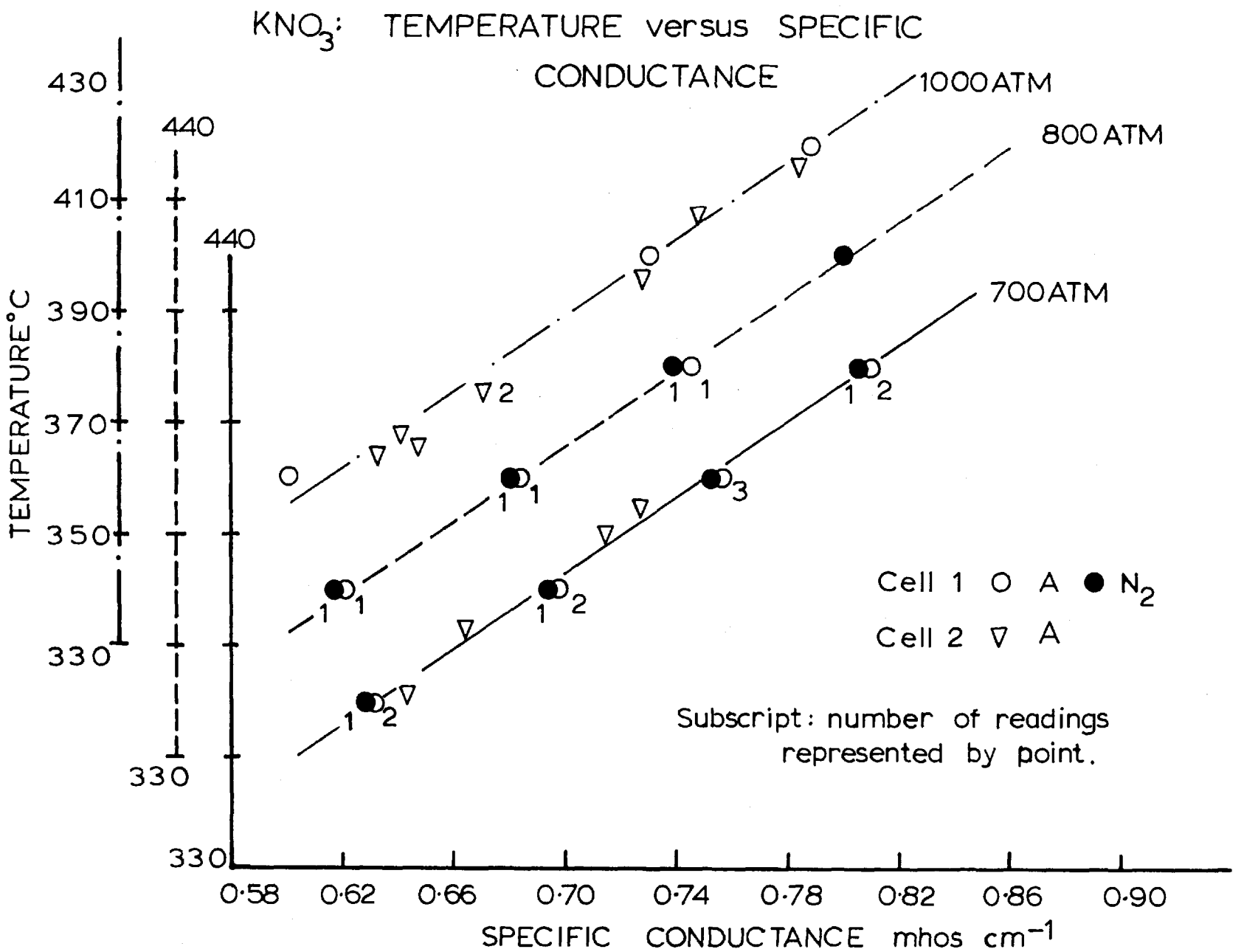
Both pressure and temperature change the cell constant, but the magnitude of the corrections, which are of opposite sign, is 0.1% and, therefore, negligible.

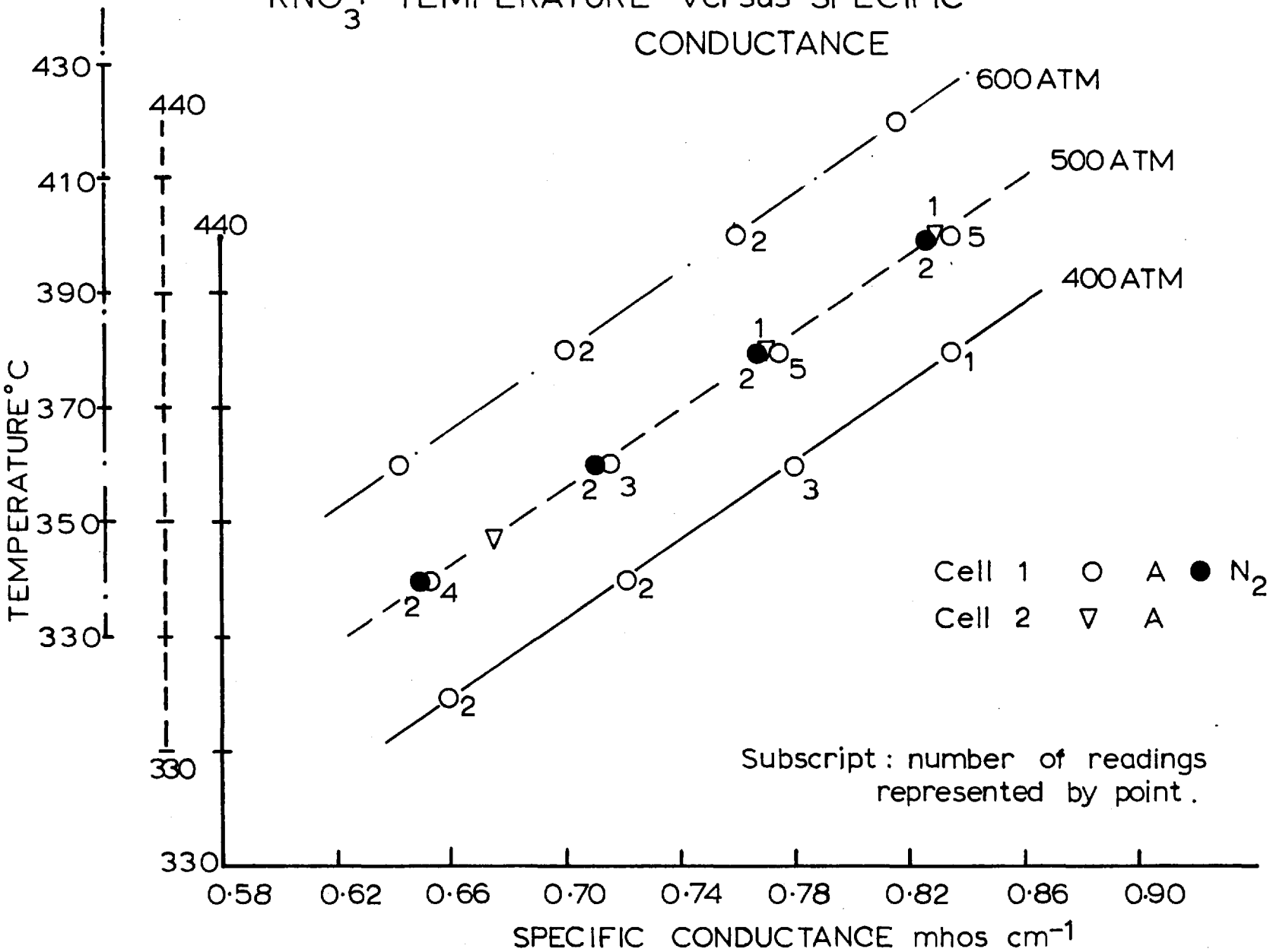
b) CONDUCTANCE MEASUREMENTS

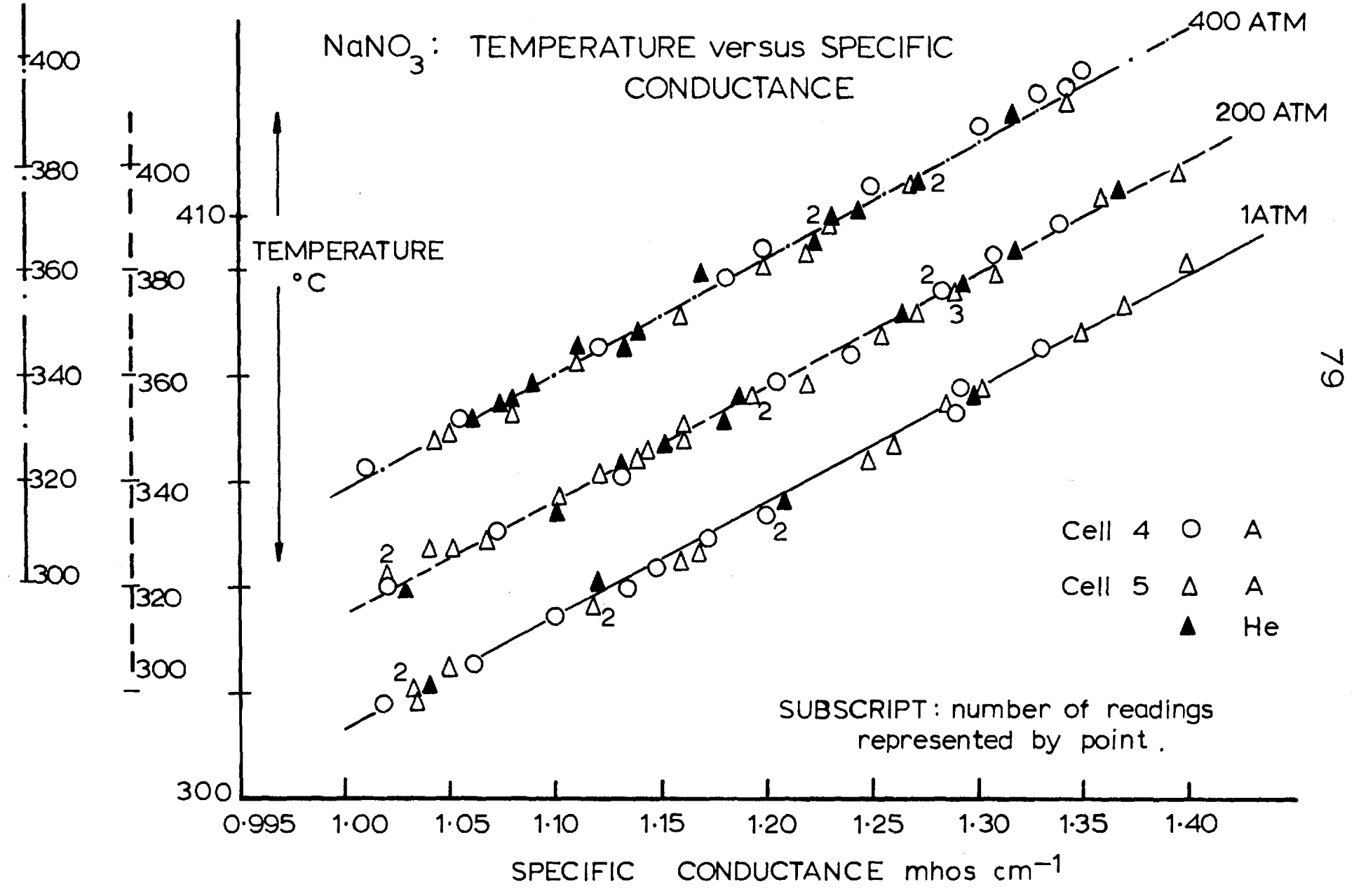
An empty cell was placed in the bomb and taken up to 500°C and 1000 atm. The conductance remained constant at 0.6×10^{-6} mhos throughout the run.

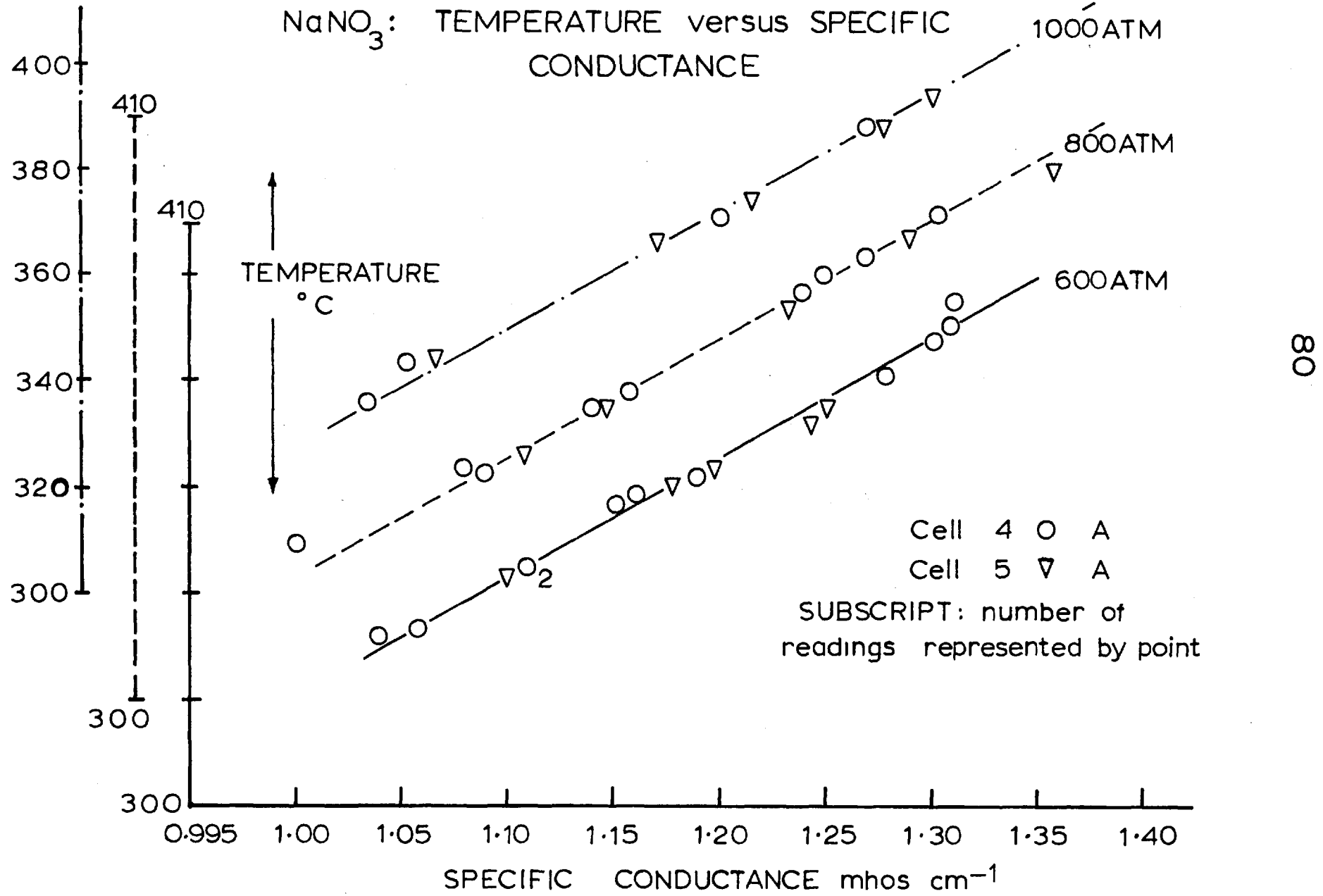
The graphs on pages 76 to 80 show temperature versus specific conductance at various pressure of argon, heli um or nitrogen for pure potassium and sodium nitrates. The results show that the conductance appears to be independent of the pressurising gas.


KNO3: TEMPERATURE versus SPECIFIC CONDUCTANCE
300 ATM
200 ATM
100 ATM
1 ATM
Cell 1 O A ● N2
Cell 2 ▽ A
Cell 3 □ A ■ He
SUBSCRIPT: number of readings represented by point.
TEMPERATURE °C
430
410
390
370
350
330
440
440
440
330
330
330
0·58
0·62
0·66
0·70
0·74
0·78
0·82
0·86
0·90
SPECIFIC CONDUCTANCE mhos cm-1


KNO3: TEMPERATURE versus SPECIFIC CONDUCTANCE
1000ATM
800ATM
700ATM
TEMPERATURE°C
430
410
390
370
350
330
440
440
330
330
0·58
0·62
0·66
0·70
0·74
0·78
0·82
0·86
0·90
SPECIFIC CONDUCTANCE mhos cm−1
Cell 1 O A ● N2
Cell 2 ▽ A
Subscript: number of readings represented by point.


KNO3: TEMPERATURE versus SPECIFIC CONDUCTANCE
600 ATM
500 ATM
400 ATM
TEMPERATURE °C
430
410
390
370
350
330
440
440
330
330
0·58
0·62
0·66
0·70
0·74
0·78
0·82
0·86
0·90
SPECIFIC CONDUCTANCE mhos cm⁻¹
Cell 1 O A ● N2
Cell 2 ▽ A
Subscript : number of readings represented by point.


NaNO3: TEMPERATURE versus SPECIFIC CONDUCTANCE
400 ATM
200 ATM
1ATM
TEMPERATURE °C
400
380
360
340
320
300
410
Cell 4 O A
Cell 5 Δ A
▲ He
SUBSCRIPT: number of readings represented by point.
0·995
1·00
1·05
1·10
1·15
1·20
1·25
1·30
1·35
1·40
SPECIFIC CONDUCTANCE mhos cm⁻¹


NaNO3: TEMPERATURE versus SPECIFIC CONDUCTANCE
1000ATM
800ATM
600ATM
TEMPERATURE °C
400
380
360
340
320
300
410
410
300
300
0.995
1·00
1·05
1·10
1·15
1·20
1·25
1·30
1·35
1·40
SPECIFIC CONDUCTANCE mhos cm−1
Cell 4 O A
Cell 5 ∇ A
SUBSCRIPT: number of readings represented by point

3. VOLUME

a) CALIBRATION

The technique was calibrated by comparing the experimentally determined number of turns of the probe for a change in temperature from 20°C to 60°C with the calculated values for mercury. The values for the densities of mercury were taken from the rubber book (123). The results are shown in table 3.2

TABLE 3.2

Calibration of Dilatometers with Mercury

Dilatometer Number	Weight Hg gm	Number of Turns Observed	Number of Turns Calculated
7	9.6031	16.1	16.0266
8	8.4728	14.1	14.1446
9	9.2153	15.4	15.3490

The values do not correspond exactly due to the fact that the level of the mercury could only be detected within 0.1 turn. Therefore, the observed and calculated values agree within the limits of experimental error.

b) CORRECTION

The bomb extended longitudinally with pressure. The corrections for this are shown in table 3.3.

TABLE 3.3

Extension of Bomb under Pressure

Pressure	Probe Position in Number of Turns	
atm.	Run 1	Run 2
1	0	0
100	—	0.1
200	—	0.2
300	0.35	0.25
500	0.45	0.4
700	0.75	0.7
1000	0.9	0.8

The runs were separated by a period of 6 months and as the results corresponded within the limits of detection it was concluded that the extension did not alter with use. These corrections represent about 4% of the actual decrease in the volume of the salt for the same pressure increment.

c) VOLUME READINGS

The weights of salt in the dilatometers are shown in table 3.3

TABLE 3.3

Weights of salt in the dilatometers

Salt	Dilatometer Number	Weight gm.
KNO_3	1	1.9390
	2	0.9712
	3	1.4101
	4	1.7690
$NaNO_3$	5	1.3196
	6	1.5037

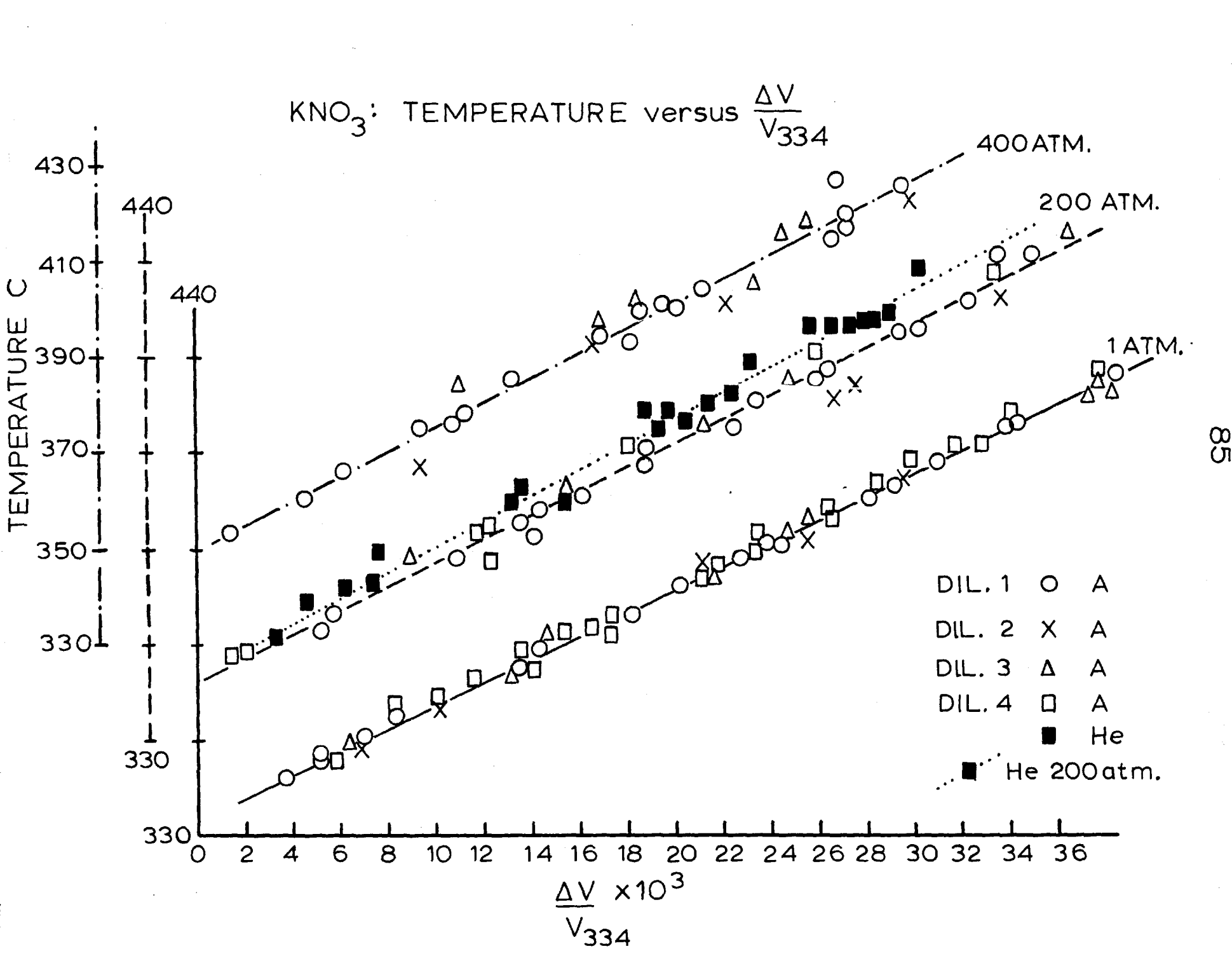
After correcting the probe positions, the values of ΔV were calculated knowing that one rotation of the "Magslip" altered the position of the probe by 1/80" and the capillary was 1.5mm precision bore.

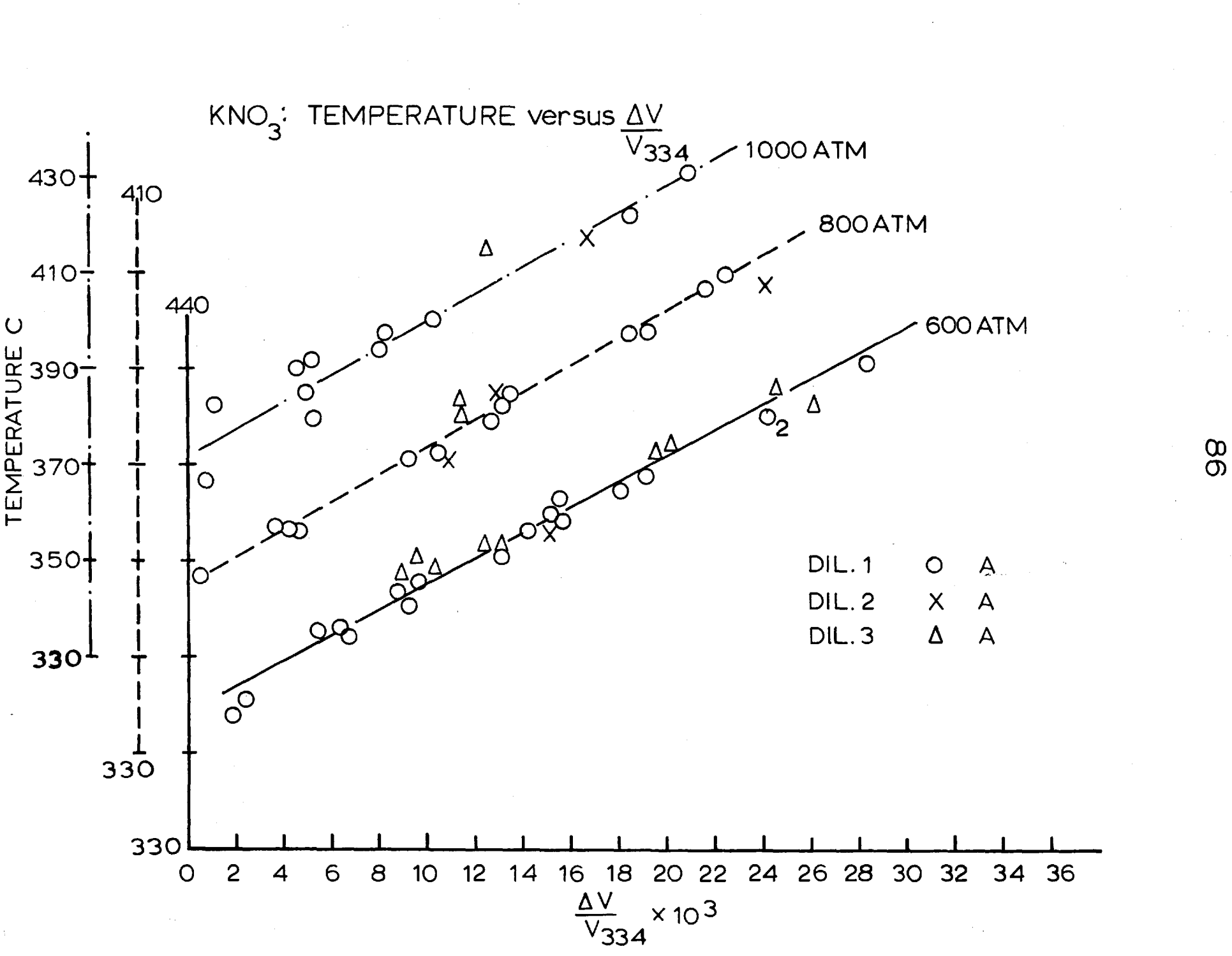
The"Magslips" were completely in phase and there was no slack in the 2.1 reduction gear. The thread on the probe was accurately machined to 40 t.p.i. in the department's workshop. The thread and the bore were correct within the limits of

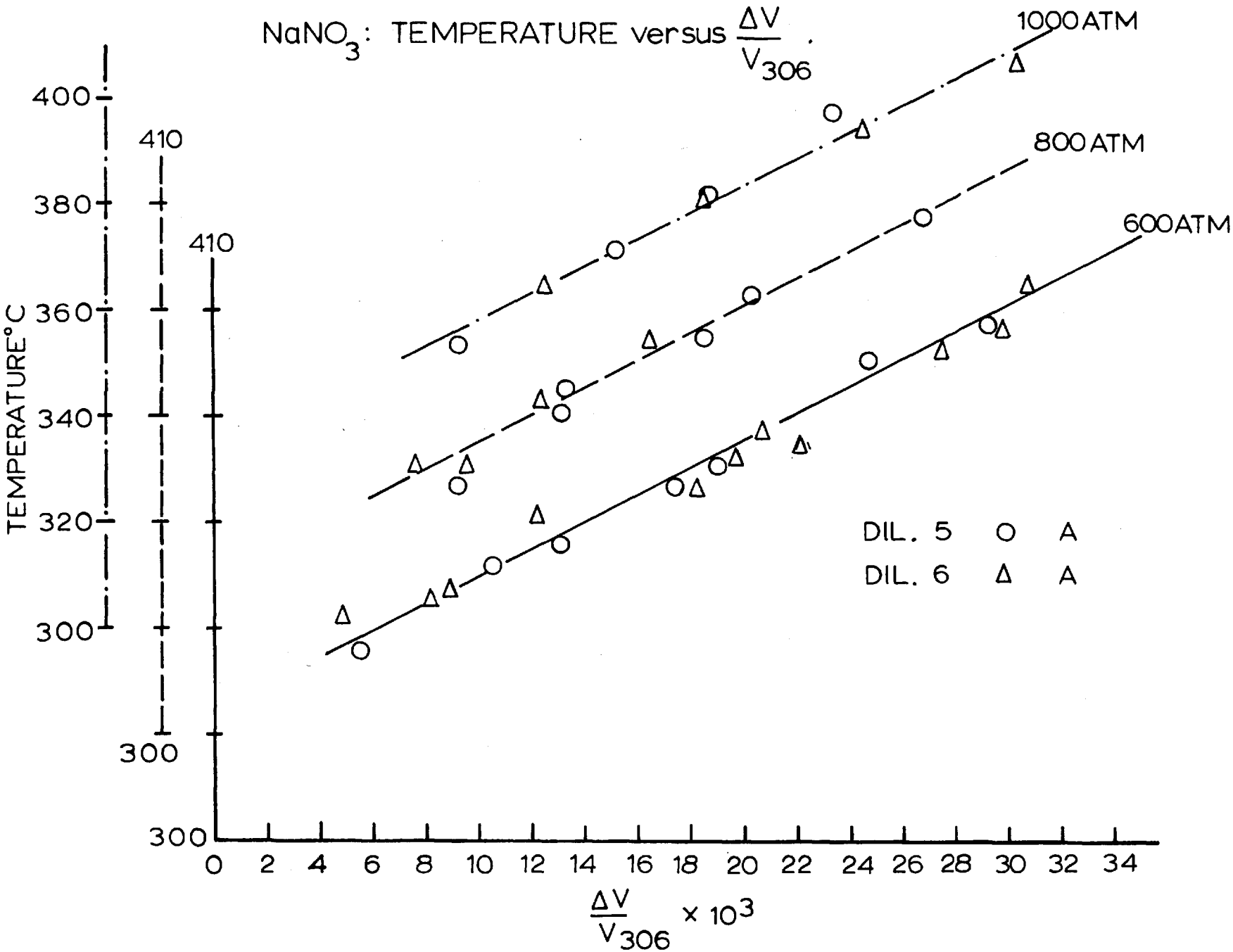
experimental error as was shown by the mercury calibration. The bore of the capillary was further checked by measuring the length of a boad of mercury in the tubing with a travelling microscope and then weighing the bead. The bore was 1.5mm ± 0.002 mm which would result in an error of ± 0.05% on the volume reading. From the mass of salt, the volume at the melting point was calculated from the equation which gave the best fit to the data. The selection of this equation is examined fully in the discussion of the results. The temperature was plotted against $\Delta V/V_{m.p.}$ for all the dilatometers and the graphs are shown on pages 85 to 88. It should be observed that there was a larger volume change with pressure with helium than with argon.

4. ANALYSIS

The method used for analysing the salt was described on page 66 in the experimental section. The sections are shown in table 3.4.


KNO3: TEMPERATURE versus ΔV/V334
400ATM.
200 ATM.
1ATM.
TEMPERATURE C
430
410
390
370
350
330
440
440
330
330
0 2 4 6 8 10 12 14 16 18 20 22 24 26 28 30 32 34 36
ΔV/V334 x10^3
DIL. 1 O A
DIL. 2 X A
DIL. 3 Δ A
DIL. 4 □ A
He
He 200atm.


KNO3: TEMPERATURE versus ΔV/V334
1000 ATM
800 ATM
600 ATM
DIL. 1 O A
DIL. 2 X A
DIL. 3 Δ A
TEMPERATURE C
430
410
390
370
350
330
440
410
330
330
0 2 4 6 8 10 12 14 16 18 20 22 24 26 28 30 32 34 36
ΔV/V334 x 10^3


NaNO3: TEMPERATURE versus ΔV/V306 .
1000ATM
800ATM
600ATM
DIL. 5 O A
DIL. 6 Δ A
TEMPERATURE°C
400
380
360
340
320
300
410
410
300
300
0 2 4 6 8 10 12 14 16 18 20 22 24 26 28 30 32 34
ΔV/V306 x 10³

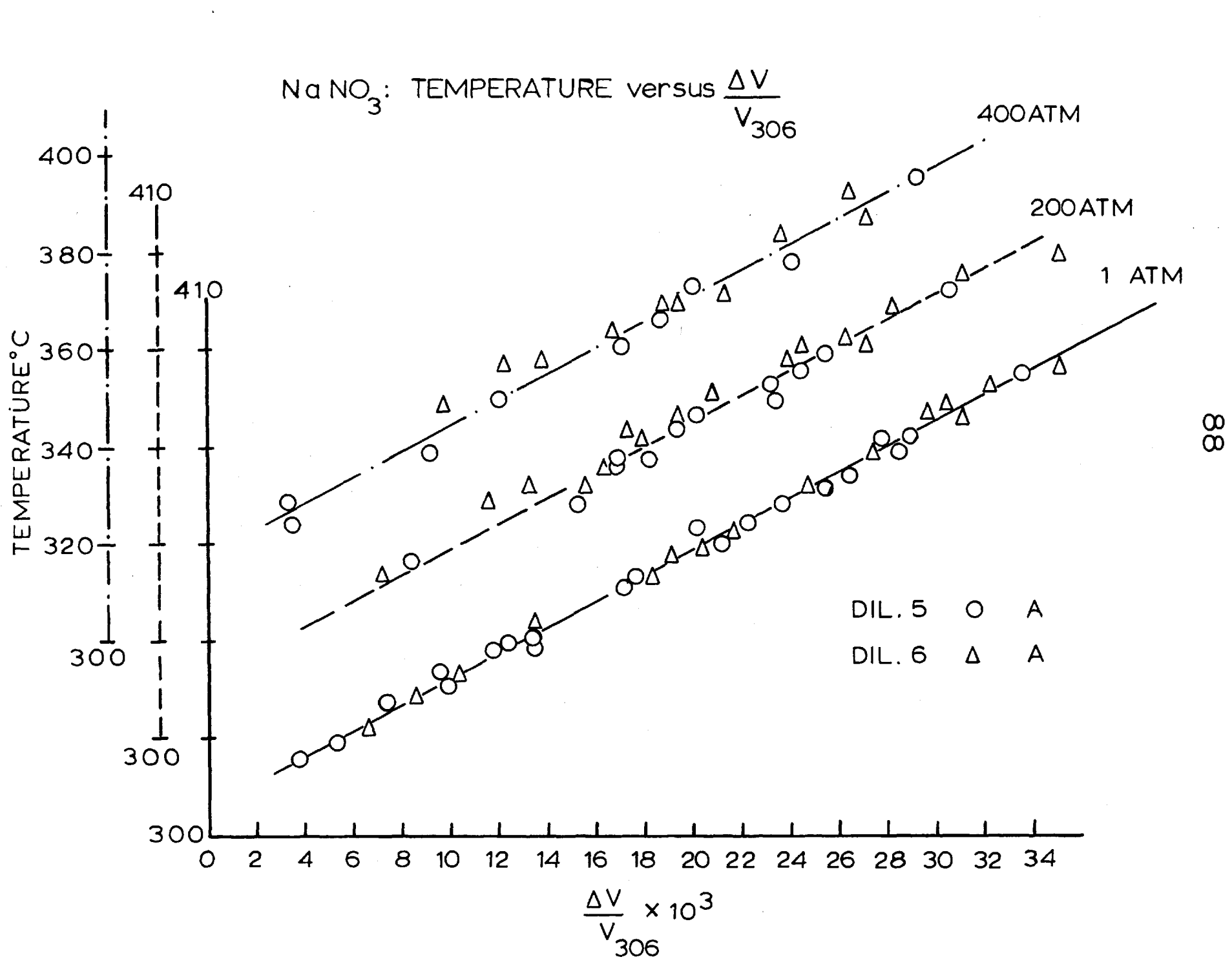

NaNO3: TEMPERATURE versus ΔV/V306
400ATM
200ATM
1 ATM
DIL. 5 O A
DIL. 6 Δ A
TEMPERATURE °C
400
380
360
340
320
300
410
410
300
300
0 2 4 6 8 10 12 14 16 18 20 22 24 26 28 30 32 34
ΔV/V306 x 10^3
88

TABLE 3.4

Analysis of Melts

Salt		% Nitrite
KNO_3	Salt from bottle	-
	Salt from filling bath	-
	Cell 1	0.48
	Cell 3	0.86
	Dil. 4	0.30
$NaNO_3$	Salt from bottle	-
	Salt from filling bath	-
	Cell 4	1.8
	Cell 5	1.6
	Dil. 6	1.9

From the table it is seen that sodium nitrate decomposes more than potassium nitrate, but in neither case does the percentage exceed 2%. This is discussed more fully in the next section.

5. CALIBRATION OF PRESSURE GAUGE

The 1500 atm. gauge calibration is shown in table 3.5.

TABLE 3.5

Pressure Gauge Calibration

True Pressure	Gauge Readings in Atm.			
Atm.	Run 1	Run 2	Run 3	Average
100	98	99	99	99
200	200	199	199	199
300	300	299	299	299
400	400	398	399	399
500	499	498	498	498
600	599	598	598	598
700	798	697	698	698
800	798	797	797	797
900	897	875	897	897
1000	997	995	997	997

Although the manufacturers give the error as $\pm$ 0.1% scale deflection it is seen that accuracy is better than this and the reproducibility is within $\pm$ 1 atm.

C EXPERIMENTAL ERRORS

a) CONDUCTIVITY

The cell constant was measured to within ± 0.2%. Chromel-alumel thermocouples were used which were frequently tested by comparing them with a standard thermocouple. The potentiometer could be read within 0.002mm or 0.04°C and the temperature was controlled within ±½°C. A change of ½°C alters the conductance by 0.2%. The conductance was measured on a Pye bridge, which was calibrated with standard resistances, and could be read to within 0.2%. The pressure gauges were calibrated against a precision balance and could be read to within 5 atm, which alters the conductance by 0.05%. The total error for each conductance reading is ±0.5%. The reproducibility was found to be within ±1% indicating that the calculated reproducibility agrees with that experimentally observed.

b) VOLUME

The liquid level could be detected to within ±0.25 turn. Each dilatometer was calib rated by comparing the coefficients of expansion of the salt in the dilatometer with that in the literature. Agreement was within the experimental error of 3%

on ΔV. The temperature control was as before and a change of $\pm\frac{1}{2}^{o}C$ alters the probe by ± 0.3 turn and, therefore, each reading is accurate to ± 0.5 turns. The effect of the error due to the pressure is negligible. This gives a $\pm$ 0.3% error on the volume and $\pm$ 1 turn of the volume changes. This results in an error of $\pm 1 \times 10^{3}$ for $\Delta V/V_{ref}$ which is the experimentally observed reproducibility.

C H A P T E R 4

DISCUSSION OF RESULTS.

1. CONDUCTIVITIES

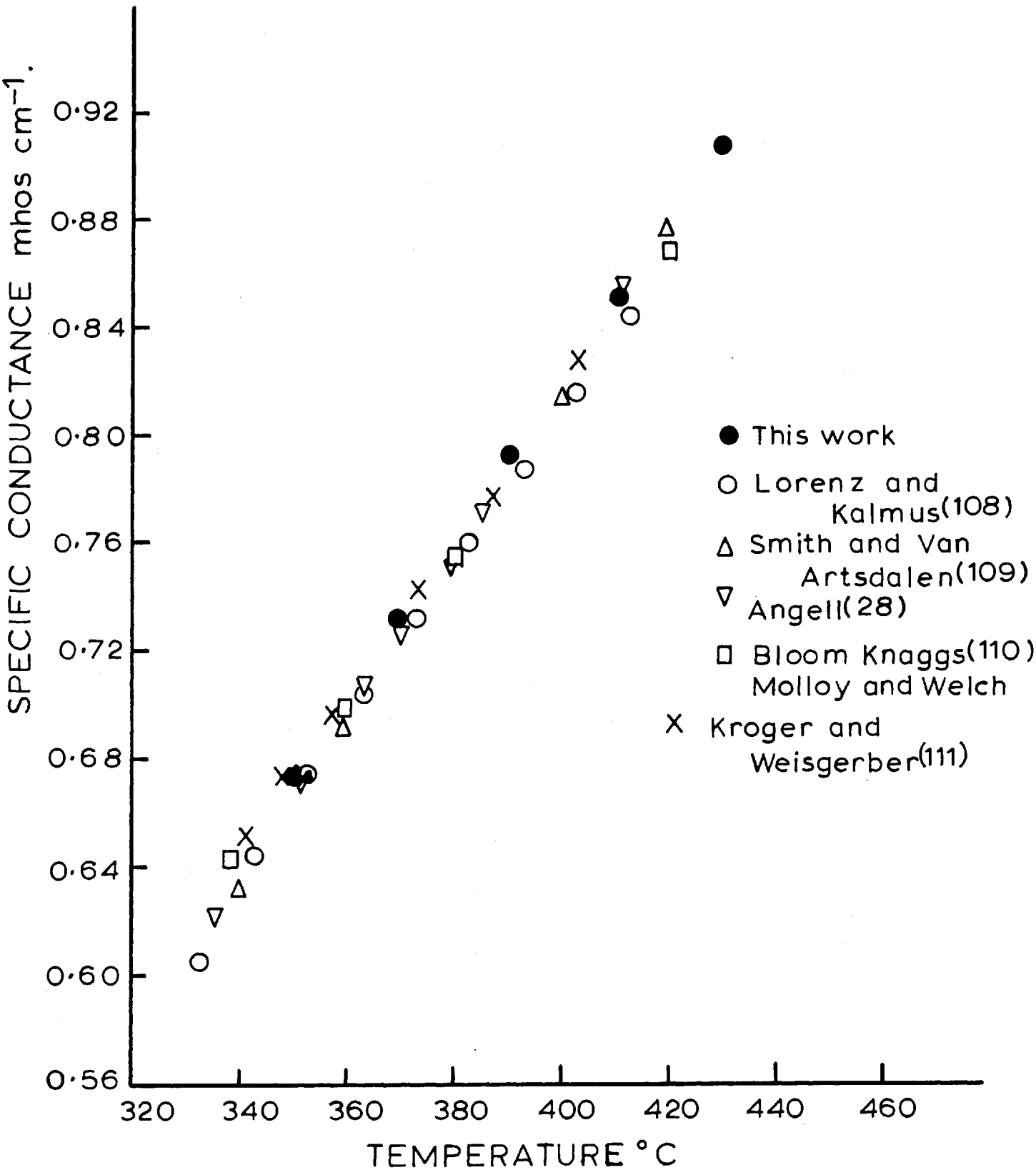
a) COMPARISON WITH OTHER WORK

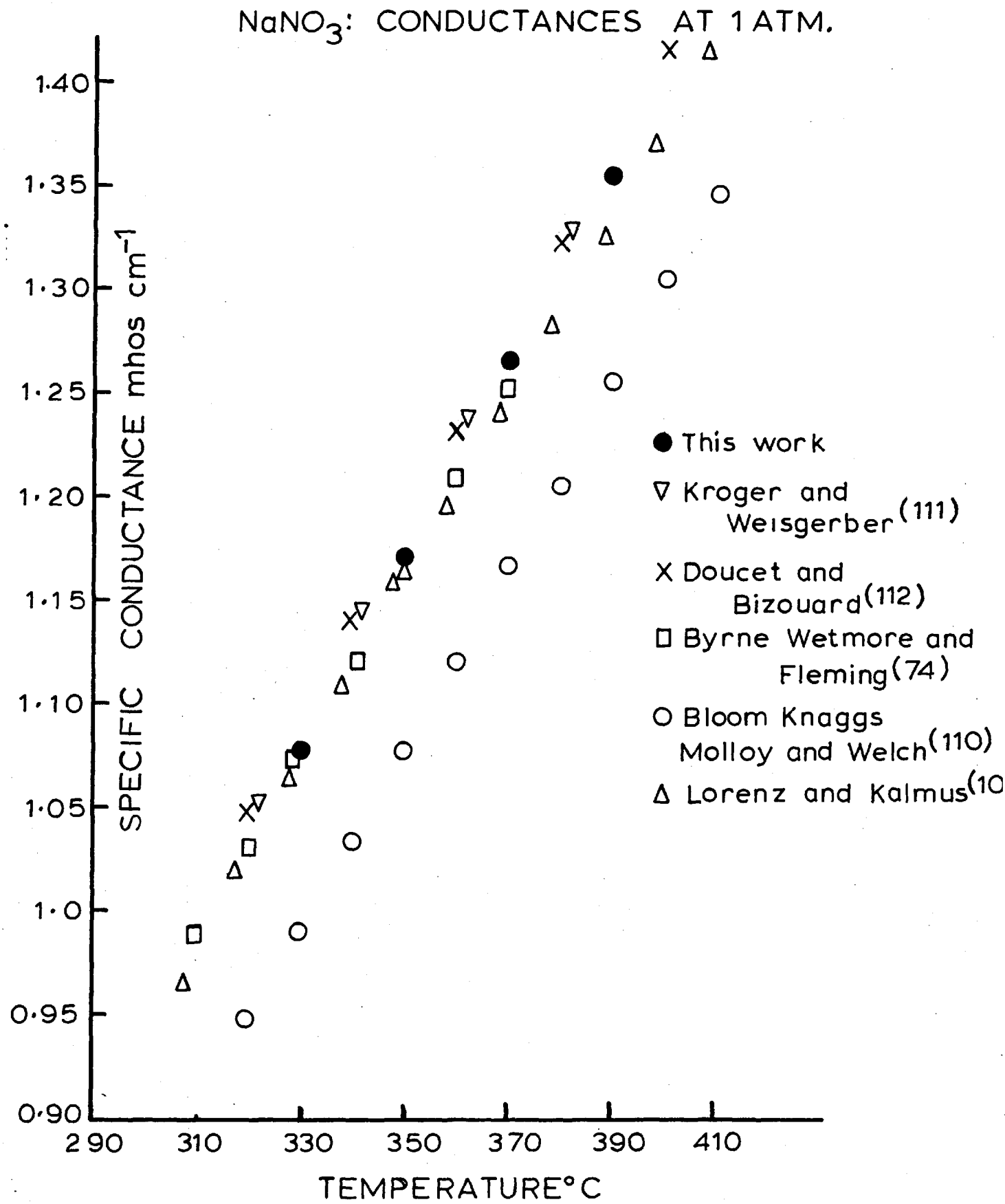
The graphs on pages95 and 96 show the values of specific conductance determined in this investigation compared to other work at 1 atm. For potassium nitrate the results found in this work agree with the other determinations with ½%. In the case of sodium nitrate the results again agree within ½% with most of the other determinations. The results of Bloom, Knaggs, Molloy and Welch appear to be in error.

In the case of sodium nitrate, Copeland and Zybko [48] have determined the specific conductance at 362 atm. of argon and 369°C. A change in conductance of 5.7% was obtained which is 2% more than the change observed in this work. As no detailed description of their apparatus is available, the experimental method cannot be criticised. However, not much reliability can be attached to a single determination.

It should be noted that the conductance of the salt is independent of the pressurising gas within the limits of experimental error. This is important as it shows that conduction is not affected by the amount of dissolved gas as helium dissolves much

KNO_3: CONDUCTANCES AT 1 ATM.




NaNO3: CONDUCTANCES AT 1 ATM.
SPECIFIC CONDUCTANCE mhos cm-1
1·40
1·35
1·30
1·25
1·20
1·15
1·10
1·05
1·0
0·95
0·90
290
310
330
350
370
390
410
TEMPERATURE°C
This work
Kroger and Weisgerber (111)
Doucet and Bizouard (112)
Byrne Wetmore and Fleming (74)
Bloom Knaggs Molloy and Welch (110)
Lorenz and Kalmus (10

more than argon. The volume of dissolved argon at 1000 atm is 1% of the total volume of salt and of helium at 400 atm. it is about 2% of the volume of the salt. However, as will be shown later, the argon forms its own holes in the melt and therefore, does not decrease the available free space in the molten salt. In the case of helium, the atoms are extremely small and are unlikely to affect the motion of the ions.

b) ACTIVATION ENERGIES AT CONSTANT PRESSURE

The values of equivalent conductance were obtained by multiplying the specific conductance by the molar volumes.

The activation energy is given by

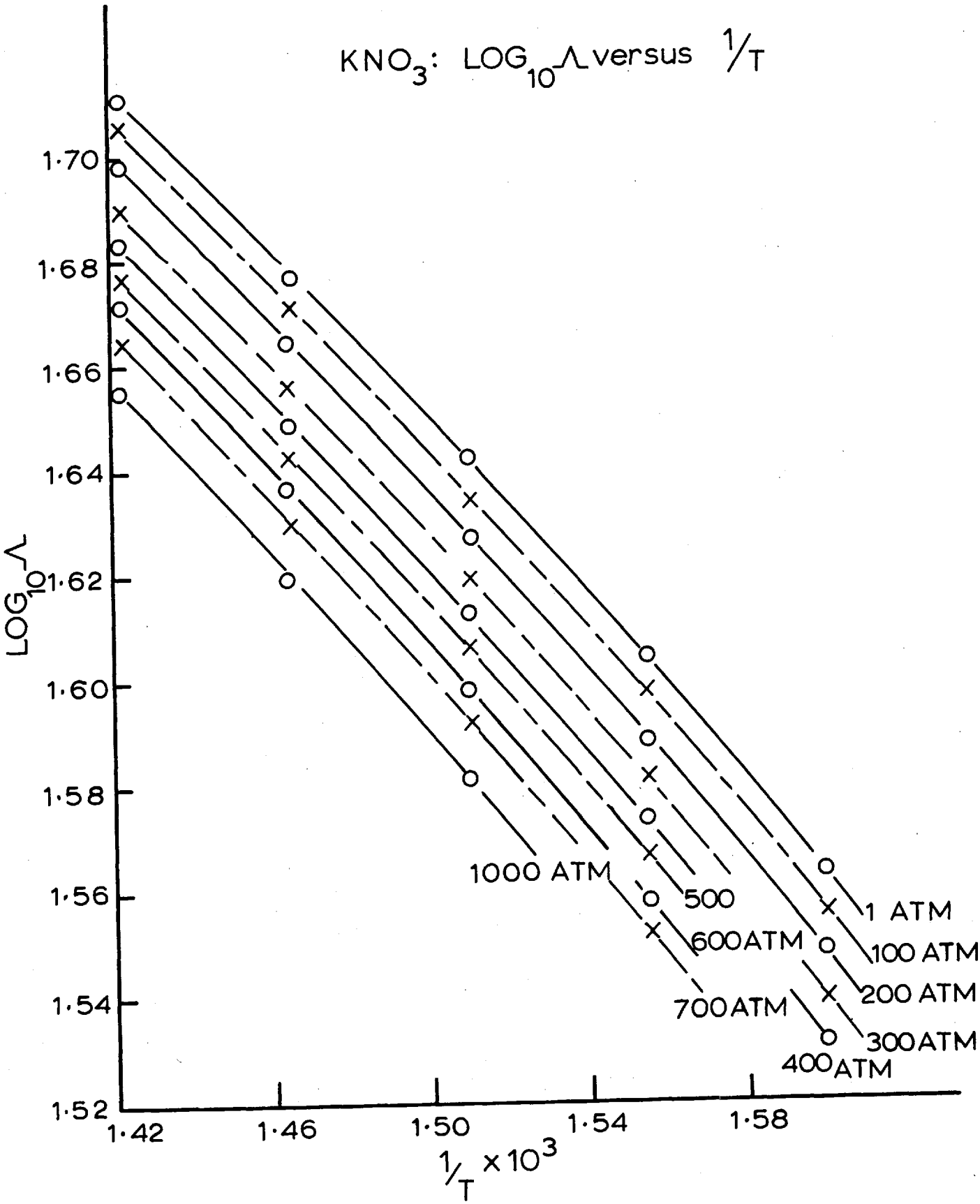
$$E_p = - R \frac{d \ln \Lambda}{d(1/T)} \qquad (4.1)$$

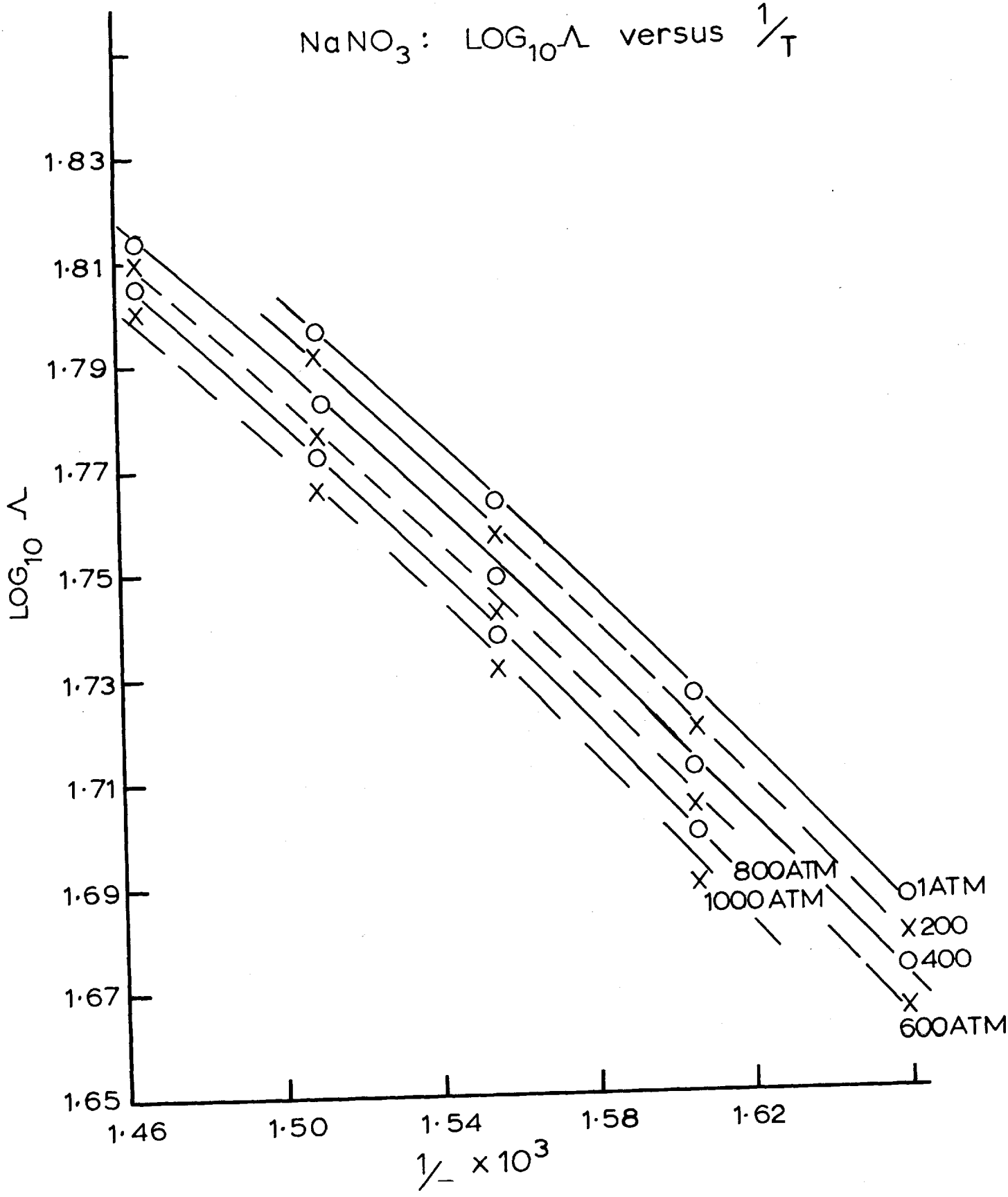
and plots of $\log_{10} \Lambda$ versus $(1/T)$ at various pressures are shown on pages 99 and 100. The activation energies obtained from these plots are shown in table 4.1.

TABLE 4.1

Activation Energies at Constant Pressure for KNO_3 and $NaNO_3$

Temperature °C	KNO_3 $(E\Lambda)_P$ Kcals (73) This Work	Cowen et al	$NaNO_3$ This Work	(74) Byrne et al
325	-	-	-	3.3
330	-	-	3.2	
345	-	-	-	3.2
350	4.1	3.9	3.1	
365	-	-	-	3.1
370	3.9	3.8	3.0	
390	3.7	3.7	2.9	
410	3.6	3.6	2.8	
430	3.5	3.6	-	


KNO3: LOG10Λ versus 1/T
1·70
1·68
1·66
1·64
1·62
1·60
1·58
1·56
1·54
1·52
LOG10Λ
1·42
1·46
1·50
1·54
1·58
1/T x 10^3
1 ATM
100 ATM
200 ATM
300ATM
400ATM
500
600ATM
700ATM
1000 ATM


NaNO3 : LOG10Λ versus 1/T
1·83
1·81
1·79
1·77
1·75
1·73
1·71
1·69
1·67
1·65
LOG10 Λ
1·46
1·50
1·54
1·58
1·62
1/T x 10^3
1ATM
200
400
600ATM
800ATM
1000 ATM

These values show the same trends as those of Cowen and Axon [73] for KNO_3 and Byrne, Fleming and Wetmore [74] for $NaNO_3$. As can be seen the values are in agreement within 0.2 Kcals. The change with temperature of $(E\Lambda)_P$ is more marked for KNO_3 than $NaNO_3$.

c) ACTIVATION VOLUMES

The activation volume is given by

$$\Delta V^* = - RT \left(\frac{\partial \ln \Lambda}{\partial P} \right)_T \qquad (4.2)$$

It is assumed that the jump distance does not alter with pressure as this distance is usually related to the interionic separation or the lattice parameter and there is no evidence that this alters with temperature or pressure.

Plots of $\log_{10} \Lambda$ versus pressure are shown on pages 103 and 104 and values of the activation volumes are given in tables 4.2 and 4.3.

TABLE 4.2

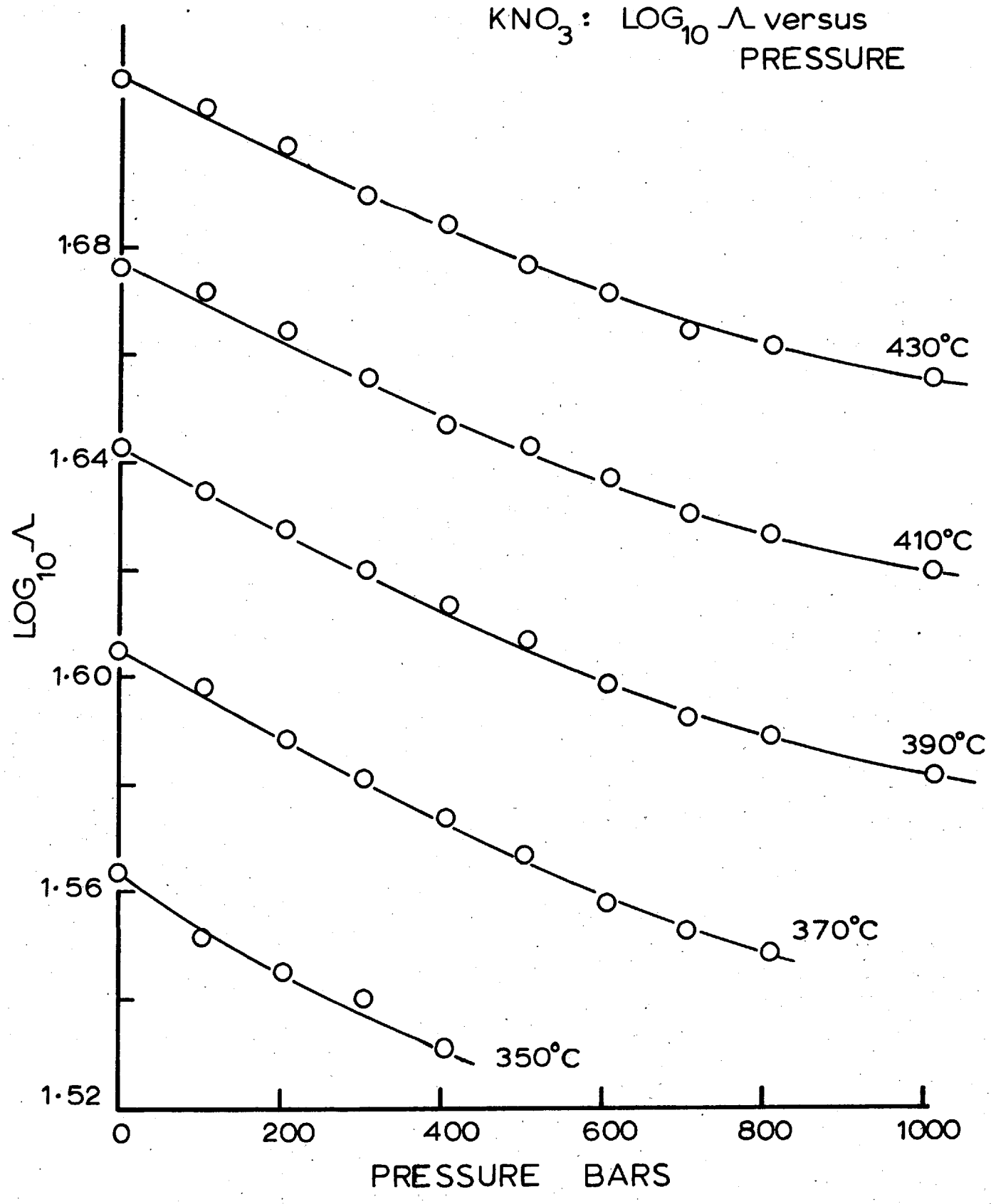
Activation Volumes of KNO_3

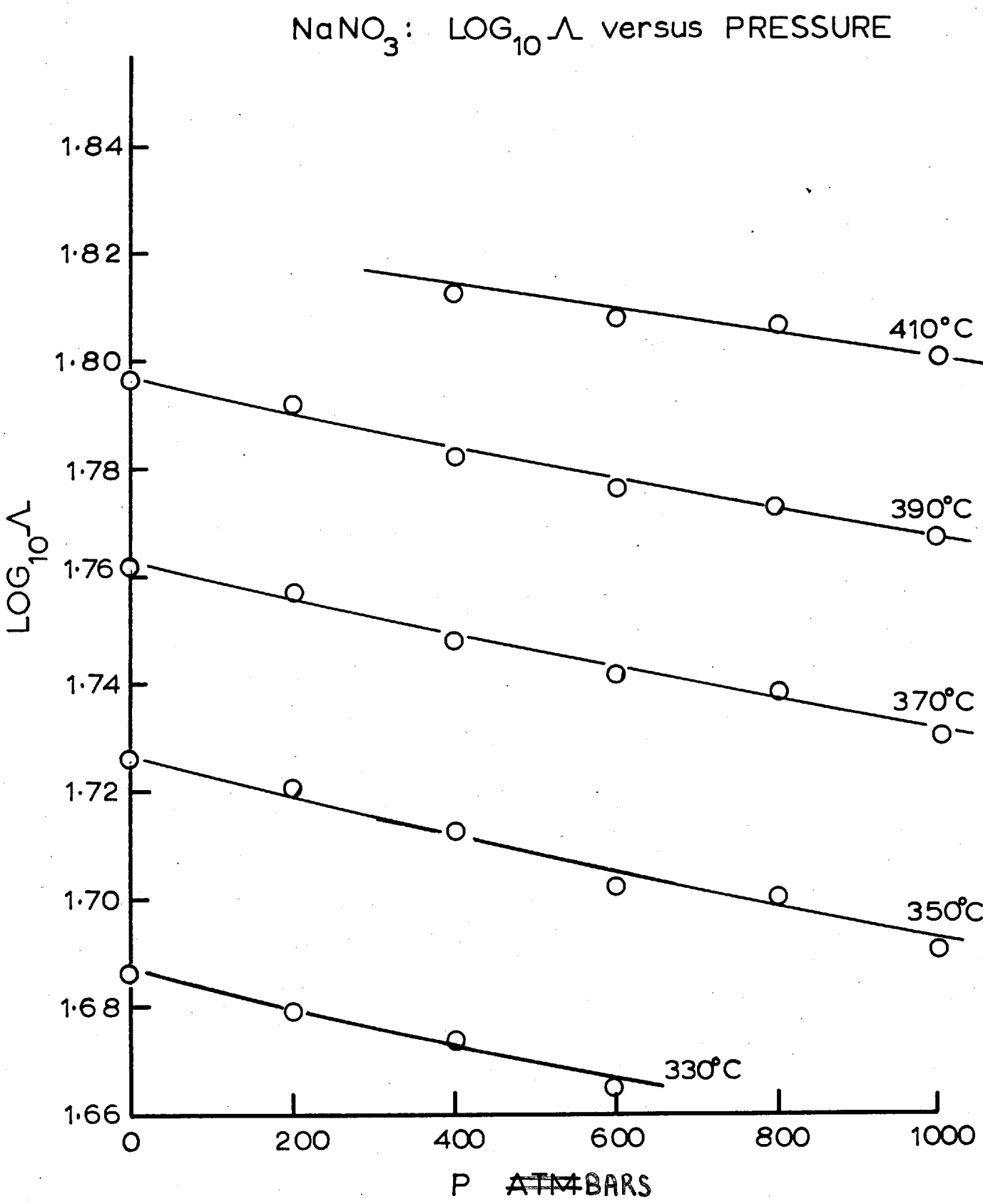
Pressure Atm.	Activation volumes in ML 370°C	390°C	410°C	430°C
100	9.5	9.5	9.3	9.7
300	9.2	9.3	8.8	8.8
500	8.1	8.4	7.7	7.8
700	7.0	5.8	5.7	6.6
900	-	3.9	4.1	5.1

TABLE 4.3

Activation Volumes of $NaNO_3$

Pressure Atm.	Activation volumes in Ml. 350°C	370°C	390°C
100	4.4	4.7	4.5
300	4.1	4.3	4.3
500	4.0	3.8	3.6
700	3.7	3.4	3.3
900	3.2	3.0	3.0


KNO3 : LOG10 Λ versus PRESSURE
1·68
1·64
1·60
1·56
1·52
LOG10 Λ
430°C
410°C
390°C
370°C
350°C
0
200
400
600
800
1000
PRESSURE BARS


NaNO3: LOG10 Λ versus PRESSURE
LOG10 Λ
1·84
1·82
1·80
1·78
1·76
1·74
1·72
1·70
1·68
1·66
410°C
390°C
370°C
350°C
330°C
0
200
400
600
800
1000
P ATM BARS

It is found that the activation volumes are positive which means that the system expands when the ion moves into the transition state. At one atmosphere, $\Delta V^{\ddagger}$ for KNO_3 is about 17% of the molar volume and for $NaNO_3$ it is 11%.

The plots show that for both salts the activation volume tends to decrease with increasing temperature and pressure. The change with pressure is considerably less for sodium nitrate than potassium nitrate and at high pressures the values of $\Delta V^{\ddagger}_{KNO_3}$ approach those of $\Delta V^{\ddagger}_{NaNO_3}$

2. VOLUMES

a) COMPARISON WITH OTHER WORK

The results obtained from the measurements are the mass of salt and the change of volume with temperature. Using the mass of salt, the volume change for a known temperature increment was calculated from the data in the literature and compared with the experimental value. The calculated and experimental values are shown in tables 4.4 and 4.5.

TABLE 4.4

Comparison of volume change for KNO_3 between 340°C and 430°C.

Dilatometer Number	Weight KNO_3 gm.	$\Delta V^{(110)}$	$\Delta V^{(109)}$	$\Delta V^{(114)}$	$\Delta V^{(115)}$	$\Delta V_{exp.}$
		ML x 10^2				
1	1.9390	3.661	3.98	4.13	3.92	3.86
2	0.9712	1.83	1.99	2.07	2.04	2.02
3	1.4101	2.66	2.89	3.0	2.88	2.89
4	1.7690	3.29	3.61	3.78	3.58	3.58

TABLE 4.5

Comparison of volume change for $NaNO_3$ between 320°C and 410°C

Dilatometer Number	Weight $NaNO_3$ gm.	$\Delta V^{(110)}$	$\Delta V^{(116)}$	$\Delta V^{(113)}$	$\Delta V_{exp.}$
		ML x 10^2			
5	1.3196	2.28	2.34	2.34	2.35
6	1.5037	2.60	2.66	2.69	2.70

References:-

(109) Smith and Van Artsdalen.

(110) Bloom, Knaggs, Molloy and Welch.

(113) Byrne, Fleming and Wetmore.

(114) Datuma.

(115) Papaioannou and Harrington.

(116) Lorenz and Frei.

Within the experimental error, the present result for KNO_3 agree with the data of Smith and Van Artsdalen[109] and for $NaNO_3$ with the data of Byrne, Fleming and Wetmore[113] and Lorenz and Frei[116].

3. COMPRESSIBILITIES

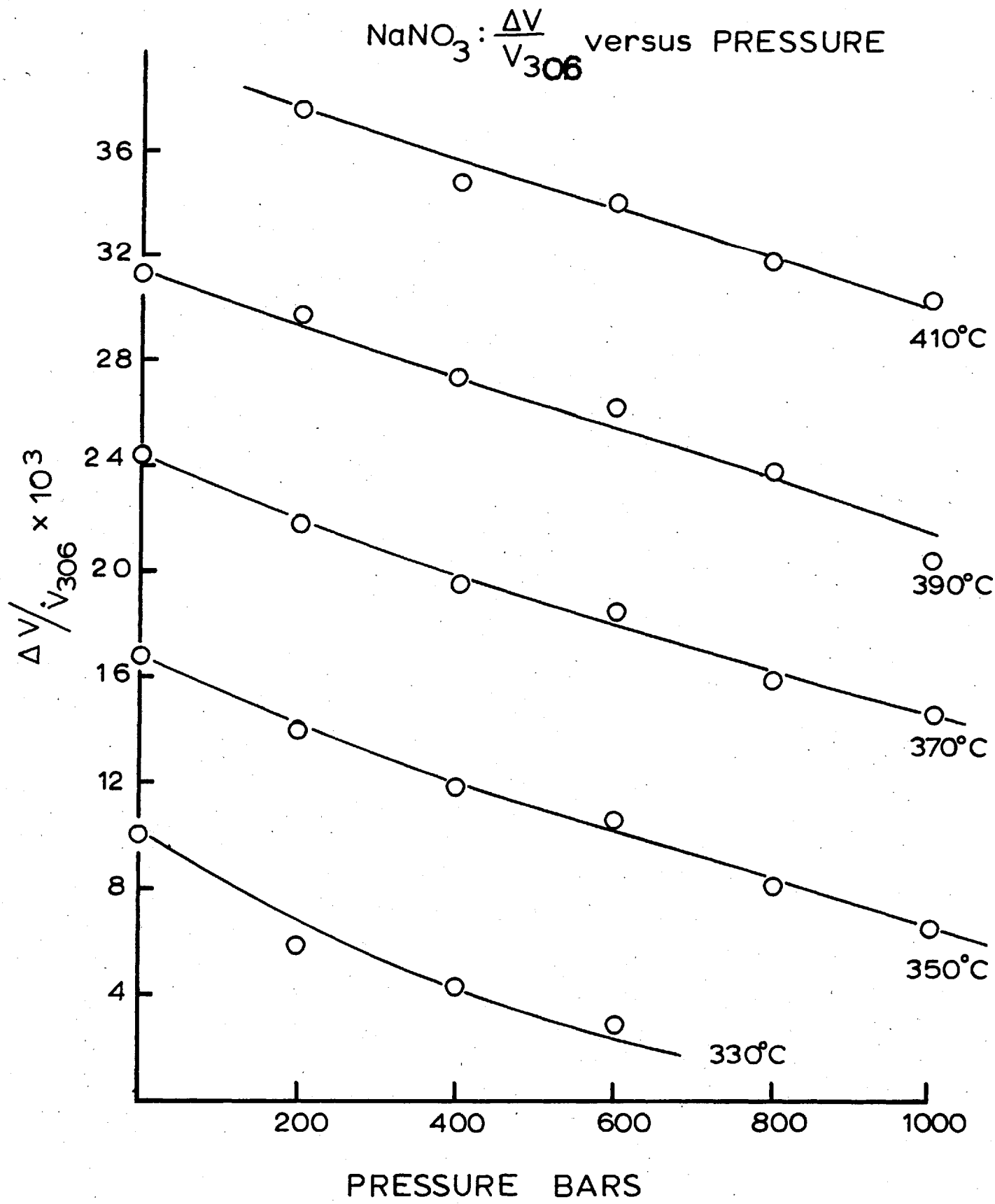
Graphs were drawn of $\frac{\Delta V}{V\ ref}$ versus pressure at constant temperature and these are shown on pages 108 and 109. Tangents drawn to the isotherms give the compressibility in the form,

$$\beta_T = -\frac{1}{Vref}\left(\frac{\partial V}{\partial P}\right)_T \qquad (4.3)$$

These values must be multiplied by $\frac{Vref}{Vo}$, where Vo is the volume of the salt in question at the temperature and atmospheric pressure, to obtain the compressibilities in their more normal form:-

$$\beta_T = -\frac{1}{Vo}\left(\frac{\partial V}{\partial P}\right)_T \qquad (4.4)$$

The values of the compressibility are tabulated in tables 4.6 and 4.7 and are plotted against pressure on pages 111 and 112. The value of the compressibility derived from the helium run was not included in the tabulation but is discussed later in this section.


NaNO3 : ΔV/V306 versus PRESSURE
ΔV/V306 x 10^3
36
32
28
24
20
16
12
8
4
410°C
390°C
370°C
350°C
330°C
200
400
600
800
1000
PRESSURE BARS

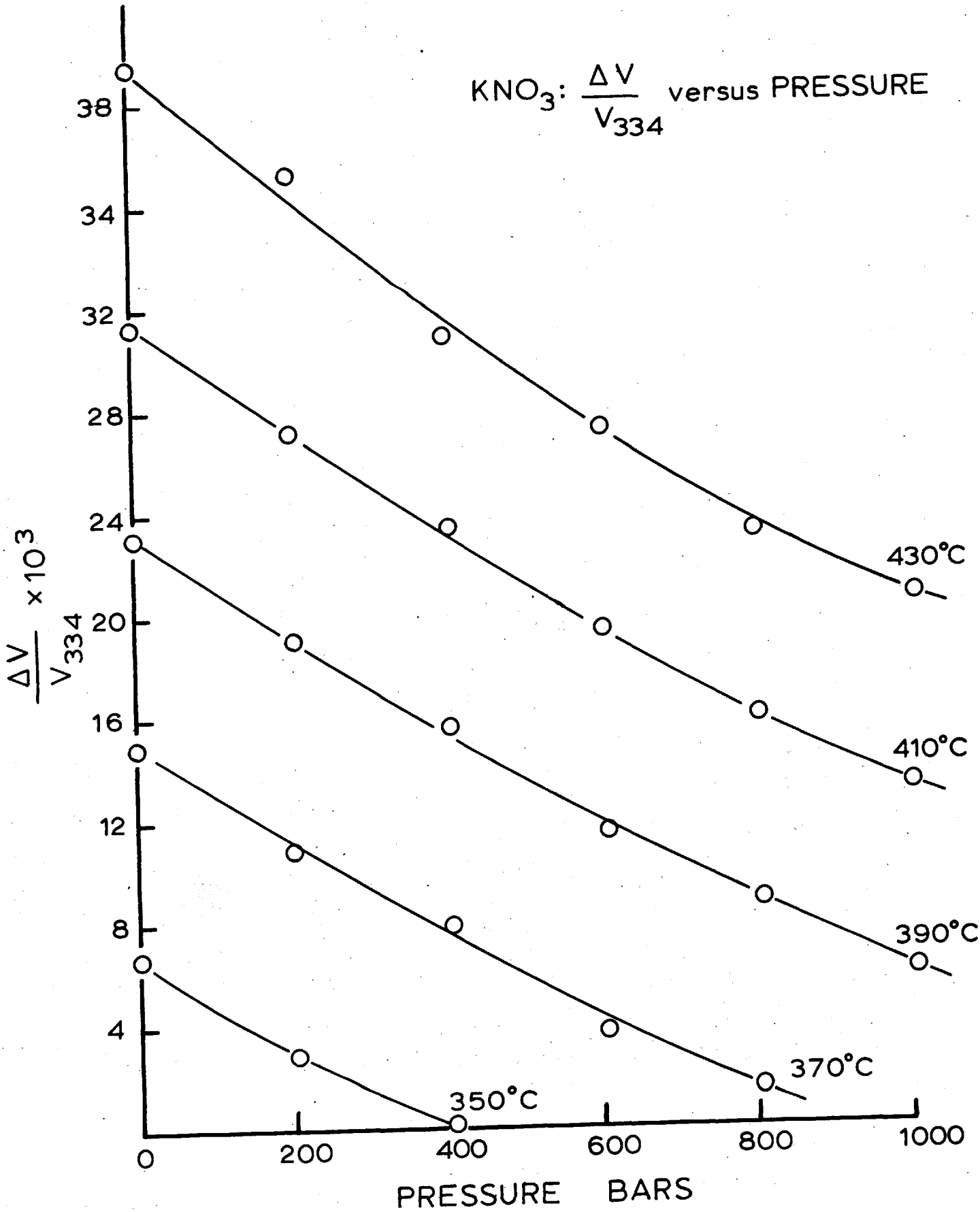

KNO3: ΔV/V334 versus PRESSURE
ΔV/V334 x10^3
38
34
32
28
24
20
16
12
8
4
430°C
410°C
390°C
370°C
350°C
0
200
400
600
800
1000
PRESSURE BARS

TABLE 4.6

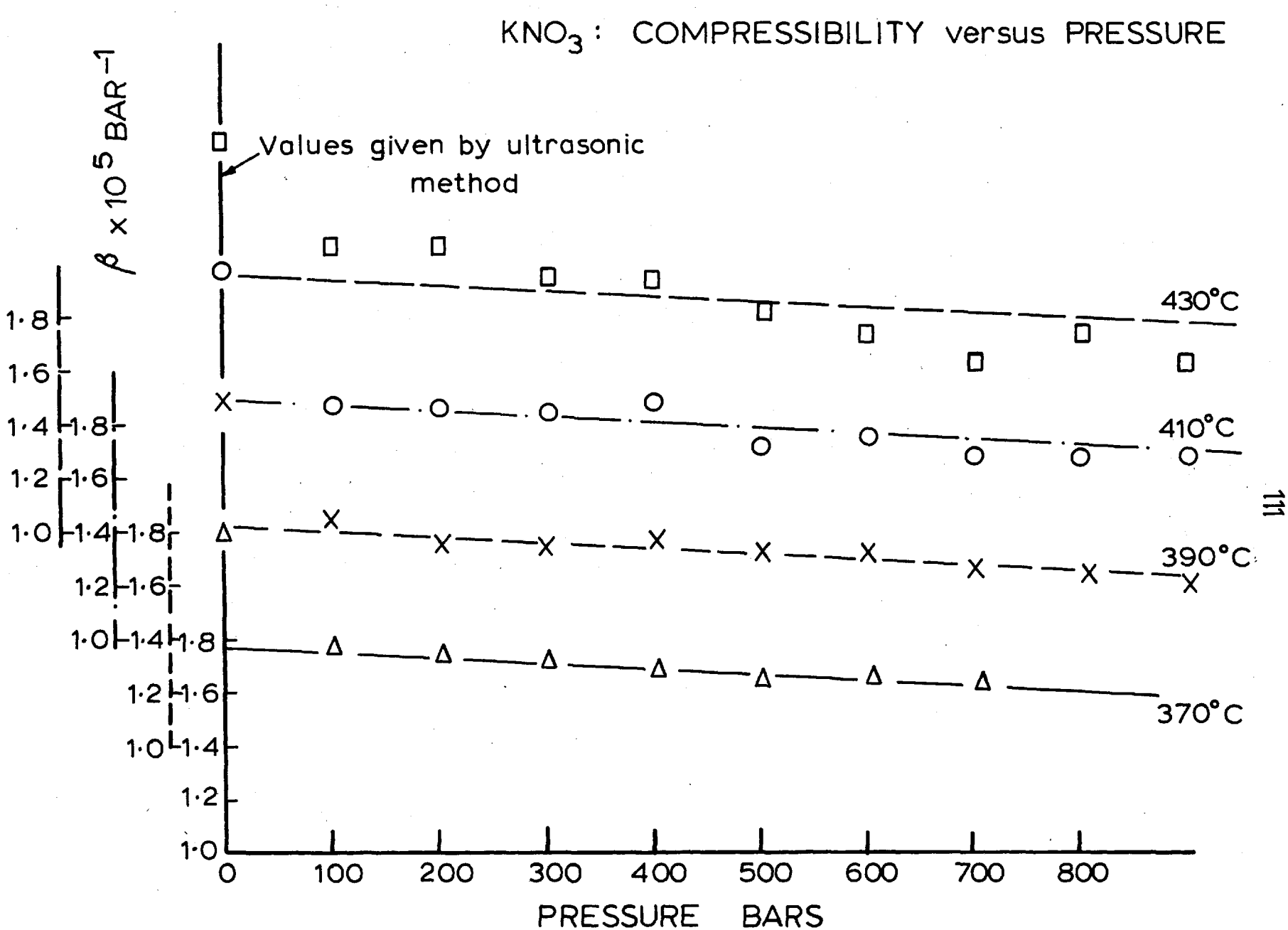
Compressibility of Potassium Nitrate.

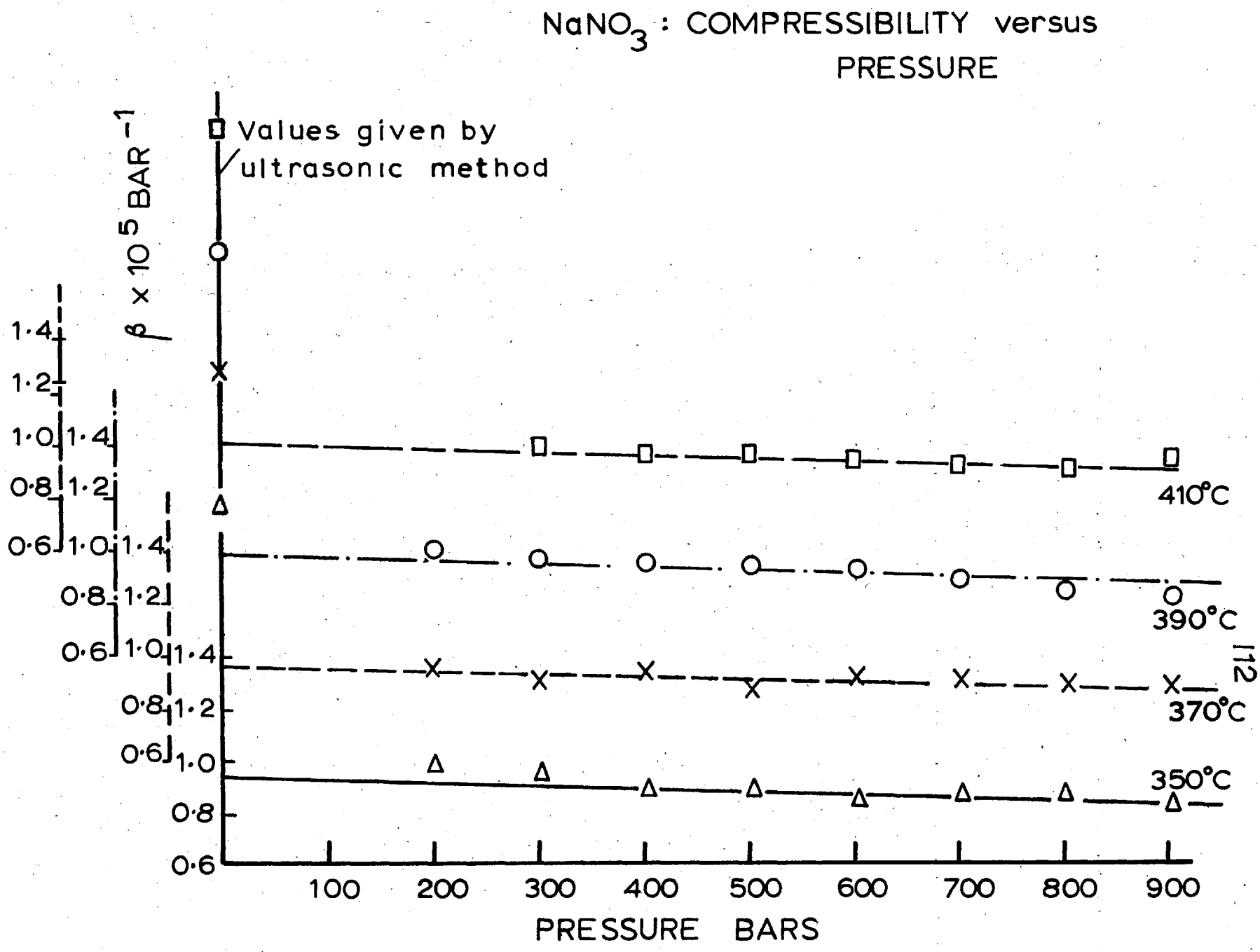
Pressure BARS	β_{370}	β_{390}	β_{410}	β_{430}
		$BARS^{-1} \times 10^5$		
101	1.78	1,86	1.88	2.08
203	1,75	1.76	1.87	2.06
304	1.71	1.75	1.85	1.95
405	1.68	1.77	1,88	1.93
507	1.64	1.73	1.73	1.82
608	1,66	1.73	1.77	1.74
709	1.63	1.68	1.68	1.63
810	-	1.65	1.68	1.75
911	-	1.62	1.68	1.63

TABLE 4.7

Compressibility of Sodium Nitrate

Pressure BARS	β_{350}	β_{370}	β_{390}	β_{410}
		$BARS^{-1} \times 10^5$		
203	0,97	0,94	0,99	0,99
304	0,93	0,89	0,96	0,96
405	0,88	0,93	0,94	0,96
507	0,83	0,87	0,93	0,94
608	0,88	0,91	0,91	0,94
709	0,86	0,89	0,89	0,90
810	0,86	0,87	0,86	0,89
911	0,84	0,87	0,82	0,92


KNO3 : COMPRESSIBILITY versus PRESSURE
β x 10^5 BAR^-1
Values given by ultrasonic method
430°C
410°C
390°C
370°C
1·8
1·6
1·4
1·2
1·0
0
100
200
300
400
500
600
700
800
PRESSURE BARS


$NaNO_3$: COMPRESSIBILITY versus PRESSURE
Values given by ultrasonic method
$\beta \times 10^5$ BAR^{-1}
1·4
1·2
1·0
0·8
0·6
410°C
390°C
370°C
350°C
100
200
300
400
500
600
700
800
900
PRESSURE BARS
112

It is seen that the compressibility increases with temperature and decreases with pressure. However, when the compressibilities are extrapolated back to atmospheric pressure, it is seen that the valves are considerably lower than those found by the ultrasonic method. The values shown in table 4.8 are slightly different from those of Bockris and Richards[1] because the compressibilities have been recalculated using the volumes found in this work and the ultrasonic velocities of Higgs and Litovitz[69]. However, both sets of values are the same if the experimental errors are considered.

TABLE 4.8

Values of the compressibility determined by the ultrasonic method.

Salt	Temperature °C	Compressibility Bars $^{-1}$ x 10^{-5}
KNO_3	370	2.28
	390	2.36
	410	2.41
	430	2.53
$NaNO_3$	350	1.96
	370	2.03
	390	2.10
	410	2.17

The reason why the data obtained in this work are so much lower than expected could be due to a rapid decrease of the compressibility with pressure in the first hundred atmospheres. The change of volume of both associated and non-associated liquids, with pressure can be represented by the Tait equation:-

$$\frac{\Delta V}{Vo} = C \log \left(\frac{B + P}{B + Po} \right) \qquad (4.5)$$

where C and B are constants, P is the pressure, and Po is the pressure at volume Vo.

$$\frac{\Delta V}{V_o} = C \log (B + P) - \log (B + Po) \qquad (4.6)$$

$$\therefore \beta = \frac{-1}{Vo} \left(\frac{\partial V}{\partial P} \right) = \frac{-C}{B + P} \qquad (4.7)$$

From the discussion in chapter 5 it is to be expected that the Tait equation will apply to molten salts, in which case a large compressibility change in the first hundred atmosphere is unlikely. The compressibility will certainly decrease smoothly with increase of pressure. As the pressure dependence of the experimental compressibility appears to be as expected, the method of calculation used by Bockris and Richards[1] will be examined. The equation used to obtain the compressibility was derived

from equations (1.14) and (1.15) and is given by:-

$$\beta_T = V\left[\frac{1}{U_L^2 M} + \frac{\alpha^2 T}{C_p}\right] \qquad (4.8)$$

where V is the molar volume, U_L is the ultrasonic velocity, α is the coefficient of expansion and C_p is the specific heat at constant pressure. Higgs and Litovitz [69] redetermined the ultrasonic velocities, and found close agreement. All the other terms are accurately known except for C_p. Although this has been determined twice for $NaNO_3$ [117] and three times for KNO_3 [117], the data are not recent and are somewhat in doubt so that C_p is probably only accurate to within ±10%. However, the second term in the bracket is about 1/5th of the first term so that any error in the C_p has a reduced effect on the compressibility and it, therefore, appears that the values of the compressibility deduced from the ultrasonic velocities are essentially correct. As there are no other alternatives, it is concluded that the difference between the two sets of data must be due to gas solubility.

It was mentioned in the introduction that Grimes [32, 46, 47] found positive heats of solution for the solubility of inert gases in molten salts and Copeland et al [48] suggested that this indicated

that the gas forms its own holes in the melt. Therefore, when the gas goes into solution the volume of the melt increases and, although this effect is very small, it will be a significant proportion when measuring very small volume changes. If it is assumed that the gas forms its own holes, the volumes will be additive leading to the following expression.

$$V_e = V_s + V_g \qquad (4.9)$$

where V_e is the experimentally observed volume, V_s is the true volume of the salt and V_g is the volume of the gas dissolved in the salt.

If $V_g = KV_sP$ where K is a pressure independent Henry's law constant, expressed in atm $^{-1}$ and P is the pressure, then

$$V_e = V_s (1 + KP) \qquad (4.10)$$

Differentiating and dividing by V_o

$$\frac{1}{V_o}\left(\frac{\partial V_e}{\partial P}\right)_T = \frac{1}{V_o}\left(\frac{\partial V_s}{\partial P}\right) + \frac{K}{V_o}\left(V_s + \frac{P\partial V_s}{\partial P}\right) \qquad (4.11)$$

$$\therefore \beta_e = \beta_s - \frac{KV_s}{V_o} + KP\beta_s \qquad (4.12)$$

where β_E is the experimentally determined compressibility and β_s is the true compressibility of the salt.

However, since in the Tait equation B is large we may write :- $\beta = \beta' - \gamma P$ (4.13)

where β' is the compressibility at 1 atm. pressure and γ is the pressure independent constant. This relation corresponds to that found experimentally.

$$-\frac{1}{V_o}\left(\frac{\partial V}{\partial P}\right) = \beta' S - \gamma P \quad (4.14)$$

integrating $-V_s = V_o\left(\beta_s' P - \frac{\gamma P^2}{2}\right) + C$ (4.15)

where $P = 0$, $V_s = V_o$ and $C = -V_o$

$$V_s = V_o\left(1 - \beta_s' P + \frac{\gamma P^2}{2}\right) \quad (4.16)$$

Assuming that $\gamma_s = \gamma_e$ and substituting into (4.12) one obtains

$$\beta_e' = \beta_s' - K\left(1 - \beta_s' P + \frac{\gamma P^2}{2}\right) + KP\left(\beta_s' - \gamma P\right)$$

$$\beta_e' = \beta_s' - K + 2P\beta_s K - \frac{P^2 3K\gamma}{2} \quad (4.18)$$

For potassium nitrate at 390°C, K = 0.5 x 10^{-5} $Bars^{-1}$, β' = 2.4 x 10^{-5} $Bars^{-1}$ and γ is 10^{-9} $Bars^{-2}$. The value of γ was taken from the experimental plot.

At 1000 atm., $\beta'_e = \beta'_s$ - 0.5 x 10^{-5} + 2.10^{-7} - 10^{-9}. As the values of the last two terms are small even at 1000 atm., it can be expected that the relation $\beta'_e = \beta_s$ - K should apply up to 1000 atm. The true compressibility is, therefore, represented by a line drawn parallel to the experimental values through the ultrasonically determined value. The value of K is the difference between the ultrasonic compressibility and the experimental value obtained in this work at 1 atm. The values of γ are 1.2 x 10^{-9} bar^{-2} and 2.1 x 10^{-9} bar^{-2} for sodium nitrate and potassium nitrate. These values are comparable to those obtained for other liquids. Because the values of γ are low, Nagarajan, Nanis and Bockris (60) would not be greatly in error in assuming that the compressibility is independent of pressure.

The fact that the compressibility of sodium nitrate is less than that of potassium nitrate is thought to be due to double repulsion. Pauling (118) shows that if the ratio r_+/r_- of the radii of the cation and anion falls below 0.414, anion - anion contact

will occur rather than cation - anion contact. Consequently, the repulsive forces are larger than they would be for either anion - cation or anion-anion contact alone. For sodium nitrate and potassium nitrate $\frac{r_+}{r_-}$ is 0.41 and 0.57 respectively and, therefore, it is much harder to compress the nitrate ions in a sodium nitrate melt than in potassium nitrate. The amount of free volume has little effect on the compressibility of molten salts: the important factor is the ion - ion interactions.

4. GAS SOLUBILITY

If the diffusivity of dissolved gas is comparable with the ion diffusivities, it might be expected that a gas dissolving in the melt would not reach saturation throughout the dilatometer due to the gas having to diffuse down the melt in the capillary. However, all the experimental evidence indicates that the saturation was achieved rapidly, thus, no matter how quickly a volume reading was taken after increasing or decreasing the pressure there was no detectable change in the volume with time. Also, the presence of gas was indicated by the occurrence of bubbles in certain cases.

All the evidence is consistent with the assumption that the melts were saturated with gas at all times. It must, therefore, be concluded either that the rate of dissolution is not diffusion controlled or that the diffusivity of the dissolved gas is high compared to the ions diffusivities. Very little is known about the diffusion of gases in liquids. A recent review by Himmelblau (122) shows that the value of the diffusion coefficient can vary from 2×10^{-2} cm^2 sec^{-1} for argon in liquid nitrogen to 40×10^{-5} cm^2 sec^{-1} for hydrocarbon gases in hydrocarbons. However, the effects of concentration, temperature and pressure on the diffusion coefficient are not known.

The values of the Henry's law constants derived from the two sets of compressibility data are shown in the 4.9 and 4.10.

TABLE 4.9.

Values of Henry's law constant for Argon in KNO_3

Temperature °C	K $bar^{-1} \times 10^5$
370	0.46
390	0.52
410	0.53
430	0.57

TABLE 4.10.

Values of Henry's law constant for Argon in $NaNO_3$

Temperature °C	K $bar^{-1} \times 10^5$
350	1.06
370	1.11
390	1.16
410	1.21

Argon is twice as soluble in sodium nitrate than potassium nitrate. This could be due to the sodium ions being able to fit interstitially between the argon atoms dissolved in the melt. For potassium nitrate, the potassium ions are unable to fit interstitially and, therefore, the negative

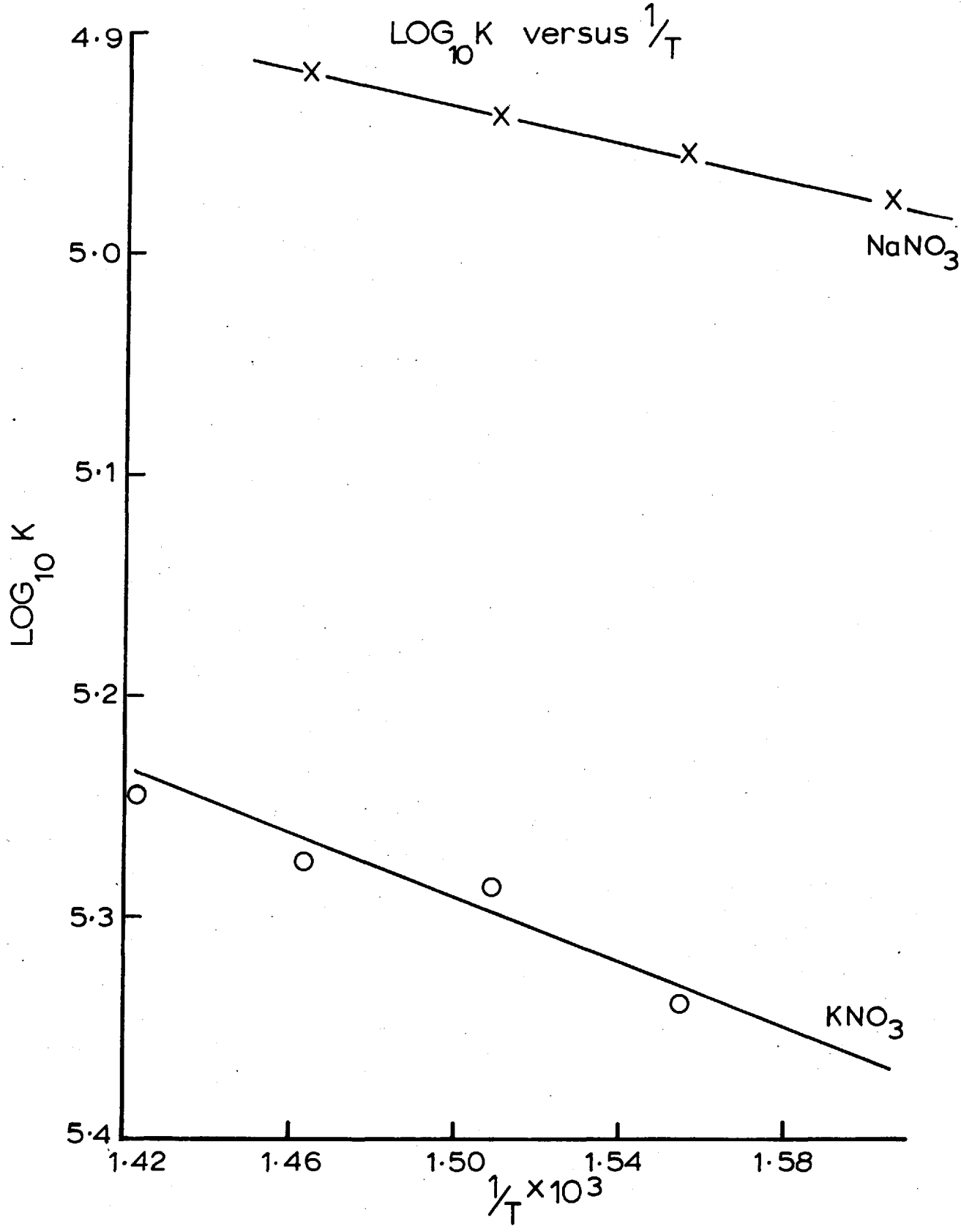
contribution to the heat of solution arising from ion - gas interactions may not be so high.

The values of the Henry's law constants are plotted logarithmically versus 1/T as shown on page 122. The heats of solution derived from this plot are 5.9 K cals. for potassium nitrate and 4.0 K cals for sodium nitrate. These heats are consistent with the explanation of the solubility difference advanced above and the values are of the same order of magnitude as the values of about 10 K cal obtained by Grimes et al (32, 46, 47) for the solubility of argon in fluoride melts.

The Henry's law constants in this work are expressed as bar^{-1}. To obtain the constant in the more usual form of moles/cc of melt atm. it must be divided by the volume of 1 mole of liquid argon at the temperature of the melt. This was calculated from the molar volume at -187°C, V_o, and the coefficient of expansion, α, by applying the equation.

$$Vt = V_o (1 + \alpha t) \qquad (4.20)$$

The coefficient of expansion for liquid argon is 4.65×10^{-3} and it was assumed that it would apply up to 400°C. The value of K was found to be 4.8×10^{-8} mole/cc melt atm. for KNO_3 and 11.0×10^{-8} mole/cc melt atm for $NaNO_3$. These values are comparable with the value of 6×10^{-8} mole/cc melt


LOG10K versus 1/T
4·9
5·0
5·1
5·2
5·3
5·4
LOG10 K
NaNO3
KNO3
1·42
1·46
1·50
1·54
1·58
1/T x 10³

atm. for argon in NaF - ZrF_4 at 700°C. Copeland Zybko [48] found the solubility for argon in $NaWO_3$ at 350°C to be 1.86 x 10^{-6} mole/cc melt atm.

This value is thirty times those obtained in this work and is probably too high as they appear to have neglected to take into account the expansion of the vessel on heating. Any slight leaks would also give rise to positive errors.

In the helium run at 200 atm. with potassium nitrate it was found that the compressibility obtained was the same as the ultrasonic value. This is surprising as it was expected that the solubility of helium should be approximately ten times that of argon. However, the helium atom is considerably smaller than the argon atom and, therefore, helium will be able to dissolve interstitially. This is confirmed by the work of Reynolds [119] who found that the solubility of argon at 500°C in glass is less by the factor of 10^3 than the solubility of helium. It, therefore, appears that the helium atom is able to accomodate itself in close packed structures whereas argon can only do this to a small degree.

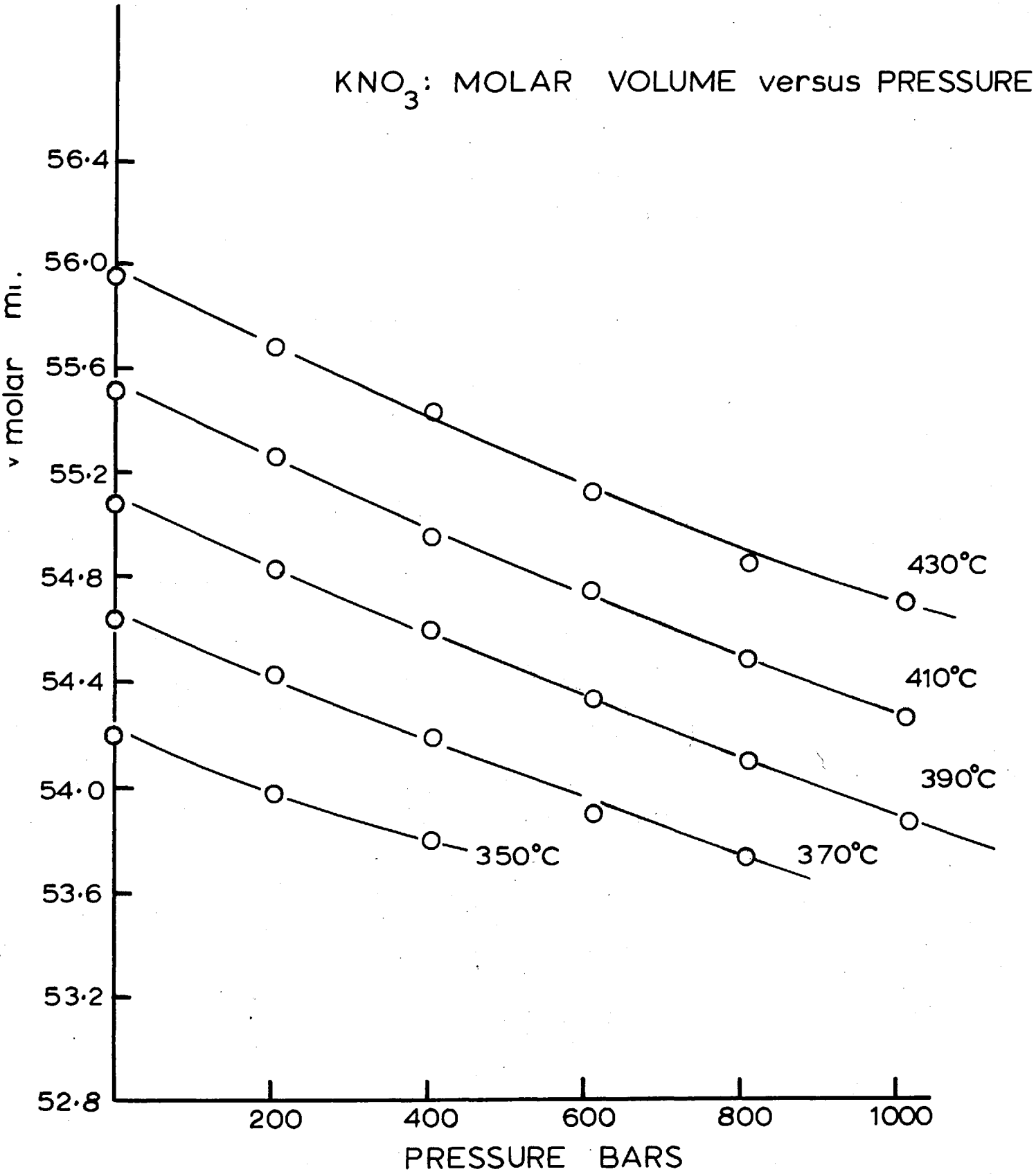
5. MEASUREMENTS AT CONSTANT VOLUME

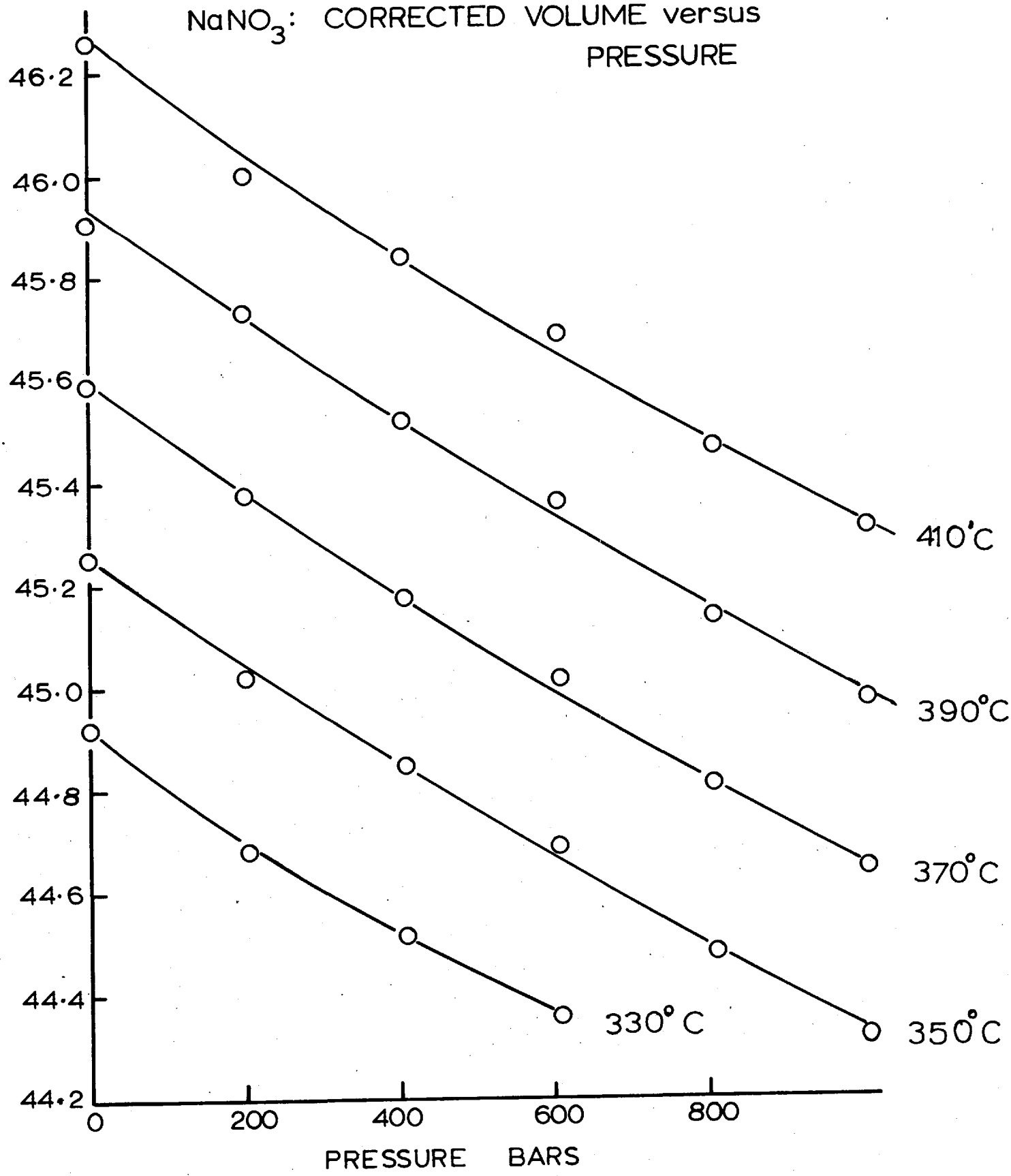
By using the expression :-

$$V_e = V_s + KPV_s \qquad (4.21)$$

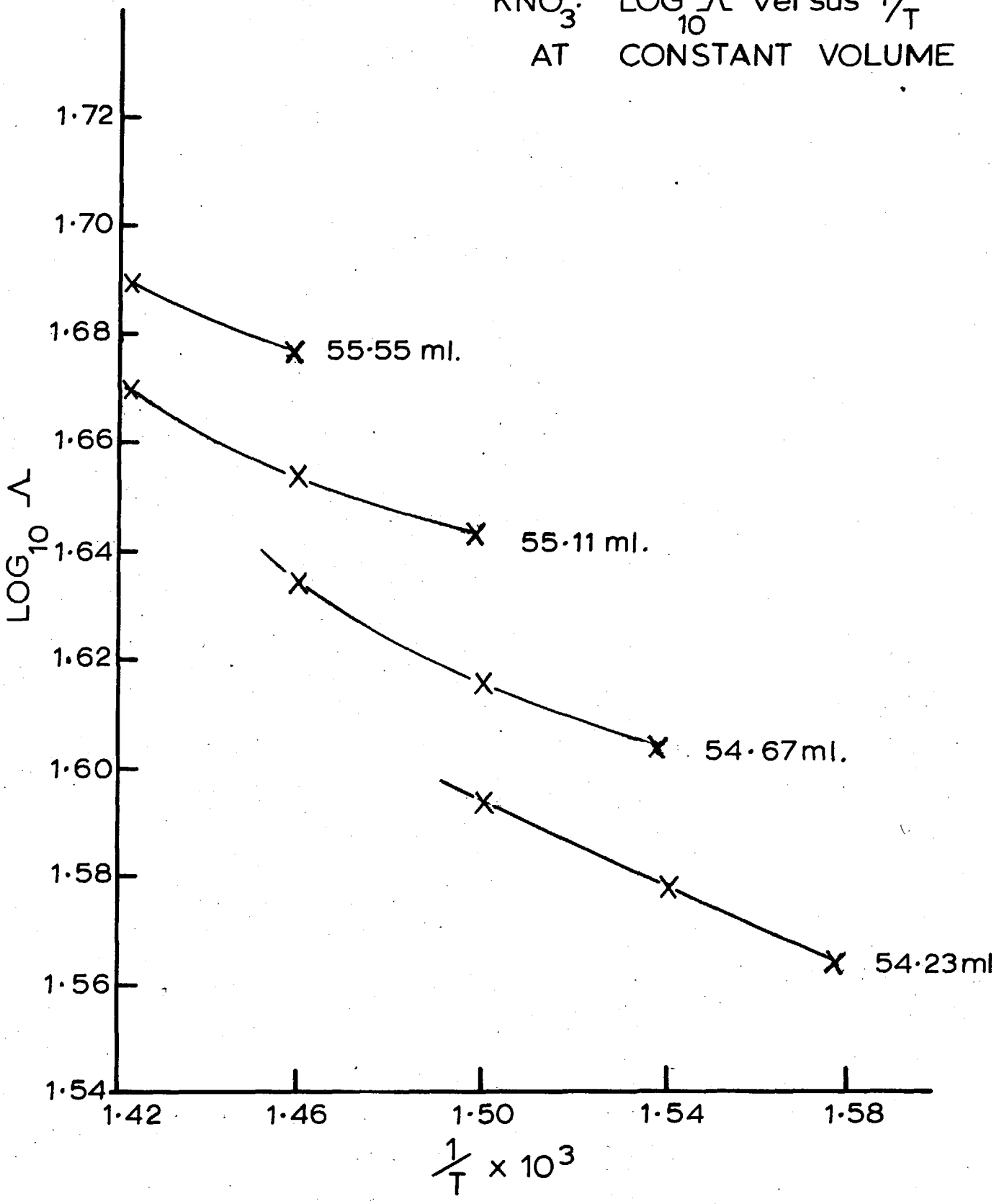
the true volume of the salt was calculated and this is plotted against pressure on pages 125 and 126. The correction was about 1/3rd of the volume change due to the pressure and was about 0.04cc/100 atm. To obtain values of the activation energy at constant volume, values of the temperature and pressure were read from the volume versus pressure plots at constant volume. $\text{Log}_{10}\Lambda$ was obtained at these temperatures and pressures from the $\log_{10}\Lambda$ versus pressure plots.

Graphs of $\text{Log}_{10}\Lambda$ versus 1/T at constant volume were constructed and are shown on pages 127 and 128. The values of the activation energies were obtained by drawing tangents to these plots and are shown in tables 4.11 and 4.12. The activation energy at constant volume for $NaNO_3$ is independent of temperature but for KNO_3, the activation energy increases with increasing temperature, mainly due to the curvature of the $\log_{10}\Lambda$ versus pressure plot. Tangents were drawn at the high and low temperature ends of the potassium plot and both values are shown in table 4.11.


KNO3: MOLAR VOLUME versus PRESSURE
v molar ml.
56·4
56·0
55·6
55·2
54·8
54·4
54·0
53·6
53·2
52·8
200
400
600
800
1000
PRESSURE BARS
430°C
410°C
390°C
370°C
350°C


NaNO3: CORRECTED VOLUME versus PRESSURE
46·2
46·0
45·8
45·6
45·4
45·2
45·0
44·8
44·6
44·4
44·2
0
200
400
600
800
PRESSURE BARS
410°C
390°C
370°C
350°C
330°C

KNO_3: $LOG_{10}\Lambda$ versus $1/T$
AT CONSTANT VOLUME



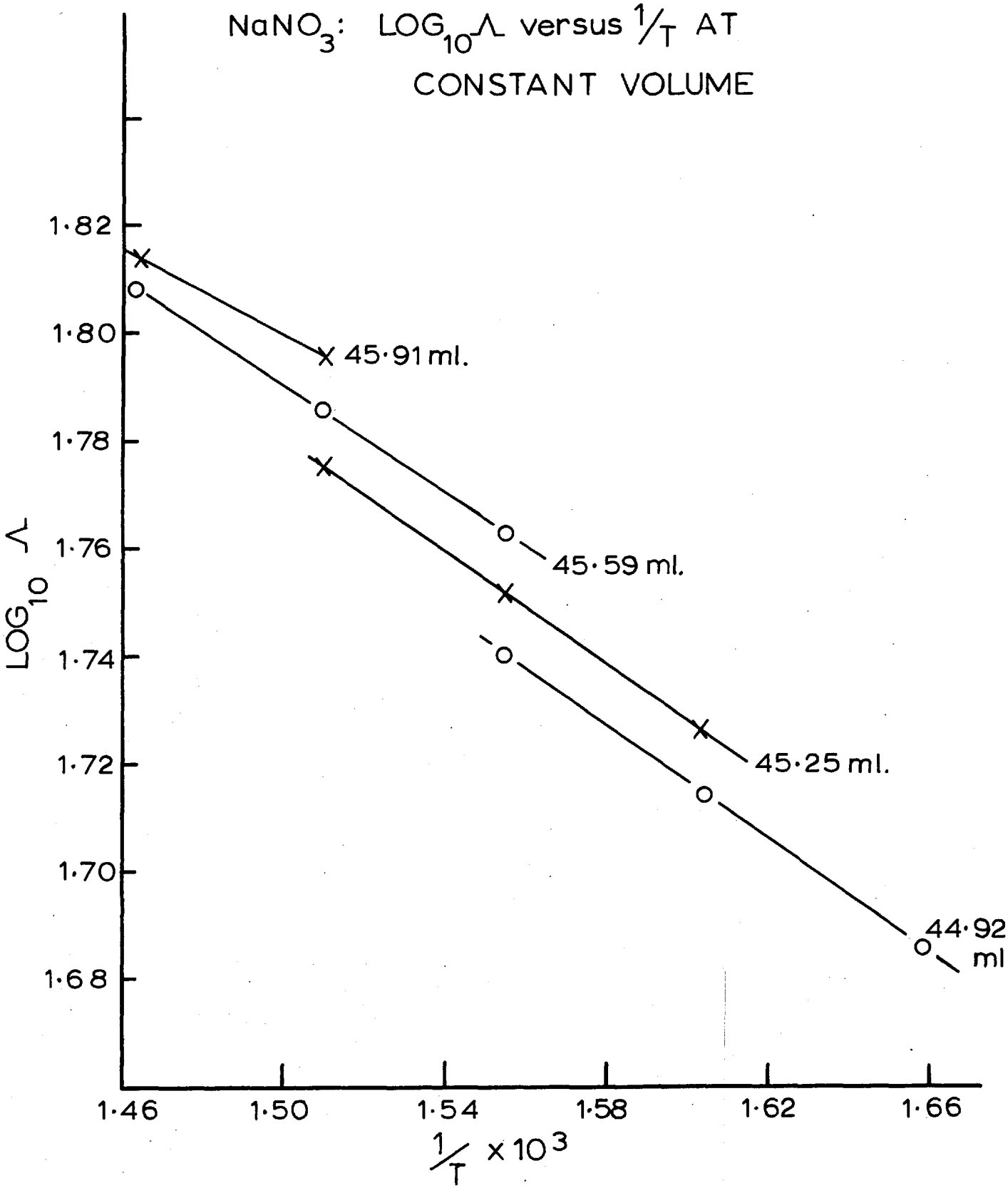

NaNO3: LOG10Λ versus 1/T AT
CONSTANT VOLUME
1·82
1·80
1·78
1·76
1·74
1·72
1·70
1·68
LOG10 Λ
45·91 ml.
45·59 ml.
45·25 ml.
44·92 ml
1·46
1·50
1·54
1·58
1·62
1·66
1/T x 10^3

TABLE 4.11

Activation Energies at Constant Volume for KNO_3.

Molar Volume	E_V Kcals.	
Ml	Low temp.	High Temp.
54.23	1.4	1.6
54.67	1.3	1.5
55.11	1.2	1.5
55.55	1.0	-

TABLE 4.12

Activation Energies at Constant Volume for $NaNO_3$

Molar Volume	E_V
Ml	Kcals
44.92	2.2
45.25	2.4
45.59	2.2
45.91	1.8

In both salts, the value of the activation energy at constant volume decreases with increasing volume.

The results for E_p and E_v can be tested to see whether they are self consistent by applying the equation (1.22)

$$E_p - E_v = RT^2 \frac{\alpha}{\beta} \left(\frac{\partial \ln K}{\partial P} \right)_T \qquad (1.22)$$

Values of $E_p - E_v$ calculated from the activation volume and α and β at 1 atm., are compared with those observed experimentally in table 4.13.

TABLE 4.13

Comparison of calculated and experimental $E_p - E_v$.

Salt	Molar Volume Ml	$(E_p - E_v)_{calc}$	$(E_p - E_v)_{exp.}$
KNO_3	54.23	2.78	2.5
	54.67	2.77	2.4
	55.11	2.77	2.4
	55.55	2.74	2.5
$NaNO_3$	44.92	1.1	1.0
	45.25	1.1	0.7
	45.59	1.1	0.7
	45.91	1.1	1.0

Although the experimental and calculated values are not in complete agreement, they agree within the experimental error of the results. Using the values of Nagarajan, Nanis and Bockris[60], there is a difference of 1.6 Kcals between the right and left hand sides of the equation. If it is assumed that their value of the activation volume is correct, the value of E_v given by the equation would be 2.5 Kcals resulting in an E_v/E_p ratio of 0.6 which corresponds to the values obtained in this work of 0.7. This value of E_v could have been obtained from the experimental results as it is possible to draw another line through the points.

Another discrepancy shown by the results obtained by Nagarajan et al[60] is that on the application of the Nernst-Einstein equation, a negative activation energy for conductance is obtained. As the Nernst-Einstein equation invariably gives values of E_Λ which are too high, a more negative value would have been expected experimentally. This has proved not to be the case.

Not much reliability can be attached to the work of Nagarajan et al[60] as their experimental method is very inaccurate. The power distribution to the furnace couldnot be altered when the pressure is

increased and only one thermocouple was used so that any temperature gradient that existed could not be detected. From experience with the apparatus used in this work, where there is considerably less free space available for corrective currents than in Bockris' apparatus, a temperature gradient of 100°C could easily exist over the melt. Moreover, the diffusion technique used has been criticised by Angell and Tomlinson [120].

6. DISCUSSION OF ACTIVATION VOLUME IN CONJUNCTION WITH E_v

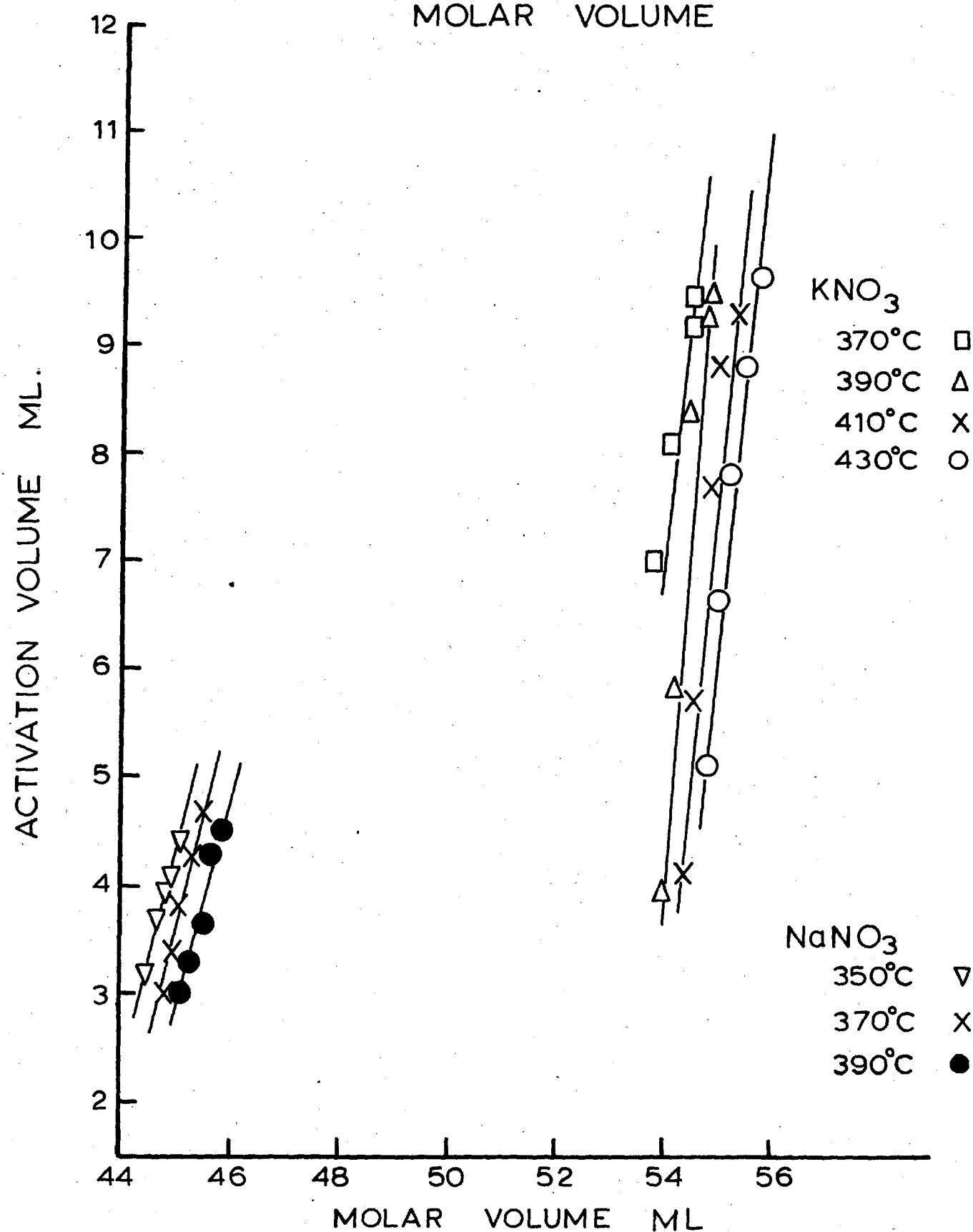
The activation volume is defined as the volume of one mole of ions in the transition state. However, it is difficult to ascribe a physical model to this definition. In the article by Bloom and Bockris [121], the activation volume is redefined as the volume of a vacancy plus the volume of an ion on the surface minus the volume of an ion in the liquid. These descriptions indicate that the volume required for the movement of an ion should remain approximately constant. However, Brummer and Hills [67] showed that, for dilute electrolyte solution in the methanol and nitrobenzene, ΔV^{*} varies considerably with both temperature and volume.

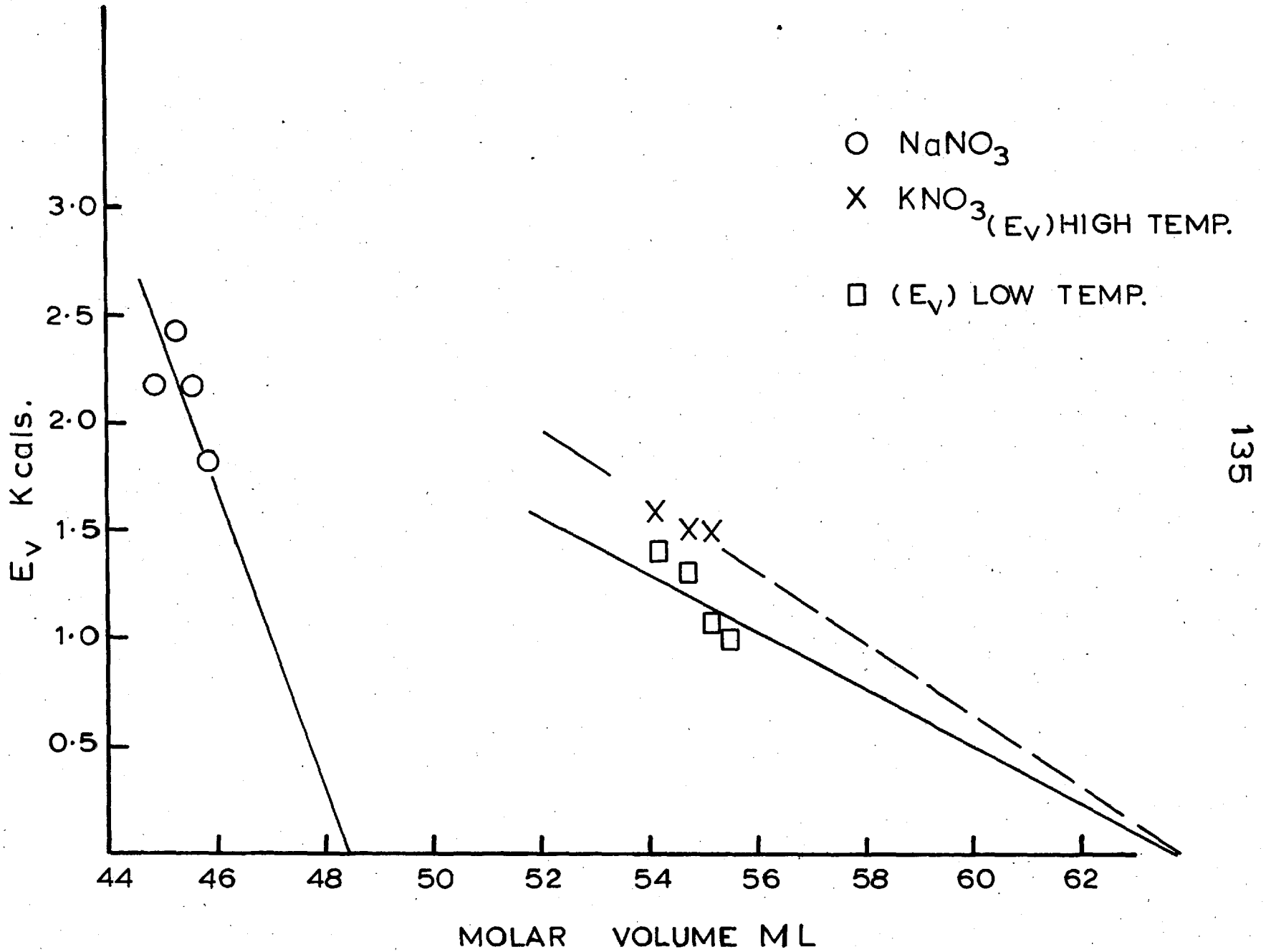
A plot of the activation volume against molar volume is found on page 134. The values of the molar volume were interpolated from the corrected volume versus pressure plots found on pages 125 and 126. It is seen that decreasing the temperature increases the activation volume at constant volume. Whereas decreasing the volume at constant temperature decreases the activation volume. This suggests that the activation volume is dependent both on the volume and the thermal energy of the melt. From similar results for dilute electrolyte solutions in methanol and nitrobenzene, Brummer and Hills (67) concluded that ΔV^* should be regarded as a composite quantity consisting of ΔV^*_j and ΔV^*_h. It was thought that the variation of ΔV^* with temperature was due to the increase in volume, ΔV^*_j, for the ion to move to a vacant site and the variation with volume was due to the change in the volume of the system for the accomodation of the migrating ion.

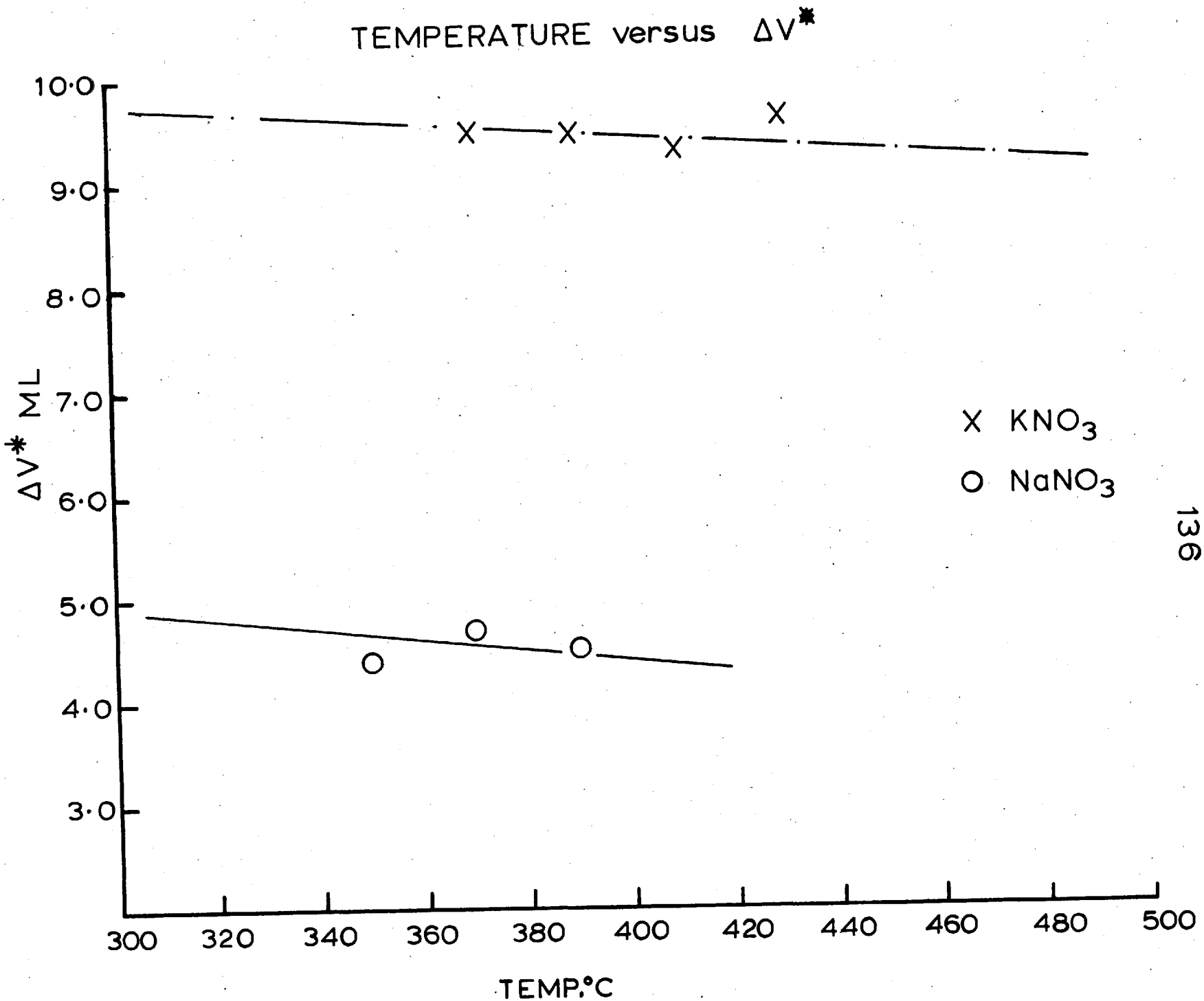
When E_v is plotted against molar volume, as is shown on page 135, and the graph extrapolated to zero E_v, a value of the molar volume is obtained which is equal to the molar volume at the melting point/(see page 136). This infers that when there is sufficient volume available for movement of

plus the activation volume at the melting point.

ACTIVATION VOLUME versus
MOLAR VOLUME




E_V versus MOLAR VOLUME
O $NaNO_3$
X KNO_3 (E_V) HIGH TEMP.
□ (E_V) LOW TEMP.
E_V Kcals.
3·0
2·5
2·0
1·5
1·0
0·5
44
46
48
50
52
54
56
58
60
62
MOLAR VOLUME ML


TEMPERATURE versus ΔV*
10·0
9·0
8·0
7·0
6·0
5·0
4·0
3·0
ΔV* ML
X KNO3
O NaNO3
300
320
340
360
380
400
420
440
460
480
500
TEMP.°C

the ions, the energy requirement is zero. From this graph and the plot on page 134, it is seen that as the molar volume of the system increases, the energy required for the movement of the ions decreases and the activation volume increases. Therefore, the activation energy at constant volume depends on the amount of free volume available for transport. It is extremely unlikely that the volume needed by a moving ion is going to alter with molar volume or temperature and therefore, it is tentatively suggested that the activation volume is the volume required by the moving ion minus the volume that the neighbouring ions sweep out to accomodate the movement. The latter would increase with temperature due to the greater thermal vibration of the ions and decrease with an increase of molar volume.

7. ANALYSIS

The values of the percentage nitrite present are shown in table 3.4 on page 89. The values appear to be high but a thermodynamic analysis indicates that they are of the right order of magnitude.

To calculate the dissociation of nitrate to nitrite a knowledge of the free energy for the reaction

$$NaNO_3 \rightleftharpoons NaNO_2 + 1/2\ O_2 \qquad (4.22)$$

is required. The heat of dissociation can be calculated from the heats of formation of the nitrite and nitrate. Values of the entropies are not known for the nitrite and nitrate and, therefore, it was assumed that they were approximately equal. The entropy change for the production of $\frac{1}{2}$ mole of oxygen is 20 e.u. and the heats of formation of sodium nitrate and nitrite are -111.54 Kcals and -85.9 Kcals and for potassium nitrate and nitrite are -117.76 Kcals and -88.5 Kcals.

The free energy changes were calculated and substituted into

$$\Delta G = -RT\ln K, \qquad (4.23)$$

where K is $\dfrac{a_{Me\ NO_2}\ P^{\frac{1}{2}}O_2}{a_{Me\ NO_3}}$

The values of K_{NaNO_3} and K_{KNO_3} were 2×10^{-2} and 1×10^{-3} respectively. The percentages of nitrite were found to be 2% and 0.1% which were in accordance with the experimental values. The differences between the calculated and observed values are probably due to the approximations made in the calculations.

8. ERROR IN DERIVED QUANTITIES

a) ACTIVATION ENERGY AT CONSTANT PRESSURE

The error in the equivalent conductance is $\pm 0.7\%$ and the error in the temperature is $\pm 0.5^{\circ}C$. The activation energy at constant pressure is given by

$$E_p = -R\left(\frac{\partial \ln \Lambda}{\partial \left(\frac{1}{T}\right)}\right)_P \qquad (4.24)$$

The derived error in E_p is $\pm$ 0.1 Kcals but to this must be added the error in drawing a tangent to the curve. It is estimated that the total error in E_p is $\pm$ 0.2 Kcals.

b) ACTIVATION VOLUME

The error in the equivalent conductance is 0.7% which gives an error in $-RT\left(\frac{\partial \ln \Lambda}{\partial P}\right)_P$ of $\pm$ 0.3 cm^2/mole. To this must be added the error in drawing a tangent to the curve and, therefore, the total error in $\Delta V^{\ddagger}$ is $\pm$ 0.6 cm^2/mole.

c) COMPRESSIBILITY AND GAS SOLUBILITY

It is extremely difficult to estimate the error in these two quantities due to the extrapolation and corrections involved. However, the scatter of the results indicates that the error on the compressibilities is ± 5% and the gas solubilities are certainly within half an order of magnitude.

d) ACTIVATION ENERGY AT CONSTANT VOLUME

The error in the equivalent conductance is ± 0.7% and it is assumed that the error on the corrected volume is the same as that on the determined volume.

To obtain values of the pressure and temperatures at the same volume required two volume measurements. An error of 0.3% on the volume causes an error of ± 70 atm. on the pressure scale. This error is transferred to the $\log_{10}\Lambda$ versus P plots resulting in an error of 2% on the $\log_{10}\Lambda$ scale. The error due to the equivalent conductance is, therefore, negligible. The error on the $\log_{10}\Lambda$ versus 1/T plot at constant volume is, therefore, 2% resulting in an error in E_v of ± 0.3 Kcals.

C H A P T E R 5

GENERAL DISCUSSION

1. GENERAL

The pressure and temperature dependence of conductance and volume of molten salts has been measured, and from the results have been dorived the values of the activation volume, compressibility, and the energy of activation at constant volume. In this section the theories of transport and the structure of molten salts will be discussed in terms of these results.

2. TRANSPORT THEORIES

a) HOLE THEORY

This theory has been extensively applied by Bockris to molten salts and the results obtained by Nagarajan et al [60] substantiate this theory. However, it has been discussed previously that these results are probably in error.

One of the basic concepts of the hole theory is that the energy of hole formation should be much larger than the energy for jumping, even though fused salts have 20% free volume. The results found show that the ratio energy of jumping to the total energy of activation is approximately 1/3rd for KNO_3 and 2/3rds for $NaNO_3$ and, therefore, transport

in these molten salts is not entirely controlled by the energy for the formation of a hole.

Nagarajan et al [60] showed a graph relating the pressure coefficient of compressibility γ, to the ratio $\frac{E_v}{E_p}$. For a value of γ of 1×10^{-9}, the ratio of $\frac{\Delta H_J}{\Delta H_{tot}}$ should be about 0.07, which has not been found.

If the work of Nagarajan et al [60] is considered correct, the mechanisms of diffusion and conductance must be different which is not in accordance with the hole theory.

b) DENSITY FLUCTUATION THEORY

The results do not substantiate Swalin's theory for although E_j is a considerable proportion of E_{tot}, the theory suggests that $E_j \approx E_{tot}$.

The activation energy should be equal to 2RT, but this has not been found with constant pressure activation energies. From these results, it can be seen that the theory applies even less at constant volume as $E_{(NaNO_3)}$ is twice $E_{(KNO_3)}$ for approximately the same temperature.

According to Swalin, transport coefficient should be proportional to T^2. From table 5.1. it is seen that conductance at constant volume depends closely on $T^{\frac{1}{2}}$ and therefore Swalin's free volume theory does not appear to be applicable to fused salts.

c) CRITICAL VOID FREE VOLUME THEORY

This theory has been applied to molten salts by Angell[28] who showed that the $1/(T-T_o)$ temperature dependence fitted for glass forming melts but that the values of the pre-exponential and $\gamma V^*/V_m$ did not correspond to those found by Cohen and Turnbull[9] for molecular liquids.

The theory indicates that a constant volume transport coefficient should depend on $T^{\frac{1}{2}}$. Values of $\frac{\Lambda_{T1}}{\Lambda_{T2}}$, $\frac{T1}{T_2}$ and $(\frac{T_1}{T_2})^{\frac{1}{2}}$ are presented in table 5.1 and it is seen that the conductivity is more dependent on $T^{\frac{1}{2}}$ than T. The pre-exponential in the Cohen and Turnbull equation, therefore, seems to give the correct temperature dependence for molten salts.

TABLE 5.1

Values of $\frac{\Lambda_1}{\Lambda_2}$, $\frac{T_1}{T_2}$ and $(\frac{T_1}{T_2})^{\frac{1}{2}}$ at constant volume.

Salt	V_M Ml	$\frac{\Lambda_1}{\Lambda_2}$	$\frac{T_1}{T_2}$	$(\frac{T_1}{T_2})^{\frac{1}{2}}$
KNO_3	54.23	0.987	0.970	0.985
	54.67	0.989	0.973	0.987
	55.11	0.987	0.971	0.986
	55.55	0.984	0.971	0.986
$NaNO_3$	44.92	0.983	0.970	0.984
	45.25	0.987	0.971	0.986
	45.59	0.985	0.970	0.985
	45.91	0.989	0.972	0.986

This theory can be further tested by using the value of T_o given by Angell and by assuming that $\gamma = \frac{1}{2}$, and $V^* = V_m$. If it is assumed that conductance can be applied to the Cohen and Turnbull theory, the pressure dependence of the conductivity at constant temperature can be calculated from :-

$$\frac{\Lambda_{1000}}{\Lambda_1} = e^{-\gamma V^* \left(\frac{1}{V_f T - \beta V_p \Delta p} - \frac{1}{V_f T}\right)} \quad (5.1)$$

The free volume is calculated from $V_m \alpha (T - T_o)$, where α is the mean coefficient of expansion, T_o is taken as the glass transition point. In the pressure dependent term, β is the compressibility at 1 atm. and $\bar{V}_p$ is the mean molar volume of the salt. The values of the mean coefficient of expansion for KNO_3 and $NaNO_3$ are 3.52×10^{-4}/C and 3.33×10^{-4}/C respectively (28).

TABLE 5.2

Values of Λ_{1000}/Λ_1 at the melting point.

Salt	Λ_{1000}/Λ_1 observed	Λ_{1000}/Λ_1 calculated $V_f = V_m \alpha (T - T_o)$	$V = V_m - V_i$
KNO_3	0.88	0.48	0.93
$NaNO_3$	0.92	0.34	0.92

From table 5.2 it is seen that the calculated values assuming $V_f = V_m \alpha (T - T_o)$ are far lower than those observed experimentally. Moreover, if the free volume is considered as the volume of the salt minus the volume of the ions, the ratio is of the correct order. Another way of obtaining the experimentally observed dependence from the Cohen and Turnbull theory is to assume that $\frac{\gamma V^*}{V_m}$

is much smaller than 1. However, even if Angell's[28] value of 0.25 for $\frac{\gamma V^*}{V_m}$ was used, the $\frac{\Lambda_{1000}}{\Lambda_1}$ only increases to 0.6 for $NaNO_3$ and 0.69 for KNO_3. However, it is thought that it is better to assume that the free volume is the total empty space in the salt rather than considering a very small critical void size.

The Cohen and Turnbull theory also gave the wrong pressure dependence for liquid metals. As the compressibility of liquid metals is insensitive to temperature, it was suggested that the expansion of a liquid metal is due to the introduction of free volume and that the contraction on the application of the pressure is due to the shrinkage of the electron gas. This idea obviously cannot be applied to molten salts.

It is not surprising that the calculated pressure dependence for molten salts is wrong as the pressure only reduces the free volume by about 10%, and, as was shown in the previous section, the amount of free volume controls the ease of movement of ions. For molecular liquids there is considerably less free volume at atmospheric pressure and, as the compressibilities are similar, the fractional decrease of free volume with pressure is greater.

The Cohen and Turnbull model is based on the simple concept that for transport to occur, a void above a critical size must be available for an ion to move into. It can be seen from these results and those of Angell's [28] that there is reasonable agreement with Cohen and Turnbull although the theory does not appear to apply entirely to conductance in molten salts. The temperature pre-exponential appears to be right, but the Cohen and Turnbull formulation of the free volume seems to be incorrect. This is to be expected as in conduction all the ions move, and, therefore, it is possible for all the free volume to be involved in transport.

5 COMPARISON OF THE PROPERTIES OF MOLTEN SALTS WITH OTHER SOLVENTS

In table 5.4 are shown the values of $\Delta V^{\ddagger}$, E_p, E_v and E_v/E_p for many liquids and solid salts. It may at once be seen that there is nothing unusual about the transport properties of molten salts. Thus the transport properties of sodium nitrate resemble those of the methanol solutions while potassium nitrate appears to resemble the non-associated liquids. It is difficult to find a satisfactory explanation for these remarkable similarities but certainly it appears that the long range coulombic forces can have little influence on transport. This view was first put forward by Rice (42) who advanced theoretical arguments to show that the relaxation time of these forces was too long for them to have any influence on transport and drew attention to the similarity of self diffusion in molten alkali halides and liquid rare gases. A possible explanation of the difference between sodium and potassium nitrates may lie in the anion - anion contact and double repulsion which occurs in sodium nitrate and, therefore, the ratio E_v/E_p in the case of this salt may be influenced by the greater repulsive and short range

TABLE 5.4

Comparison of data

Mechanism System	$\triangle V^{\ddagger}$ ml	E_p Kcals	E_v Kcals	E_v/E_p
Conductance KNO_3 (1) (ℓ)	5-10	3.5-4.1	1-1.5	0.3
$NaNO_3$ (1) (ℓ)	3-5	2.8-3.2	1.8-2.2	0.7
KNO_3 (10) (s)	1.10	-	-	-
0.01168N $NaNO_3$ in Methanol (67)	3.5-4.5	2.27	1.59	0.7
0.00931N n-Bu_4NPi in Methanol (67)	7-10	2.41	1.78	0.74
0.00855N n-Pr_4NPi in Nitrobenzene (67)	13-15	2.94	1.13	0.38
0.0014N n-Bu_4NPi in Nitrobenzene (67)	13-15	2.98	1.097	0.37
Diffusion Methanol (76)	—	3.8	2.7	0.7
Benzene (75)	22	2.78	0.78	0.3
Sulphur in Benzene (75)	8-29	3.34	1.0	0.4
Iodine in Benzene (75)	15	2.78	1.23	0.44

References:-

(1) This work
(67) Brummer and Hills
(76) Hiraoka, Izui, Osugi and Jono.
(75) Hiraoka, Osugi, Jono.
(10) Cleaver

attractive forces between the ions. This difference may be paralleled by the difference between associated and non-associated liquids since short range forces are structurally more important in the former class.

TABLE 5.5

Values for $\eta B/\eta S$ for molten salts, associated and non associated liquids.

MOLTEN SALTS		ASSOCIATED LIQUIDS		NON ASSOCIATED LIQUIDS	
	$\eta B/\eta S$		$\eta B/\eta S$		$\eta B/\eta S$
KNO_3	9.5	Diphenyl pentachloride	3.03	Carbon disulfide	800
$AgNO_3$	5.5	Water	2.66	Benzene	140
$NaNO_3$	3.9	Methyl alcohol	2.19	Chloroform	63
$LiNO_3$	2.0	Butanediol 2.3	1.60	Carbon tetrachloride	35
$CdCl_2$	1.7	Ethyl alcohol	1.44	Toluene	13
		Glycerol	0.80	Acetone	3.8

Further evidence for the similarity between the nitrates and organic liquids is shown by the work of Higgs and Litovitz [69] who measured the absorption of sound in molten nitrates. In liquids, the ultrasonic absorption is larger than the shear viscosity and is accounted for by assuming the existance of a bulk viscosity term η_B in addition to the shear velocity η_S. The ratio of η_B/η_S is shown in table 5.5 for molten salts and other liquids. It is seen that there is a similarity between the nitrates and other solvents as was found with the E_v/E_p ratio. As before, potassium nitrate tends to behave like a non-associated liquid while sodium nitrate behaves like an associated liquid. It is also interesting to note that the value of ΔV^* for molten potassium nitrate at the melting point is almost the same as that of the solid, at the melting point which indicates that there is some similarity between the process of transport in both the liquid and the solid state. This could be due to the low volume change on fusion. On the other hand, the activation volume in the solid increases with temperature while in the liquid it decreases. However, in view of the large difference between the activation energies it is not possible to take this comparison any further.

4 CONCLUSIONS AND SUGGESTIONS FOR FURTHER WORK

From the pressure dependence of the conductance and the ratio E_v/E_p, it appears that of the three theories of transport discussed in this work the Cohen and Turnbull critical void free volume theory applies best to nitrates. However, this theory will need some modification if it is to be applied with complete success to the conductance of molten salts. These results have shown that the pre-exponential term shows the correct temperature dependence and that the whole of the free volume in the salt must be considered to obtain a correct pressure dependence of conductance.

Provided that the solubility of argon is considered, the compressibilities of the salts correspond to the values found by Bockris, Higgs and Litovitz. Further confirmation of the correctness of the assumptions involved in evaluating the true dependence of volume on pressure and temperature is desirable.

There is a growing amount of evidence that molten salts are very similar to other liquids. This was shown by the similarity of $\Delta V^{\ddagger}$ and the ratio, E_v/E_p for nitrates and simple organic liquids and solutions. It would be interesting to

measure E_v for the other group I_a nitrates to observe whether, a consistent dependence on r_+/r_- occurs. Thus E_v should approach E_p in the case of lithium nitrate due to double repulsion.

There was a remarkable agreement between Cleaver's value of the activation volume of the solid at the melting point and the result obtained in this work. It would be useful to examine the pressure dependence of the conductance of other solid nitrates and to compare the activation volumes to see if the agreement was purely fortuitous in this case due to the low volume of fusion at the melting point.

Eventually it is hoped to extend the use of this apparatus to higher temperatures to enable the alkali halides, which are structurely much simpler than the nitrates, to be studied.

APPENDIX.

1. CONDUCTANCE RESULTS

a) POTASSIUM NITRATE

SPECIFIC CONDUCTANCE OF KNO_3

	TEMP °C	K MHOS CM^{-1}	T	K	T	K
1 atm	340.1	0.645	340.1	0.644	360	0.704
	360	0.704	360	0.709	360.1	0.709
	360.7	0.714	380	0.770	380	0.767
	380.1	0.769	380.4	0.766	386.7	0.802
	399.8	0.826	399.9	0.826	400	0.826
	400	0.826	400.2	0.826	419.9	0.888
	420	0.887	420.1	0.887		
100 atm.	339.7	0.626	340	0.626	340	0.625
	340	0.626	340	0.634	340.1	0.622
	340.1	0.626	340.3	0.626	357	0.680
	359.9	0.686	359.9	0.686	359.9	0.696
	360	0.685	360.1	0.696	360.1	0.686
	360.1	0.686	360.2	0.695	365.1	0.706
	378.5	0.758	380	0.756	380	0.754
	380	0.755	380	0.749	380.1	0.751
	380.1	0.756	380.2	0.750	386.6	0.769
	387.4	0.774	390.5	0.789	400	0.809
	400	0.815	400	0.813	400	0.814
	400.2	0.818	400.3	0.809	401.1	0.818

SPECIFIC CONDUCTANCE OF KNO_3

	T	K	T	K	T	K
100 atm (cont'd)	413.2	0.851	419.6	0.879	419.9	0.872
	420	0.880	420	0.870	420	0.879
	420	0.869				
200 atm	345.1	0.634	346.1	0.636	355.5	0.666
	357	0.676	368.8	0.702	374.9	0.726
	384.4	0.747	391.3	0.780	392.4	0.781
	394.8	0.784	399.7	0.806	408.4	0.831
	415	0.848	423.5	0.870	425.6	0.885
250 atm	339.4	0.627	340	0.626	360	0.686
	360	0.687	380	0.746	380.1	0735
	380.1	0.741	399.9	0.809	400	0.814
	400.2	0.781	400.2	0.781	420.1	0.852
	420.2	0.870				
300 atm	359.9	0.670	360	0.670	360	0.664
	360.1	0.672	360.1	0.671	360.2	0.670
	364.9	0.690	380	0.731	380	0.731
	380	0.731	380.1	0.731	396.8	0.780
	399.9	0.789	399.9	0.789	400	0.789
	400	0.790	400	0.790	400.1	0.789
	420	0.843	420	0.844	420	0.852
	420	0.850	420	0.854	420	0.846

SPECIFIC CONDUCTANCE OF KNO_3

	T	K	T	K	T	K
400 atm	359.9	0.659	360.1	0.659	380	0.721
	381	0.721	400	0.780	400.2	0.780
	400.2	0.781	420	0.835		
500 atm	360	0.649	360	0.649	360	0.652
	360	0.654	360	0.653	360	0.654
	367	0.676	379.5	0.709	380	0.711
	380	0.711	380	0.712	380.1	0.714
	399.9	0.771	399.9	0.766	400	0.770
	400	0.770	400	0.770	400	0.771
	400	0.770	402.4	0.775	420	0.826
	420	0.826	420	0.830	420	0.830
	420.1	0.830	420.1	0.826	420.2	0.826
	420.4	0.829				
600 atm	360	0.642	380	0.700	380	0.700
	400	0.760	400.2	0.760	420	0.816
700 atm	359.9	0.629	360	0.631	360.1	0.631
	363.5	0.644	374	0.665	379.9	0.696
	380	0.684	380	0.694	391	0.716
	395.3	0.727	400	0.756	400	0.756
	400.2	0.756	400.2	0.746	420	0.805
	420	0.809	420.1	0.814		

SPECIFIC CONDUCTANCE OF KNO_3

	T	K	T	K	T	K
800 atm	360	0.618	360.1	0.622	379.9	0.686
	380	0.681	399.9	0.739	400	0.744
	419.9	0.801				
1000 atm	360.1	0.602	365.2	0.634	367	0.649
	369	0.645	377.5	0.671	378.6	0.674
	397.1	0.729	400.2	0.731	409	0.750
	417	0.786	419.6	0.789		

SPECIFIC CONDUCTANCE OF $NaNO_3$

	TEMP °C	K MHOS cm^{-1}	T	K	T	K
1 atm	318	1.018	318.4	1.034	320.4	1.040
	320.9	1.041	321	1.045	324.7	1.050
	325.4	1.061	334.7	1.100	336.4	1.119
	337	1.116	338	1.130	339.4	1.133
	340.5	1.120	343.1	0.1148	343.8	1.162
	346.2	1.168	349.7	1.169	353.1	1.201
	354.5	1.202	355.8	1.209	363.6	1.249
	366.2	1.261	372.9	1.288	373.9	1.282
	375.1	1.300	376.6	1.318	376.7	1.292
	385	1.331	387.4	1.351	393.5	1.372
	400.7	1.403				

SPECIFIC CONDUCTANCE OF $NaNO_3$

	T	K	T	K	T	K
200 atm	319.2	1.031	320.5	1.020	320.9	1.024
	321.3	1.022	326.8	1.042	327.5	1.051
	329.6	1.071	330.4	1.072	335	1.100
	337.8	1.101	341.4	1.132	342.7	1.119
	343	1.131	345	1.138	346.3	1.142
	346.8	1.153	348.9	1.162	351.2	1.162
	351.21	1.182	355.7	1.191	356.1	1.191
	356.5	1.200	358	1.204	360.4	1.219
	363.8	1.240	367.8	1.253	371.8	1.270
	371.9	1.269	375.3	1.291	375.6	1.293
	376	1.281	376.6	1.285	377.2	1.284
	377.8	1.300	378.5	1.300	379.8	1.310
	382.5	1.306	383.4	1.319	388.1	1.340
	393	1.358	394.7	1.369	397.1	1.398
	397.7	1.398				
400 atm	322.5	1.010	327.7	1.042	327.7	1.043
	328.3	1.051	330.8	1.060	332.2	1.059
	332.8	1.079	333.5	1.072	334.9	1.077
	338.1	1.091	343.2	1.112	343.5	1.111
	345.2	1.136	345.3	1.118	345.6	1.111
	347.8	1.140	350.7	1.160	358.3	1.182
	359.9	1.169	360.3	1.200	363.7	1.218

SPECIFIC CONDUCTANCE OF $NaNO_3$

	T	K	T	K	T	K
400 atm Cont'd	363.8	1.221	363.9	1.199	364.8	1.221
	368	1.229	369.6	1.238	369.7	1.242
	370.2	1.241	375.8	1.250	375.9	1.278
	376.1	1.259	377.6	1.270	387	1.304
	389.2	1.318	391.5	1.341	393.8	1.330
	394.2	1.340	397.6	1.351		
600 atm	332.3	1.041	334.2	1.059	343.4	1.102
	345.2	1.111	345.7	1.111	357.8	1.152
	359.3	1.161	360	1.178	362.5	1.190
	363.7	1.199	373.5	1.246	375.2	1.252
	381.6	1.279	389.1	1.302	391.8	1.308
	395.8	1.308				
800 atm	330	1.001	343.3	1.092	344.8	1.080
	346.6	1.110	355.2	1.149	355.5	1.142
	358.4	1.157	373.4	1.238	377.5	1.240
	380.6	1.250	383.1	1.279	387	1.291
	392	1.303	400	1.358		
1000 atm	336.4	1.035	343.6	1.070	344	1.053
	367	1.173	370.6	1.201	374	1.218
	388.5	1.280	388.6	1.270	393.7	1.302

2 VOLUME RESULTS

a) POTASSIUM NITRATE

$\frac{\Delta V}{V_{334}}$ FOR KNO_3

	TEMP °C	$\frac{\Delta V}{V_{334}} \times 10^3$	TEMP °C	$\frac{\Delta V}{V_{334}} \times 10^3$	T	$\frac{\Delta V}{V_{334}} \times 10^3$
1 atm	342.8	3.77	345.4	5.06	346.4	5.99
	347.0	5.01	348.6	6.91	349.9	6.66
	350.8	6.80	355.6	8.20	356.4	10.09
	358	8.22	359.7	10.10	363.9	11.79
	366.41	13.89	366.5	13.73	367	10.36
	369	13.65	369.3	14.10	372.2	14.48
	373.1	17.20	373.5	15.21	374.2	16.38
	374.8	16.42	376.5	18.08	376.7	17.22
	382.4	20.03	384.5	21.68	386.5	21.62
	387.4	21.38	388.9	22.74	389.3	25.35
	390.3	23.19	391.6	24.44	391.8	25.3
	391.9	23.95	392.5	24.61	392.9	25.02
	393.3	23.44	396.7	26.32	396.71	25.82
	398.6	26.25	400.5	28.02	403.2	29.05
	404.4	29.3	404.6	29.3	404.61	28.5
	408.7	31.0	409.3	29.8	412.1	32.98
	412.9	31.6	416.2	33.82	416.8	34.2
	419.2	34.0	422.8	37.12	424.7	38.21
	424.7	42.9	425.4	37.75	427.7	38.4
	428.5	37.7				

$\frac{\Delta V}{V}$ 334 FOR KNO_3

	T	$\frac{\Delta V}{V}_{334} \times 10^3$	T	$\frac{\Delta V}{V}_{334} \times 10^3$	T	$\frac{\Delta V}{V}_{334} \times 10^3$
200 atm	344.3	0.00	348.2	2.14	352.6	5.06
	365.4	5.69	358.1	5.96	361.4	6.4
	367.1	12.3	368.4	10.98	368.6	8.99
	372.1	14.11	374.9	11.8	375.4	12.01
	375.6	13.48	378.7	14.38	381.5	16.12
	384.2	15.51	387.4	18.9	388.3	18.8
	391.3	18.61	391.9	18.11	395.2	22.75
	397.4	21.10	401.2	23.41	402	26.61
	404.4	27.62	405.5	260	406.1	24.60
	407.8	26.4	411.9	25.8	415	29.4
	415.8	30.21	421.1	32.21	422	33.6
	436.7	36.25				
200 atm under Helium						
	351.4	3.17	359.5	4.55	361.4	6.22
	363	7.08	369.4	7.76	373	12.0
	379.4	13.27	381.8	14.42	382.7	13.7
	395.3	19.2	396.6	20.42	398.7	19.6
	398.8	18.82	400	21.25	402.5	22.1
	409.7	23.1	416.3	27.39	416.5	26.39
	417.2	28.4	417.21	28	417.8	25.65
	418.8	28.9	428.3	30.4		

$\frac{\Delta V}{V}$ 334 FOR KNO_3

	T	$\frac{\Delta V}{V}$ 334 x 10^3	T	$\frac{\Delta V}{V}$ 334 x 10^3	T	$\frac{\Delta V}{V}$ 334 x 10^3
400 atm	353.3	1.49	360.8	4.56	366.1	6.16
	367.0	9.31	375.4	9,6	376.3	10.81
	378.2	11.23	384.5	11.0	385.4	13.18
	393.0	18.25	393.01	16.9	393.4	16.89
	398.2	16.91	399.4	18.61	399.9	20.15
	400.8	22.12	402.3	19.6	402.8	18.54
	404.1	21.20	405.0	21.21	405.7	23.39
	414.7	26.62	416.2	24.62	416.6	27.08
	419.6	25.5	419.7	27.2	422.0	29.95
	425.1	29.55	427.5	26.82		
600 atm	357.5	1.911	361.9	2.44	374.4	6.75
	375.7	5.58	376.2	6.43	380.5	9.25
	383.6	8.93	385.8	9.75	388.4	10.54
	388.6	9.0	391.3	9.86	391.7	13.21
	392.7	13.2	394	12.62	395.7	15.09
	396.6	14.18	398.9	15.55	399.3	15.22
	400.7	15.04	403.9	15.59	405	18.05
	408	19.09	413.7	19.71	414.7	20.18
	420.4	24.21	421.4	24.01	422.7	26.19
	426	24.65	432	28.39	433.6	28.2

$\frac{\Delta V}{V}$ 334 FOR KNO_3

	T	$\frac{\Delta V}{V}_{334} \times 10^3$	T	$\frac{\Delta V}{V}_{334} \times 10^3$	T	$\frac{\Delta V}{V}_{334} \times 10^3$
800 atm	367	0.59	376.1	4.58	376.2	4.41
	376.8	4.05	377.5	3.83	391.3	10.61
	391.6	9.3	393.2	10.49	399.8	12.71
	401.8	11.49	402.9	13.2	403.8	11.49
	404.6	12.91	405	13.51	417.3	18.61
	417.4	19.28	427.1	24.07	427.3	21.85
	430	22.41				
1000 atm	381.2	5.32	383	1.06	385.2	5.0
	390.7	4.89	391	5.16	395	8.11
	397.9	8.16	400.6	10.29	412.1	15.19
	415.2	12.6	417.4	16.89	422.5	18.27
	431.1	20.93				

b) SODIUM NITRATE

$\frac{\Delta V}{V306}$ FOR $NaNO_3$

	Temp °C	$\frac{\Delta V}{V306} \times 10^3$	T	$\frac{\Delta V}{V306} \times 10^3$	T	$\frac{\Delta V}{V306} \times 10^3$
1 atm	361	4.0	319	5.55	323.1	6.94
	327.7	7.25	328.9	8.75	331.3	10.1
	333.5	9.85	334.2	10.52	337.4	13.66
	338.7	11.81	339.5	12.32	342.4	13.59
	344.0	13.52	351.4	17.3	353	17.69
	353.3	18.16	357.4	19.11	359.1	20.5
	360.6	21.05	362.4	21.8	363.7	20.25
	364.6	22.3	368.7	23.82	372	25.55
	372.7	24.99	374.2	26.55	379.3	28.6
	380.5	27.68	382.1	28.78	382.8	29
	386.3	31.12	387.6	29.75	388.9	30.3
	392.8	32.19	395.1	33.65	395.4	35.01
200 atm	333.7	7.13	336.2	8.36	348.6	15.3
	349.3	11.6	351.4	15.61	352.6	13.07
	355.8	16.81	356.2	16.48	357.5	16.98
	357.9	18.30	361.4	18.0	363.2	17.42
	364.7	19.7	366.3	19.48	366.6	20.25
	369.6	23.72	370.9	20.92	373.4	23.21
	375.8	24.45	378.3	24.0	379.8	25.61

$\frac{\Delta V}{V}_{306}$ FOR $NaNO_3$

	T	$\frac{\Delta V}{V}_{306} \times 10^3$	T	$\frac{\Delta V}{V}_{306} \times 10^3$	T	$\frac{\Delta V}{V}_{306} \times 10^3$
200 atm	380.8	24.40	381.4	27.18	383.4	26.10
cont'd	389.2	28.05	392.5	30.85	396.2	31.25
	401.5	35.2				
400 atm	324.8	3.6	329.4	3.4	339.5	9.28
	349.6	9.9	350.1	12.04	357.3	12.19
	358.4	13.8	360.6	17.03	363	16.62
	367.8	18.8	369.5	18.9	370.2	18.9
	371.6	21.4	373.8	20.0	378.3	24.2
	384	23.81	387.7	27.1	392.4	26.5
	395.5	29.28				
600 atm	335.9	5.56	342.3	4.79	346.8	9.23
	347.3	9.81	351.7	10.5	356.8	13.25
	362.1	12.32	366.8	18.18	367.2	17.72
	371.3	19.21	371.9	19.61	376	22.18
	377.5	20.92	390.1	24.8	393	28.62
	397.5	29.82	398.6	29.13	405.1	30.99

$\frac{\Delta V}{V306}$ FOR $NaNO_3$

	T	$\frac{\Delta V}{V306} \times 10^3$	T	$\frac{\Delta V}{V306} \times 10^3$	T	$\frac{\Delta V}{V306} \times 10^3$
800 atm	347.6	9.35	351.4	7.64	351.5	9.6
	361.6	13.18	362.5	12.42	365.1	13.38
	374.3	16.55	375.3	18.3	383.1	20.41
	398	26.4	408.1	31.6		
1000 atm	353	9.28	365.4	12.59	371.6	15.29
	381.8	18.31	382.9	18.5	394.7	24.62
	397.2	23.41	406.8	30.42		

ACKNOWLEDGEMENTS

The author is indebted to Professor F.D.Richardson for the provision of research facilities and to D.S.I.R. for financial support throughout this work.

In particular, the author wishes to express his gratitude to his supervisor, Dr. J.W.Tomlinson, for his interest, guidence and encouragement throughout the course of this work.

Thanks are also due to Dr. E.H.Baker, Dr. K.E.Weale, Dr. K.E.Bett and Dr. R. Ross for many interesting discussions and advice regarding the high pressure aspects of the apparatus.

Finally, an expression of sincere appreciation to the members of the Nuffield Group Workshop, especially Mr. P. Worner, Mr. R. Green and Mr. R. Chamberlain, whose patience, skill and advice enabled the apparatus to be successfully operated.

The Nuffield Research Group,
Royal School of Mines,
S.W.7.

REFERENCES

1. Bockris and Richards. Proc. Royal Soc.A 1957, 241, 44.

2. Zarzcki, Compt. rend., 1957, 224, 758, J. Physique Rad.A, 1957, 18, 65; 1958, 19, 13; Non-Crystalline solids (Wiley.N.Y.,1960) pp 117-143.

3. Levy and Danford, "Molten Salt Chemistry", (Wiley. N.Y., 1964)

4. Frenkel, Acta Phy sicochim URSS 1935) 3,633, 913.

5. Bresler, Acta Phy sicochim URSS, 1939 10, 491.

6. Lumsden, "Private Communication".

7. Zermicke and Prins, Z. Physik, 41, 184.

8. Swalin, Acta Met. 1959, 7, 736.

9. Cohen and Turnbull, J. Phys. Chem 1959,31, 1164.

10. Cleaver "Private Communication".

11. Ubbelohde, Disc. Farad. Soc. 1961,32, 72.

12. Førland, "Fused Salts" (McGraw-Hill 1964).

13. Janz and James, Electrochim Acta, 1962 7, 427.

14. Kleppa and Hersh, Disc. Farad. Soc., 1961,32, 155.

15. Furukawa, Disc. Farad. Soc., 1961,32, 53.

16. Rhodes, Smith and Ubbelohde, Proc. Royal Soc. A. 1965, 285 263.

17. Angell, J. Phys. Chem. 1965, 69, 399.

18. Kleppa and Hersh, J. Chem. Phys., 1961,34, 351.

19. Bockris, Kitchener, Ignatowicz and Tomlinson Trans. Faraday Soc., 1952, 48, 75.

20. Bockris, Crook, Bloom and Richards. Proc. Royal Soc. A., 1960,255, 558.

21. Mills and Godbole, J. Amer-Chem. Soc., 1960, 82, 2395.

22. Laity, J. Chem, Phys., 1959, 30, 682.

23. Sundheim "Fused Salts" (McGraw-Hill 1964) P.244.

24. Bockris and Hooper, Disc. Farad. Soc., 1961, 32, 218.

25. Klemm, Z Naturforsch, 1953, 8a, 397.

26. Klemm, Z. Naturforsch, 1953, 15a, 173.

27. Laity, Ann. N.Y. Acad. Sci 79, 997.

28. Angell, J. Phys. Chem. 1964, 68, 1917.

29. Bockris, Disc. Farad. Soc., 1961, 32, 71

30. Reiss, Frisch and Lebowitz J. Chem. Phys., 1959 31, 369.

31. Stillinger "Phys. Chem. of Molten.Salts. (Interscience.1964).

32. Blander, Grimes, Smith and Watson. J. Phys. Chem. 1959, 63, 1164.

33. Nanis and Bockris, J. Phys. Chem., 1963 67, 2865.

34. Frenkel, "Kinetic Theory of Liquids" (Oxford, 1946).

35. Nachtrieb and Petit, J. Chem. Phys. 1956, 24, 1027.

36. Waser and Pauling J. Chem. Phys., 1950 18, 747.

37. Eyring, Ree and Hirai, Proc. Nat. Acad. Sci, 1958, 44, 683.

38. Lunden, Trans. Chalmers, Univ. of Tech., Gote. burg, Sweden. 1961, 241, 1.

39. Angell. PhD. thesis London (1961)

40. Dietzel and Poegel. Proc. of the Third International Glass Congress, Venice, Italy 1953 p.219.

41. Rice and Allnatt, J. Chem. Phys 1961, 34, 2144.

42. Rice, Trans. Farad. Soc. 1962, 58, 499.

43. Angell and Tomlinson. To be published.

44. Stillinger, J. Chem. Phys., 1961, 35, 1581.

45. Reiss and Mayer, J. Chem. Phys. 1961, 34, 12001.

46. Grimes, Smith and Watson. J. Phys. Chem. 1958, 62, 862.

47. Watson, Evans, Grimes and Smith. Chem. Eng. Data., 1962, 7, 285.

48. Copeland and Zybko. J. Amer. Chem. Soc., 1964, 86, 4734.

49. Frame, Rhodes and Ubbelohde. Trans. Farad. Soc., 1961, 57, 1075.

50. Bockris, Pilla and Barton. J. Phys. Chem., 1960, 64, 507.

51. Markham and Kobe. Chem. Revs., 1941, 28, 519.

52. Frohlich, Tauch, Hogan and Peer, Ind. Eng. Chem. 1931, 23 548.

53. Uhlig. J. Phys. Chem., 1937, 41, 1215.

54. Jobling and Lawrence Proc. Royal Soc. A 1951, 206, 257.

55. Haycock, Alder and Hildebrand. J. Chem. Phys., 1953, 21, 1601.

56. Watts, Alder and Hildebrand. J. Chem. Phys., 1955, 23, 659.

57. McCall, Douglass and Anderson. Phys. Fluids, 1959 2, 87.

58. Nachtrieb and Petit. J. Chem. Phys 1956 24, 756.

59. Tricklebank, Nanis and Bockris. Rev. Sci. Inst., 1964 35, 80.

60. Nagarajan, Nanis and Bockris. J. Phys. Chem., 1964, 68, 2726.

61. Nagarajan, Nanis, Bockris. J. Electrochem. Soc., 1965, 112 78c.

62. Jost and Nehlep. Z. Physik Chem. 1936, B.34, 348.

63. Shapiro and Kolthoff. J. Chem. Phys. 1947, 15, 41.

64. Shapiro and Kolthoff. J. Phys. Chem. 1948 52, 1319.

65. Kurnick. J. Chem. Phys. 1952, 20, 218.

66. Colladon and Sturm. Ann Chim. Phys. 1827, 36, 225.

67. Brummer and Hills. Trans. Farad. Soc., 1961, 57, 1816, 1823.

68. Bridgeman "The Physics of High Pressures". (Bell. London 1958).

69. Higgs and Litovitz. J. Acc. Soc. Amer. 1960 32, 1108.

70. Owens. J. Electrochem. Soc., 112, 83c (1965).

71. Van Artsdalen and Yaffe, J. Phys. Chem. 1955 59 118.

72. Klemm, Disc. Farad. Soc., 1961, 32, 265.

73. Cowen and Axon, Trans. Farad Soc., 1956, 52, 242.

74. Byrne, Fleming and Wetmore. Can. J. Chem. 1952, 30, 922.

75. Hiraoka, Osugi and Jono. Rev. Phys. Chem. Japan. 1958 28, 52.

76. Hiraoka, Izui, Osugi and Jono. Rev. Phys. Chem. Japan 1958, 28, 61.

77. Fürth, Proc. Cambridge Phil. Soc. 1941, 37, 252, 276, 281.

78. Bett and Newitt "The Design of High Pressure Vessels", Chem. Eng. Pract. p.5 (1958)

79. Dodge, "High Pressure Technique", Chem. Eng's. Handbook (McGraw-Hill 1950).

80. Ihrig, Ind. and Eng. Chem., 1949, 41, 2516.

81. Bridgeman "The Physics of High Pressure" (G. Bell and Sons 1958)

82. Adams, Williamson and Johnston J. Amer. Chem. Soc. 1919, 41, 12.

83. Goranson, Amer J. Sci., 1931, 222 481.

84. Birch, Phys. Rev., 1932, 41, 641.

85. Bett and Weale "Private Communication".

86. Lazarre, Saunel and Vodar. J. Res. C.N.R.S. Bellevue, 1954 26.

87. Gugan. J. Sci. Instr., 1956, 33, 160.

88. Paul, Benedek and Warschauer, Rev. Sci. Instr. 1959, 30, 874.

89. Balain and Bergeron, Rev. Sci. Instr., 1959, 30, 1058.

90. Loving, Ind. Eng. Chem., 1957 49, 1744.

91. Browne, Hileman and Weger. Ind. Eng. Chem. 1961, 53, 52A.

92. Comings, "High Pressure Technology" (McGraw-Hill 1956)

93. Porter, Lobo and Sliepcevich. Ind. Eng. Chem., 1956, 48, 841.

94. Kiefer. Ind. Eng. Chem. 1951, 49, 2017.

95. Smyth and Adams. J. Amer. Soc., 1923, 45, 1172.

96. Johannin and Vodar, Ind. Eng. Chem., 1957, 49, 2041.

97. Johnston and Adams. Amer J. Sci. 1911, 31, 505.

98. Birch. Rev. Sci. Instr., 1939, 10, 137.

99. Bundy. J. App. Phys., 1961, 32, 483.

100. Newitt, "The Design of High Pressure Plant and the Properties of Fluids at High Pressures" (O.U.P., 1940)

101. Boardman, Dorman and Heyman, J. Phys. Chem., 1949, 53, 375.

102. Shartsis and Spinner. J. Res. Nat. Bur. Stand., 1951, 46, 176.

103. Vogel "Textbook of Quantitative Inorganic Analysis" (Longmans, Green and Co. 1951)

104. Brummer PhD. Thesis (1961), London.

105. Plester, Ubbelohde Proc. Royal Soc. A. 1956, 235, 469.

106. Murphy and Wetmore, Can. J. Chem., 1959, 37, 1397.

107. Rice, Phys. Rev. 1958, 112, 804.

108. Lorenz and Kalmus, Z. Physik Chem, 1907, 59, 17.

109. Smith and Van Artsdalen. Semi-annual Prog. Rept. Oak Ridge Lab. ORNL - 2159, 80 (1956)

110. Bloom, Knaggs, Molloy and Welch, Trans. Farad Soc., 1953, 49, 1458.

111. Kroger and Weisgerber, Z. Physik Chem. (Frankfurt) 1955, 5, 192.

112. Doucet and Bizouard, Bull Soc. Chem. France, 1570 (1959)

113. Byrne, Fleming and Wetmore Can. J. Chem. 1952, 30, 922.

114. Datuma, Z. Anarg. Chem. 1928, 175, 1.

115. Papaioannou and Harrington, J. Phys. Chem. 1964, 68, 2424.

116. Lorenz, Frei and Jabs. Z. Physik Chem., 1908, 61, 468.

117. Kelley, Bureau of Mines Bulletin 476.

118. Pauling, "The Nature of the Chemical Bond" (O.U.P. 1963)

119. Reynolds, U.S. Atomic Energy Commission Dept. KAPL - 1612, 1956, p 25.

120. Angell and Tomlinson, Disc. Farad Soc., 1961, 32, 237.

121. Bloom and Bockris "Fused Salts" (McGraw-Hill, 1964)

122. Himmelblau. Chem. Revs. 1964, 64, 527.

123. Handbook of Physics and Chemistry. (The Chemical Rubber Co., 1964)